Dissertation

submitted to the
Combined Faculties for the Natural Sciences and for Mathematics
of the Ruprecht Karl University of Heidelberg, Germany,
for the degree of
Doctor of Natural Sciences (Dr. rer. nat.)

Presented by

MSc. Molecular Bioengineering **Carlos Alberto Hung Low**

Born in Caracas, Venezuela

Oral examination: November 16^{th}, 2010

Screening the cell adhesion activity of muscle skeletal progenitor cells on defined nanopatterns

Referees:
Prof. Thomas Holstein
Prof. Joachim P. Spatz

To my mother

Contents

Symbols and abbreviations

BM	Basement membrane
BSA	Bovine serum albumin
CAM	Cell Adhesion Molecule
CS	Chondroitin sulfate
DS	Desmartan sulfate
DGC	Dystrophyn-gycoprotein protein
DMEM	Dulbecco's modified eagle medium
DMSO	Dimethylsulfoxide
ECM	Extra cellular matrix
FA	Focal adhesions
FAK	Focal Adhesion Kinase
F-actin	Filamentous actin
FB	Fibrillar adhesions
FBS, FCS	Focal calf serum, Foetal calf serum
FC	Focal complexes
FN	Fibronectin
FG	Fibrinogen
GAG	Glycosaminoglycan
GAPs	GTPase activating proteins
GEF	Guanine nucleotide exchange factors
HA	Hyaluronic acid
He	Heparin
HTPS	High throughput screening
HS	Heparan sulfate
KS	Keratan sulfate
LM	Laminin
MAPK	Mitogen activated protein kinase
MHC	Myosin heavy chain
MRF	Myogenic regulatory transcription factors

MPCs	Muscle progenitor cells
PAK	p21-activated kinase
PBS	Phosphate buffered saline
PDMS	Poly(dimethylsiloxane)
PEG	Polyethylene glycol
PFA	Paraformaldehyde
PG's	Membrane-bound proteoglycans
siRNAs	Small interfering RNAs
shRNAs	Short hairpin RNAs
Src	Kinase
SAM	Self Assemble Monolayer
qRT- PCR	Quantitative real time polymerase chain reaction
YFP	Yellow fluorescent protein

Summary of the thesis

In living systems, the extracellular matrix (ECM) is a complex structural network of proteins that confine and supports cells adherent to it. In the process of cell adhesion, the cells spread out on the supporting microenviroment generating intracellular tension (mediated by actomyosin contractility). Such mechanical force modulates the formation of focal adhesion structures (FA). The "local" generation of mechanical force in FA causes "global" changes in cell shape and motility , modulation of gene expression and changes in cell proliferation, differentiation and survival. Due to their importance, FA are attractive targets for drug discovery and functional genomics studies. However, less is known about how cells mechanically sense and transduce external chemical and physical signals via FA as surface mechanosensors. The process of cell adhesion is mediated mainly through attachment and clustering of transmembrane integrins of the cell to ECM macromolecules, such as fibronectin, vitronectin, collagen and laminin. ECM proteins have been shown to contain ligand peptides that can influence cell behavior. In this thesis, the interaction of cells with different ECM peptide ligands is examined in order to determine the importance of this relationship in cell adhesion and differentiation.

In this thesis, the immobilization of peptides on engineered surfaces is used to mimic proteins in the ECM and to characterize their influence on cellular functions. The engineered surfaces consist of nanometer spaced, hexagonally arranged gold-particles on glass surfaces, which can be specifically decorated with the desired peptide, and the interparticle spacing modulated. In particular, progenitor C2 cells were chosen as reporter cells, as a well-documented model for studying cell differentiation, with the potential to differentiate into bone or muscle cells. For the quantification of cell-ECM matrix interaction, the C2 cells were manipulated to express fluorescent paxillin, a common FA component in cell adhesion screens. Further, in this thesis, cell adhesion experiments on nanopatterns were optimized to a cell based, multi-parametric and high-throughput screening (HTPS) system.

Using this HTPS platform at fixed 52 nm spacing between gold particles, a peptide library (perturbation) containing 33 different ECM derived peptides from fibrino-

gen, tenascin, collagen, fibronectin and laminins was examined. The screen ranked the response of the C2 cells based on a quantitative evaluation for cell attachment and a qualitative phenotypic rating. Out of this library, 5 adhesive peptide ligand candidates were chosen (3 laminin, 1 fibronectin, and 1 fibrinogen) based on their ability to induce a substantial phenotypic change in the cells as compared to the control peptide ligand RGDfK. The 5 peptide candidates finally examined are linear in structure, non RGD containing and up to 20 amino-acid long.

Both chemical (peptide ligand exposure) and spatial (nano particle spacing) cues were more thoroughly studied using the five chosen peptide ligands. Each of the peptide ligands was bound to the nano-patterns surfaces but this time 3 spaces were tested: 52 nm, 70 nm and 116 nm. In each case, the phenotypic response of the cells was measured; cell shape (spreading and elongation), FA morphology (area and length), and FA number in treated versus control cells were statistically compared.

The results specific to the chemical cues at 52 nm showed that 1 laminin peptide (sequence designation F-9) induced an increase in cell spreading (50%) and number of FA structures (100%) as compared to the control RGDfk peptide. Additionally, the fibrinogen peptide ligand (sequence designation P2) triggered a rare cluster phenotype.

When evaluating adhesion dependence upon the peptide ligand spacing, it was observed that the number of adherent cells decreased by 50% and 70% at 70nm and 116 nm respectively, as compared to 52nm-spaced nanopatterns. Similar decreasing trends were also observed in cell area, FA number and FA area. Only cell elongation and FA elongation seemed unaffected by peptide ligand spacing.

The study addresses the importance of ligands as active sites in cellular response producing specific changes in the cell cystoskeleton and FA, subjected by the ligand spacing. Such intrinsic phenotypes shed light on novel specific receptor-ligand interaction on cell shape.

As a final step, the identified peptide ligands were used to explore preliminary relationships between ECM molecule signaling and cell myogenesis and osteogenesis on 52 nm spaced nanopatterns. It is known that without any additional inducing factor, cell-cell contact between C2 cells induced differentiation to muscle fibers. These muscle fibers, or myofibers, were observed to be larger in area and length after 96 hours when the C2 myoblasts were cultured on laminin F-9 and fibrinogen P2 as compared to the RGDfk control. On the other hand, in response to the bone morphogenetic protein (BMP), osteogenic differentiation is induced and markers such as alkaline phosphatase ALP is detectable. Cells culture on Laminin F-9 produced an increase in ALP of 15% over both fibrinogen P2 and RGDfk, suggesting that laminin F-9 is an ECM peptide ligand that enhance osteogenesis in the presence of

BMP.

To conclude, a strategy for quantitative analysis of cell-matrix interactions is presented here. It is envisioned that this methodology will be beneficial in several biological fields: (i) in system biology for elucidating the biological functions of ECM adhesive sites and their role in the regulation of cytoskeleton assembly, as well as mechano-adhesive signaling, (ii) in drug development aimed at treating human diseases by identifying inhibitors and activators of cell adhesion, and (iii) in regenerative medicine by collecting adhesive ECM peptide ligands that provide a framework for understanding the environmental niches in which adult stem cells can adhere, proliferate, and differentiate.

Zusammenfassung der Dissertation

Die extrazelluläre Matrix (EZM) ist eine komplexe Struktur, welche Zellen im lebenden Organismus umschließt und unterstützt. Wenn Zellen an diese Mikroumgebung adhärieren, nehmen sie eine flache Form an, wobei durch Aktin-Myosin-Kontraktilität vermittelte intrazelluläre Spannungen entstehen. Die so erzeugten Kräfte beeinflussen die Bildung von sogenannten fokalen Adhäsionskontakten (FA). Diese lokalen mechanischen Kräfte an einem FA können eine globale Änderung der Zellform, Zellmigration, Genexpression, Zellproliferation und Zelldifferenzierung bewirken und entscheiden außerdem über das Zellüberleben. Aufgrund dieser vielfältigen Zusammenhänge sind FA sehr interessante Ansatzpunkte für die Medikamentenentwicklung und die Genforschung. Bislang ist nur wenig darüber bekannt, wie die eigentliche Signalübertragung an den Zell-EZM-Kontakten abläuft. Der Zelladhäsionsprozess wird durch die Anbindung und Clusterbildung von Proteinen in der Zellmembran, den Integrinen, an EZM-Proteine, wie z.B. Fibronektin, Vitronektin, Kollagen oder Laminin, vermittelt. Es ist bekannt, dass diese EZM-Proteine einzelne Peptidabschnitte enthalten, die das Zellverhalten beeinflussen können. In der vorliegenden Arbeit wurde die Wechselwirkung von Zellen mit verschiedenen EZM-Peptidliganden untersucht, um die Bedeutung dieser Beziehung für die Zelladhäsion und Zelldifferenzierung zu bestimmen.

Mit Hilfe der Immobilisierung von Peptiden auf funktionalisierten Oberflächen wurden Proteine in der EZM imitiert und deren Einfluss auf die Zellfunktionen charakterisiert. Die funktionalisierten Oberflächen bestehen aus im Nanometerbereich hexagonal angeordneten Goldpunkten auf Glasoberflächen, die spezifisch mit den gewünschten Peptiden funktionalisiert werden können und deren Abstand definiert eingestellt werden kann. Progenitor-C2-Zellen wurden speziell als Reporterzellen gewählt, da sie sich zu Knochen- oder Muskelzellen differenzieren können und ein gut dokumentiertes Modell zur Untersuchung der Zelldifferenzierung darstellen. Zur Quantifizierung der Zell-EZM-Wechselwirkung wurden C2-Zellen so moduliert, dass sie fluoreszierendes Paxillin exprimieren. Ein häufiges Protein, das mit FA assoziiert wird. Außerdem wurden die Zellädhäsionsexperimente auf den nanostrukturi-

erten Oberflächen zu einem zellbasierten, Multi-Parameter-Hochdurchsatzverfahren (HPTS) optimiert.

Mit Hilfe dieser HTPS-Plattform wurde bei einem festen Abstand der Goldpartikel von 52 nm, eine Peptidbibliothek (Perturbation) aus 33 verschiedenen EZM-Peptiden von Fibrinogen, Teskanin, Kollagen, Fibronektin und Laminin untersucht. Das Screening sortierte die Reaktion der C2-Zellen auf Basis der quantitativen Analyse der Zellhaftung und einer qualitativen Einordnung des Phänotyps. Aus dieser Bibliothek wurden fünf Kandidaten für Adhäsionspeptidliganden (drei Laminine, ein Fibronektin und ein Fibrinogen) ausgewählt und zwar aufgrund ihrer Fähigkeit eine deutliche phänotypische Veränderung der Zellen hervorzurufen im Gegensatz zu den Kontrollpeptidliganden RGDfK. Die fünf ausgewählten Peptide haben alle eine lineare Struktur, sind nur 20 Aminosäuren lang und enthalten keine RGD-Sequenz.

Sowohl chemische (Exposition der Peptidliganden) als auch räumliche (Abstand der Nanopartikel) Signale wurden mit Hilfe der fünf ausgewählten Peptidliganden genauer untersucht. Jeder Peptidligand war an die nanostrukturierten Oberflächen gebunden und es wurden drei Abstände getestet: 52 nm, 70 nm und 116 nm. Jedes Mal wurde die phänotypische Reaktion der Zellen im Hinblick auf Zellform (Ausbreitung und Dehnung), FA-Morphologie (Fläche und Länge) untersucht und die FA-Anzahl bei behandelten Zellen und Kontrollzellen statistisch verglichen.

Die Ergebnisse zeigten, dass die chemischen Signale bei einem Abstand von 52 nm bei einem Lamininpeptid (Sequenzbezeichung F-9) eine Zunahme der Zellausbreitung (50%) und der Anzahl der FA-Strukturen (100%) bewirken gegenüber dem Kontrollpeptid RGDfK. Außerdem führte ein Fibrinogen-Peptidligand (Sequenzbezeichnung P2) zu einem seltenen Clusterphänotyp.

Bei der Auswertung der Adhäsionsabhängigkeit vom Abstand der Peptidliganden konnte beobachtet werden, dass die Anzahl der adhärierenden Zellen um 50% bei 70 nm und um 70% bei 116 nm abnahm im Gegensatz zu den mit 52 nm strukturierten Oberflächen. Eine ähnlich abnehmende Tendenz zeigte sich auch bei der Zellfläche, FA-Anzahl und FA-Fläche. Nur die Zelldehnung und FA-Dehnung scheint vom Abstand der Peptidliganden nicht beeinflusst zu werden.

Die vorliegende Arbeit beschäftigt sich mit der aktiven Rolle von Liganden bei der Zellreaktion, die spezifische Veränderungen des Zellzytoskeletts und des FA bewirken in Abhängigkeit vom Ligandenabstand. Solche intrinsischen Phänotypen tragen dazu bei neue spezifische Rezeptor-Liganden-Wechselwirkungen im Hinblick auf die Zellform zu verstehen

In einem letzten Schritt wurde mit Hilfe der identifizierten Peptidliganden eine erste Beziehung zwischen der Signalübertragung von EZM-Molekülen und der Zellmyogenese und Osteogenese auf mit 52 nm strukturierten Oberflächen untersucht. Es ist

bekannt, dass ohne zusätzlichen auslösenden Faktor, der Kontakt von Zelle zu Zelle zwischen C2-Zellen eine Differenzierung zu Muskelfasern bewirkt. Diese Muskelfasern oder Myofasern wiesen eine größere Fläche und Länge nach 96 Stunden auf, wenn die C2-Myoblasten auf Laminin F-9 und Fibrinogen P2 kultiviert wurden, verglichen mit dem Kontroll-RGDfK. Das Potenzial der C2-Zellen in Osteoblasten zu differenzieren wurde untersucht, indem nach Zugabe von Knochen-morphogenetischem Protein (BMP) die Aktivierung osteogener Marker wie der alkalischen Phosphatase (ALP) detektiert wurde. Zellkulturen auf Laminin F-9 erzeugten einen Anstieg von ALP von 15% gegenüber sowohl Fibrinogen P2 als auch RGDfK. Daraus lässt sich schließen, dass Laminin F-9 ein EZM-Peptidligand ist, der die Osteogenese bei Zugabe von BMP fördert.

In der vorliegenden Arbeit wird eine Methode zur quantitativen Auswertung der Zell-EZM-Wechselwirkung vorgestellt. Mit Hilfe dieser Methode könnten verschiedene Fragestellungen aus mehreren biologischen Forschungsgebieten untersucht werden: (i) In der Systembiologie, um einen Einblick in die biologische Funktion der EZM-Adhäsionsstellen und deren Rolle bei der Zytoskelettregulation sowie der mechanisch-adhäsiven Signalübertragung zu erhalten. (ii) In der Medikamentenentwicklung, zur Behandlung von Krankheiten durch Identifizieren der Inhibitoren und Aktivatoren der Zelladhäsion. (iii) In der regenerativen Medizin, indem adhäsive EZM-Peptidliganden erfasst werden, um so die Nischen, in denen adulte Stammzellen adhärieren, proliferieren und sich differenzieren können, besser verstehen zu können.

Chapter 1

Introduction

1.1 Elucidating cellular environments

Multicellular organisms are constituted of specialized tissues. From prokaryotes to multicellular organisms, a cell can sense and respond to a wide range of external signals. Cells require exposure to many factors from their environment in order to function properly: cell adhesion to other cells, soluble factors and physical-chemical attachment to the extracellular matrix (ECM) [169].

The ECM is a well organized network of proteins, complex in composition and specific to the tissue functionality, supporting the cells that inhabit it. In mammals, the ECM is commonly present in the connective tissues such as cartilage, bone or the skin. Interestingly, ECM proteins contain domains (peptide ligands) that can influence cell behavior. Receptors located on the surface of a cell can recognize such domains that can function as their counterparts (ligand; key lock principle)[141]. The extracellular membrane bound receptors on cells, posses dimensions down to nanoscale size.

Cells of the connective tissue, if they are not adherent, have a spherical shape and diffuse cytoskeleton. Upon adhesion, the cells spread out on the supporting substrate, generating intracellular tension in the process. The cells do not adhere over the whole surface, but only in certain points, the so called focal adhesion plaques. These "sites" are termed focal contacts or focal adhesions (FA) and provide a structural link to the actin cytoskeleton [204] . The "local" generation of mechanical force in FA causes "global" changes in cell shape and motility , modulating gene expression [23] and producing changes in cell proliferation, differentiation and survival.

The process of cell adhesion is mediated mainly through engagement of transmembrane integrins by extracellular matrix ligands (present in fibronectin, vitronectin,

collagen and laminin) [179]. Focal adhesion sites of attachment to the ECM, are mainly induced by clustering of integrins, that are directly involved in propagating extracellular signals ([52]).

The complex interplay between the mechanical role of cell adhesions and their 'intructive role' which is manifested by the activation of a wide variety of signalling networks, is mediated by a group of proteins known as the "adhesome" [201]. The updated adhesome network includes 180 integrin mediated cell-ECM adhesion components [201]. The sensory machinery or adhesome is constituted of adhesion receptors, adaptors, actin regulators and the associated cytoskeleton. The number of direct interactions reported between these components (180 nodes) is at least 742 in the integrin adhesion network only.

To summarize, cells exist in a complex microenvironment in which they must adapt and react to cues present in their surroundings. While much effort has been dedicated to understand the cellular response to soluble signals, less is known about how cells mechanically sense and transduce signals both chemical and physical. Comprehensive understanding of adhesion-mediated signaling requires characterization of (i) the sensory machinery of the cell and (ii) the sensed surface [51].

Much effort has been invested to engineer surfaces that mimic and contain native ECM proteins. However, a mixture of proteins with random unfolding, orientation and conformational states presents a divergence from natural, intentionally arranged protein layers. Immobilization of entire native proteins to surfaces can provide many functions because of the various domains within the molecule.

An alternative approach is using peptides instead of complete proteins. This approach allows a more specific investigation of the interaction and the effect of specific domains in the ECM proteins. Peptides based on the primary structure of the receptor binding domain of an entire protein such as RGD from fibronectin (FN), aim to target specific cellular interactions. Displaying short peptides appeared to enhance the availability and activity of receptor binding domains as compared with presenting the entire native protein [102].

Which ligands and which receptors are involved in the regulation of cytoskeletal assembly, force transduction and signaling activities? At what spatial resolution does adhesion mediated signaling occur? How to integrate and interpret, collected FA information about the chemical and physical properties of the cell's environment triggering long range signalling responses? [190].

Moreover, the mechanisms that regulate cell differentiation, include both autonomous (stem cell intrinsic) and non-cell-autonomous (microenviroment / epigenetic) components. The microenviroment regulates the maintenance of stem cell and progenitor pools, through extrinsic and intrinsic factors, creating niches [76]

[156] [146]. How can we develop a strategy to elucidate environments, such as stem cell niches to gain information on the ECM components that regulate adhesion and differentiation?

To investigate these open questions in cellular adhesion, system biology studies require large data sets on multiple conditions with profiling of many samples. Recently, high-throughput screening and high-resolution light-microscopy have been established as a combined platform methodology for characterizing cellular phenotypes [93] [135] [134]. The pipeline analysis consist on the quantification of multiple subcellular features (for example structure and organization of focal adhesions) and statistical comparisons of their distributions in treated vs. control cells [134].

The development of advanced perturbation techniques such as surface nanoengineering has opened up new possibilities for the systematic modulation of individual surface features. Multiple parameters include ECM specificity, adhesive ligand density, surface compliance and dimensionality [51].

The sensory machinery of the cell has been explored by screening (i) a chemical library of combinatorial natural products [134] and (ii) by siRNA technology [189] as perturbations targeting focal adhesions as pivotal adhesion structures in adhesion-mediated signaling. However, surface ECM components as ligand-receptor perturbations have not been explored as input variabled to study the epigenetic variables in FA formation, cell adhesion behavior or signaling.

1.2 Aims

Elucidating the surface cues that mediate affinity to ECM is of central importance for a wide variety of biological processes such as differentiation, cytoskeletal organization, cell migration and adhesion-signaling. This thesis will describe:

1. The design of a screening platform and how it is used to screen a library of ECM ligands as chemical and physical perturbations.

2. The use of the screen to identify spatial cues and target ECM ligands peptides that produce significant cytoskeletal changes.

3. The use of the chosen ligands to further study the effect of ECM upon cell differentiation on muscle skeletal C2 progenitor cells.

Chapter 2

Literature review

2.1 The extra cellular matrix (ECM)

In living systems, the extracellular matrix (ECM) is a complex network of proteins that confine and support cells. In mammals, the ECM is commonly present in the connective tissues such as cartilage, bone or the skin. Variations in the organization and quantity of the ECM components change the type and form of the ECM. The ECM is produced and maintained by the cells within specific tissues. The proteins within the ECM can be classified according to their function and structure [3].

The most important class is the *structural class* of ECM proteins. It contains to a large extent the collagen and elastin families of proteins. The role of collagen fibers is to strength and organize the matrix; while elastin fibers give flexibility and resilience. The *adhesive class* plays an integral role within the ECM matrix and includes fibronectin, laminin, and tenascin. These proteins mediate cell attachment and form crosslinks within the matrix. Last but no least, the *stabilizer class* consisting of proteoglycans and heparan sulfate containing proteins. They form a highly hydrated gel-like mixture within the aqueous microenvironment of the ECM. Proteoglycans interact with several components including: hyalunoran, lectins, and numerous growth factors and cell surface receptors. Figure 2.1 illustrates the main components of the ECM .

Interestingly, cells recognized specific ECM components and cell adhesion molecules (CAM). Such proteins have been demonstrated to contain domains that can influence cell behavior[159]. Receptors located on the surface of a cell can recognize such domains that can function as their counterparts (ligand; key lock principle)[141].

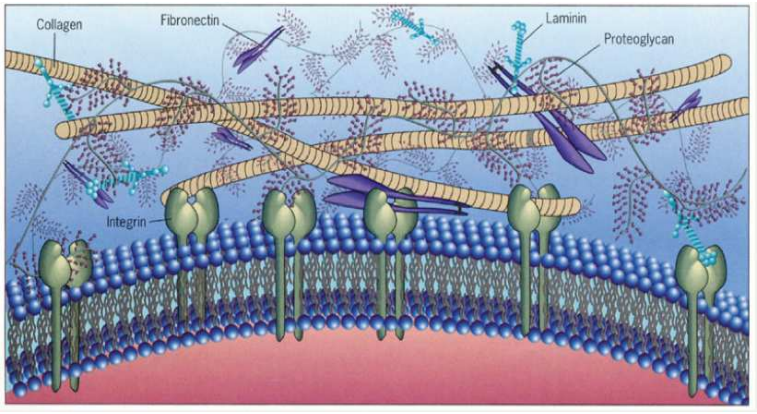

Figure 2.1: Main components of the extracellular matrix.

2.1.1 Collagens

The collagen family is the main protein component of connective tissues and basement membrane. Its often responsible for the rigidity or flexibility of structures, compartmentalization, and cellular restriction. Known collagen types (of which there are 19) contain repeating-Gly-X-Y-sequences [145], and can be classed on the basis of structural features. The most abundant are fibril-forming (types I, II, III, V and XI) collagens, which together with network-forming (types IV, VIII and X), are the fundamental cell adhesive collagens [3].

2.1.2 Fibronectin

Fibronectin (FN) is found primarily as dimers in blood and as high multimers in the insoluble ECM [73][119] [133]. Each monomer is composed of three different types of homologous repeating units. FN contains 12 type I repeats, two type II repaets and 15-17 type III repeats. In addition, one particular region, designated IIICS (also known as V region), can be inserted intact or in part by alternative splicing.

Fibronectin can be ligand for a dozen members of the integrin receptor family [142]. The best known minimal integrin-recognition sequence is *RGD* in the FN repeat III10 [141][196]. Next to this tripeptide, in the ninth type III repeat (III9), the sequence *PHSRN* promotes specific $\alpha_4\beta_1$ binding to fibronectin [40][128] [6][124]. PHSRN is known as synergy site, because it works in cooperation with RGD.

Independently from the RGD, two peptides sequences with cell adhesive activity are *LDV* near the amino terminus and *REDV* near the the carboxy-terminus [71].

Both of them are recognized by the $\alpha_4\beta_1$ integrin [121] [59] and by the $\alpha_4\beta_7$ integrin [133]. These sequence are located in the alternatively spliced IIICS or V region [70, 71][133].

Also recognized by $\alpha_4\beta_1$ integrin are the sequences *IDAPS* and *KLDAPT*. They are located in repeats III4 and III5, respectively (the later also binds to $\alpha_4\beta_7$ integrin). Another adhesive sequence of interest is *EDGIHEL* located within the alternated spliced EDA. It binds to $\alpha_4\beta_1$ as well as $\alpha_9\beta_1$ and has been reported to play a role during wound healing [92].

2.1.3 Laminin

Laminin (LN) is a the main component of the basement membrane. The basement membrane is a thin sheet-like ECM underlying epithelia and endothelia and surrounding muscle, adipose and peripheral nerve cells, essential for tissue formation in early development and in adult tissue. LN promote neurite outgrowth, tumor metastasis, and angiogenesis [113] [200]

The old nomenclature refers to three polypeptides chains, A, B1, and B2 [108]. In an update nomenclature, these chains a reassigned to three non identical polypeptide chains as α, β, and γ respectively [22]. There are 16 laminin isoforms that can be named combinations of five α, three β, and three γ (γ1-γ3) [113] [22] [137]. A simplified nomenclature is summarize in figure 2.2. For example, LN trimers can be name on the basis of chain composition $\alpha5\beta1\gamma1$ or in an abbreviate manner 511 instead of laminin-10 [8].

Cell adhesion regions of laminin include an RGD sequence on the amino-terminal half of the α chain; and a Tyr-Ile-Gly-Ser-Arg (YIGSR) sequence on the β chain, that promotes adhesion and migration, modulates morphological differentiation and inhibits angiogenesis and tumor growth [56].

A third cell adhesive site, with the sequence Ser-Ile-Lys-Val-Ala-Val (SIKVAV), is found near the carboxy terminus of the α chain. In vitro, SIKVAV induces neurite outgrowth, and formation of tubelike networks by endothelial cells. In vivo it enhances tumor cell growth, metastasis,and angiogenesis [172][57].

Cell morphology was altered by the addition of active laminin-derived synthetic peptides, YIGSR-NH2 and CSRARKQAASIKVAVSADR-NH2, but not by an active RGD-containing peptide. When coated directly on plastic, all three peptides promoted cell adhesion, demonstrating that bone cells interact with specific molecular domains of laminin. These data demonstrate that basement membrane plays a key role in formation of a network of cytoplasmic processes resembling the osteocyte canalicular network in bone [184].

Nomenclature of 16 laminins

Standard	Abbreviated	Previous
α1β1γ1	111	1
α2β1γ1	211	2
α1β2γ1	121	3
α2β2γ1	221	4
α3Aβ3γ2	332, or 3A32	5, or 5A
α3Bβ3γ2	3B32	5B
α3Aβ1γ1	311, or 3A11	6, or 6A
α3Aβ2γ1	321, or 3A21	7, or 7A
α4β1γ1	411	8
α4β2γ1	421	9
α5β1γ1	511	10
α5β2γ1	521	11
α2β1γ3	213	12
α4β2γ3	423	14
α5β2γ2	522	–
α5β2γ3	523	15

Figure 2.2: Simplified laminin nomenclature, adapted from [8].

Laminin-based peptides, such as the adhesion ligand YIGSR have been used to promote cell spreading and stress fiber formation when its conformation was constrain by covalent inmobilization through glycine residues at the N terminus [103] [25]

2.1.4 Tenascin

Tenascin with both adhesive and anti-adhesive properties, is transiently expressed in many developing organs such as connective tissues, epithelial organs, and also the central and peripheral nervous systems. Tenascin has a distinctive hexabrachion (six-armed) structure [29]. Each arm in this structure is a single polypeptide folded into an irregular series of independent globular domains. The globular domains in each arm can be separated into EGF-like (epidermal growth factor), FN-III (fibronectin type III) and FBG (fibrinogen). There are of four types of tenascin: tenascin-C, X, R and W [178]. Two types of tenascins (tenascin-C and tenascin-W) are significantly regulated by the tissue microenvironment. The distinctive and highly regulated expression of tenascin has provoked interest in trying to identify possible functions of tenascin in cell-cell and cell-substrate adhesion, cell migration, growth, and cell differentiation [178] [3].

2.1.5 Proteoglycans

Proteoglycans belong to large family of complex macromolecules with more than 40 different members. They are mainly, but not exclusively, located at the cell membrane and within the extra-cellular matrices of most vascular tissues.

Proteoglycans have been categorized and named depending on their distribution, biochemical structure, and, when possible, their function [74]. They consist of a protein core to which is attached one or more glycosaminoglycan (GAG) side chains. The later are covalently attached to the protein backbone, usually via serine residues, although keratan sulfate has been shown to coupled to asparagine residues [48]. The major types of GAG chains that have been isolated and characterized include chondroitin sulfate (CS), desmartan sulfate (DS), keratan sulfate (KS), hyaluronic acid (HA), heparan sulfate (HS), and heparin (He). Each type of GAG chain has a distinctive polymeric structure in which the repeat disacharides are linked by certain bonds [49].

Proteoglycans play a role in ECM organization and composition since it binds to many ECM proteins. As a receptor heparan sulfate proteoglycans bind, via their sulfated glycosaminoglycans chains, to ECM proteins such as fibronectin, laminin, collagen, and trombospondin [110] [38] [12].

2.1.6 Fibrinogen

Fibrin(ogen) (FG) is a protein produced by the liver.This protein operate by helping blood clots to form. It provides scaffold for the intravascular thrombus and also accounts for clot viscoelastic properties. FG molecules are comprised of two sets of disulfide Aα, Bβ, and γchains. Each molecule contains two outer D domains connected to a central E domain by a coiled-coil segment [118]. Fibrin(ogen) participates in biological functions involving unique binding sites, such as leukocyte binding to FG via integrin alpha(M)beta2 (Mac-1) [180, 195]. [94].

2.2 Cell cytoskeleton and focal adhesion (FA) signalling

The cytoskeleton gives structure to the cell, allows for a segregation of cellular compartments (for instance in cell division), exerts mechanical tension on the surroundings (wound healing) and is fundamental for cell motility [55]. It is composed of three groups of proteins: the micro-filaments wich consist of actin, the microtubuli and the intermediate signals.

Cells of the connective tissue, if they are not adherent, have a spherical shape and a diffuse cytoskeleton. Upon adhesion, the cells grow increasingly flat and spread out on the supporting substrate, generating a certain intracellular tension in the process.

Mechanical forces are generated by the associated polymerizing actin or by actomyosin - driven contractility. The local generation of mechanical force causes global changes in cell shape and motility , modulating gene expression [23] and producing changes cell proliferation, differentiation and survival.

The process of cell adhesion is mediated mainly through engagement of transmembrane integrins by extracellular matrix ligands (fibronectin, vitronectin, collagen and laminin) [179]. The cells do not adhere over the whole surface, but only in certain points, the so called focal adhesion plaques. These "sites" are termed focal contacts or focal adhesions and provide a structural link to the actin cytoskeleton (figure 2.3) [204].

There are a variety adhesion contacts, including focal complexes (FC), focal adhesions (FA), fibrillar adhesions (FB) and podosomes. These sites of attachment to the ECM, are mainly induced by clustering of integrins, that are directly involve in propagating extracellular signals ([52]).

In this manner, clustering of integrins leads to their activation and results in several intracellular signal events (i) activation of phosphorilation and G-protein mediated pathways (ii) pH and calcium level changes (iii) activation of the mitogen-activated protein kinase (MAPK) cascade [179].

Nascent Focal adhesions normally develop into mature focal adhesions as a consequence of the activation of Rho [32] and recruit intermediate proteins such as Vinculin, Paxillin and Talin [204].

Among FA components, talin seems to form the most important link between the cytoplasmic portion of beta-integrin and the actin filament. it is also required for integrin activation [186] and FA formation [206].

Paxillin is a 559 amino acid protein (68kd) considered a molecular adaptor. Paxillin phosphorilation has long been associated with the cordinate formation of focal adhesions and stress fibers [149][58].

The complex interplay between the mechanical role of cell adhesions and their 'intructive role' which is manifested by the activation of a wide variety of signalling networks, is mediated by a group of proteins collectively known as adhesome [201]. The adhesome provide a structural link and reorganisation to the actin cytoskeleton or are directly involved in propagating extracellular. To date more than 180 focal adhesion-associated molecules have been located at the interface between the transmembrane adhesion receptors, and the actin cytoskeleton signals[202] [201].

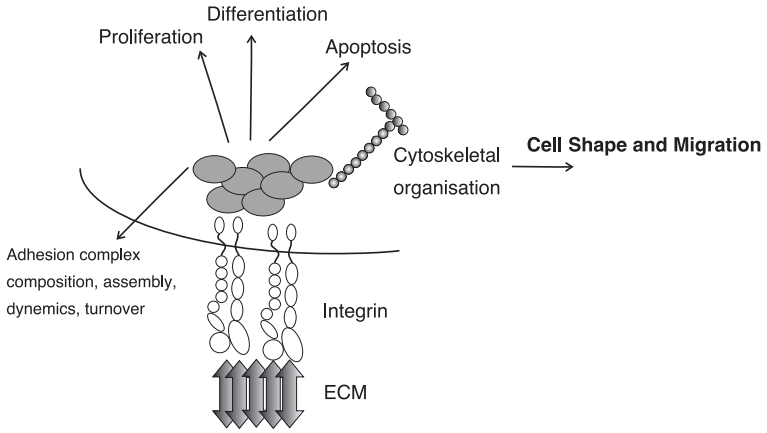

Figure 2.3: Assembly between integrin and the ECM organizes the cytoskeleton which controls cell shape, polarity and migration. Recruitment of adaptors and signaling enzymes controls proliferation, apoptosis and diffenrentiation. Adapted from [169].

2.2.1 Integrins and other receptors systems

The cell-surface receptors that mediate cell-ECM adhesion are primarily members of two gene families - the integrins and the syndecans.

Integrins are hetero-dimers of alfa and beta subunits, that contain a large extracellular domain responsible for ligand binding (figure 2.4). In mammals 18 alpha and 8 beta integrin genes encode polypeptides that combine to form 24 alpha-beta receptors [72]. The exact subunit combination of these dictates the binding specificity of the integrin to different ECM components. A specific ECM molecule can nevertheless be bound by different types of integrins, and specific integrins can bind to different types of ECM molecules [204]. Integrin diversity is increased further through the expression of intra and extracellular splice variants for several subchains. The β_1 integrin family forms the largest group of integrin receptors for extracellular matrix proteins [105].

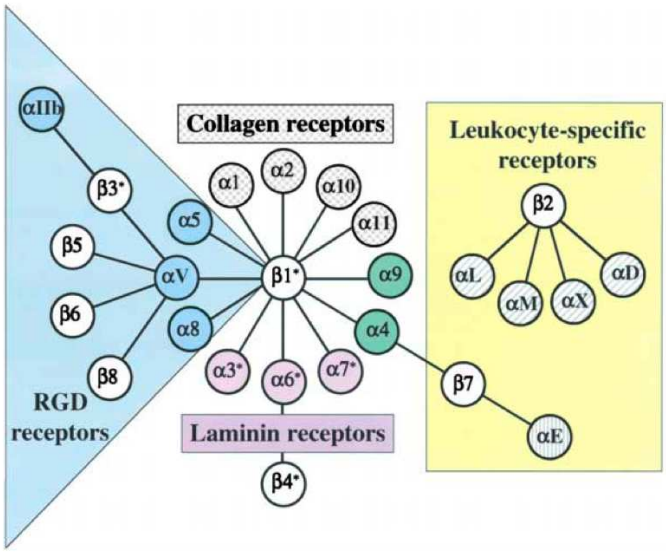

Figure 2.4: The integrin receptor family. In mammals 18 alpha and 8 beta integrin genes encode polypeptides that combine to form 24 alpha-beta receptors. Adapted from [72].

Central to the process of cell adhesion is integrin clustering [169]. This occurs through integrin aggregation co-ordinated by: (i) close proximity or periodicity of ligand binding sites within the crosslinked matrix of ECM molecules; (ii) lateral associations of integrins ([91, 41, 65]) and (iii) interactions between integrin cytodomains

via structural dimers (e.g talin) [207] [169].

In addition to integrins, several membrane molecules have been reported to be localized at focal contacts, including proteoglycans [204]. Syndecans are a family of membrane-intercalated proteoglycans, each comprising a protein core with covalently attached heparan sulphate (HS) or glycosaminoglycan sugar chains (GAG).There are four members of the syndecan family in mammals (figure 2.5), of which three (syndecan 1, 2 and 3) have a restricted tissue distribution — the fourth (syndecan 4) is expressed ubiquitously. Syndecan 4 encompasses a binding site for protein kinase Cα (PKCα) that is primary focus of investigation into syndecan signalling.

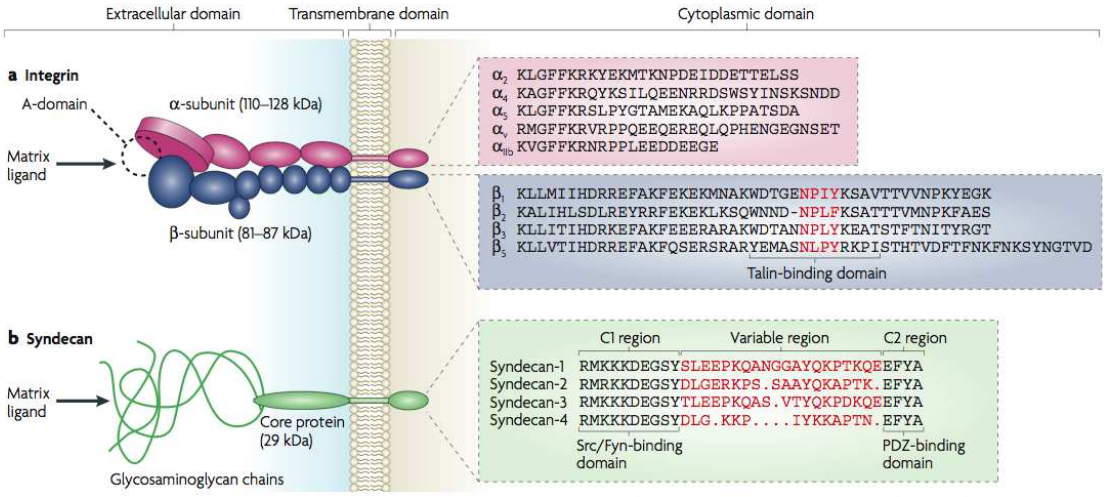

Figure 2.5: Domain Structures of Integrin and Syndecans. Adapted from [116].

The syndecans act as receptors for ECM proteins and growth factors, engaging ligands through the large flexible GAG chains that make them ideal receptors for ligands that are dilute or distant from the membrane.

There is substantial evidence that a cell-adhesion response requires engagement of both types of receptors, integrins and proteoglycans. Although mechanisms of direct receptor crosstalk have not yet been identified, *in vitro* analyses have demonstrated clear synergy between signalling cascades downstream of the two families [116] [169].

There are reports presenting that the protein cores of the extracellular domains of syndecans themselves act as integrin ligands [188, 107, 10]. This might represent an alternative mechanism of receptor cooperation, although this has not yet been investigated in depth.

Integrins also colocalize and coprecipitate with several growth factor receptors, for example the epidermal growth factor receptor (EGFR). The close physical proximity of adhesion and GF molecules facilitates such coordination [179].

2.2.2 Adhesome: actin-integrin linking proteins

The adhesome is a group of proteins that mediates the activation of a wide variety of signalling networks; as a consequence of the complex mechanical interaction between cell adhesion and their environment.

The update adhesome network include 180 integrin mediated cell-ECM adhesion components [201]. The integrin adhesome is constituted of adhesion receptors, adaptors, actin regulators and the associated cytoskeleton.

On the cytoplasmic side of the adhesion sites, integrins can interact with at least 12 different adaptor proteins [202]. Among these molecules five of them provide a direct link to the actin cytoskeleton. These molecules are tensin (TNSI), filamin (FLNA), talin (TLN1), plectin (PLEC1) and α actinin. Alternatively, plectin may interact with the intermediate protein Paxillin (PXN) and link to microtubules.

Link to the cytoskeleton is further reinforce, by a second and third level of adaptor molecules, with the purpose to stabilize the adhesome network and connect to various filament systems of the cell [201].

The number of direct interactions reported between these components (180 nodes) is at least 742 only in the integrin adhesion network. The interactions between components of the adhesome is recently discuss in detail in several excellent reviews [202] [201]. Adhesome components, with its know interactions can be review as an interactive map at www.awesome.org.

The role of talin

Talin has a special role as it binds to the cytoplasmic domain of β integrin subunit. It triggers the transition of the entire αintegrin and βintegrin dimer from an inactive to an active conformation that is capable of high afinity interactions with ECM ligands [170][9][51]

However the exclusive binding of talin seems to be insufficient for complete integrin activation. According to recent research, kindlin 2 and 3 are neccesary for maximal integrin activations [115][117][97]. The coordinated effect of talin and kindlin on both integrin activation an on the subsequent assembly of FA is additionally enhance by mechanical forces from the cytoskeleton [51].

Paxillin and focal adhesions

In cell based adhesion screens, cell lines usually target fluorescent Paxillin as a prominent component in FA complex [135] [134] [189]. Paxillin is an intermediate protein in FA development . The 559 amino acid protein (68kd) is considered a molecular

adaptor or scaffold protein. It is a highly conserved protein between species, with 90% identity between chicken and humans.

Paxillin contains 2 structural domains (i) the amino terminus which contains SH3 and SH2 binding domains and (ii) the carboxyl terminus which consist of four LIM domains (Lin-11, IS1-1, Mec3, LIM1-4). Paxillin is a cellular target for tyrosin kinases that are activated as a result of integrin signalling after either cell adhesion or stimulation of quiescent cells with soluble growth factors and cytokine [179].

Paxillin phosphorilation has long been associated with the cordinate formation of focal adhesions and stress fibers [149][58]. Signaling culminate in changes in cell shape, and motility and gene expression [179].

2.2.3 Nascent adhesions, maturation and disassembly of focal adhesions

Nascent focal adhesions evolve from initial (punctuate, dot like, focal complexes) at the cells leading edge into mature structures [14]. Nascent FA either disappear or rapidly grow centripetally, undergoing transition into elongated, mature FA's [190].

Nascent FAs (or focal complexes) are short live structures (in the order of seconds) [190] that appear as spots of 100 nm in diameter, and sometimes even smaller (30–40 nm) structures that contain integrin and some associated adhesion plaque proteins [51].

Among FA components, talin appears to be the main link between the cytoplasmic portion of beta-integrin and the actin filament. It is also necessary for integrin activation [186] and FA formation [206]. In addition to actin and beta integrin, talin binds another FA component, vinculin.

The "leading edge" of moving and spreading cells can be subdivided into peripheral "lamellipodium" and the internal "lamellar proper". Initial FA mainly form underneath the "lamellipodium" and appear as paxillin (or vinculin) positive dots [190]. The lamellipodia is described as thin, flat, cellular extensions.

Transition from nascent to mature FA creates a symetry break in the FA structure. An elongated polar structure with a distal tip (toe) and proximal end (heel) associated with the growing actin bundle, emerges [190].

The maturation of focal adhesion progress in a centripetal direction, from the initial adhesion (toe)toward the cell center (heel), correlating with the centripetal direction of actin flow [4]. Mature focal adhesions are elongated and localized at the termini of stress fibres. Stress fibres consist of actin filament bundles that contain a multitude of accessory proteins. The cross-linker α-actinin, along with myosinII, are among the first proteins to appear in the actin filament bundle growing from the

heel portion of the maturing FA [30]

The formation and further growth of focal adhesions depend on myosin II and, particularly, on myosin IIA [51]. Experiments with RNAi mediated knockdown of myosin II isoforms revealed that myosinIIA plays a major role in FA growth and maintenance, at least in cultured fibroblasts and epithelial cells [190]. . MyosinIIA produces contractile forces via the stress fibers that focal adhesions experience continuous pulling forces, which they then transmit, through the associated integrins, to the ECM [51].

The interactions between integrin-mediated adhesion and actin cytoskeleton are bidirectional. The mechanical force by the actin system modulate FA assembly and maturation, while simultaneously the growing FA can regulate the assembly of the actin system [51]. The figure 2.6 illustrate the main stages of FA formation and maturation.

Once the maturation stage is complete, the FA adhesion within the lamella domain stop growing, remaining stationary for up to 10 minutes, and gradually disappear. *The disassembly of focal adhesions* is not completely understood. It is known that FA dis assembly can be trigger by any treatment interfering with myosinIIA driven contractility both in the presence and in the absence of microtubules [13].

While FA grow under tension centripetally 'toe-to-heel', the FA tend to fade upon mechanical relaxation in the opposite direction (heel to toe). FA organization is mainly driven by mechanical forces, actin along the interface between the cytoskeleton and the ECM attached membrane [190].

FA mechanosensory units corresponding to stretching forces by growth, and to relaxation by disassembly. On average the force required to maintain the FA is about 5nNper square micrometer [15] though some adhesions at the leading edge can experience stronger forces [11].

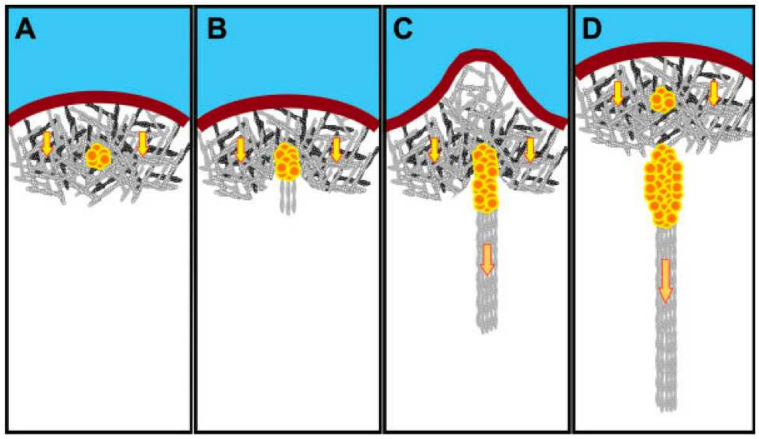

Figure 2.6: Cartoon illustrate the main stages of FA formation and maturation, and the parallel advancement of the boundary between the fast lamellipodium and the slow lamella domains. Formation of FAs is followed by the advance of the lamellipodium-lamella boundary. Maturation and elongation undergoes in the direction of flow. The substrate is label blue; the plasma membrane at the cell edge illustrate as a brown line. In orange-yellow circular "subunits" nascent and mature FAs. The lamellipodium is filled with a dense, branched network of actin filaments; yellow arrows symbolize the centripetal actin flow characteristic of that area. The forces generated by the actomyosin contraction in the stress fibers are indicated by arrows. The stress fibers are shown as actin filament bundles; cross-linking proteins and myosin-II are not shown.(A) Nascent focal adhesion underneath the branched actin network in the lamellipodium. (B) Early stage of FA maturation, formation of the precursor of a stress fiber (by filament nucleation and crosslinking) and appearance of a new border between the lamellipodium and the lamella. (C) Formation of a contractile stress fiber and force-dependent growth of FAs. Simultaneously, bulging of the lamellipodial protrusion just opposite the growing FA occurs. (D) The lamellipodial network moves forward due to FA-triggered disassembly and the assembly at the tip. The mature FA and the associated stress fiber continue to grow in the lamella, while a new, nascent adhesion appears in the lamellipodium. The sequence of events is based on references [4] [30] adapted from [190].

2.2.4 Mechano sensitivity of focal adhesions and signalling

FAs are also referred as mechanosensors do to its function. The network of interconnected molecules, respond cooperative to the internal mechanical forces applied by the actin system. Mechanical forces can also be induce externally, applying sheer stress or stretching the ECM matrix. In the early stage of FA assembly, mechanical force is necessary. The stress fibers associated with focal adhesions, grow and incorporate new components, mainly at the focal adhesion stress fiber interface [67].

The mechanical force developed by contractile stress fibers within the cell can (i) induce a local Ca+ influx near focal adhesions, (ii) produce the transition of β-integrin subunit from inactive to active conformation and also (iii) unfold or change the conformation of the ECM ligand fibronectin [51].

Focal adhesions and signalling

Signaling from FA to the cytoskeleton occurs via the Rho family GTPases. Primarily Rho and Rac are the main regulators in actin cytoskeleton function. The activation of Rho GTPases is mediated by guanine nucleotide exchange factors (GEF), which catalyze the exchange of GDP for GTP. The activation of Rac by matrix adhesion occurs also via a GEF known as DOCK180-ELMO complex [96]. This complex is activated by a pathway that involves the FA proteins paxillin and p130CAS both of which respond to mechanical stimulation [203].

In addition to GEFs, integrin adhesions also negatively regulate RhoA activity through GTPase activating proteins (GAPs).

The regulation activity and transduction of integrin signals to GEFs and GAPs is directed by other key elements. A well documented example is focal adhesion kinase (FAK) [176]. FAK can bind, phosphorylate and activate both GEF's and GAPs in cooperation with Src. Fundamental for the mechanosensory function of focal adhesions [51].

Paxillin phosphorilation has long been associated with the cordinate formation of focal adhesions and stress fibers [149][58]. Several paxillin binding proteins (FAK, Src and PAK) are pivotal in regulating gene expression through activation of various MAPK cascades. But tyrosene phosphorilation of paxillin is not required for localization of focal adhesions. Signaling culminate in changes in cell shape, and motility and gene expression [179].

2.3 Modeling microenviroments

Cells require exposure to many factors in order to function properly; physical attachment to the ECM (I) , soluble factors (II) but also cell adhesion to other cells (III) [169]. Cells exist in a complex microenviroment in which they must adapt and react to cues present in their surroundings. The mentioned factors interplay and regulate signaling cascades that govern many cell behaviors, including cell proliferation, apoptosis, polarity, motility and differentiation [81, 28, 15]. While much effort has been dedicated to understand the cellular response to soluble signals, less is known about how cells mechanically sense and transduce signals (mechano transduction).

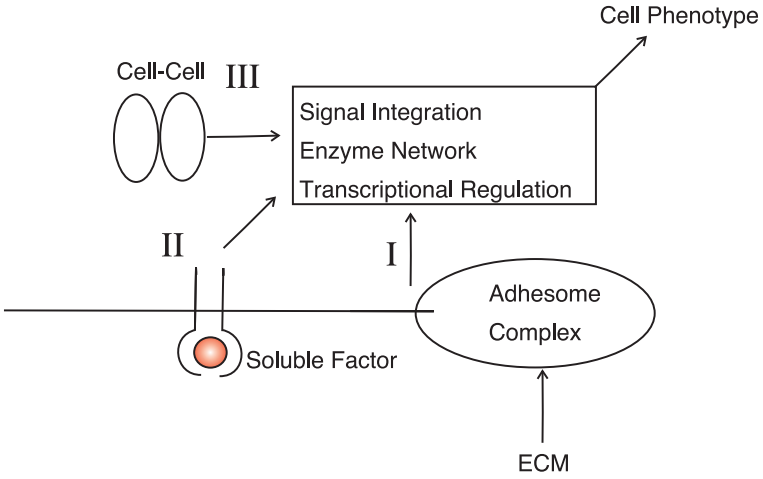

Figure 2.7: Soluble factors control development temporarily (II), but their signals are only interpreted by the cell in the context of integrin adhesion complexes (I), and cell-cell interactions (III), which together provide microenviromental checkpoints for cell fate (phenotype decisions). Adapted from [169].

2.3.1 Natural cellular environments

Natural ECM environments are structurally well organized, complex in composition and specific to the tissue functionality, with dimensions down to nanoscale size. For example, figure 2.8 shows the abundant interactions between a muscle cell and its associated basement membrane, mainly constituted of laminin. Cell associations occur at distinct sites every 10-25 nm, an enormous number of interactions when considered over the entire surface [109].

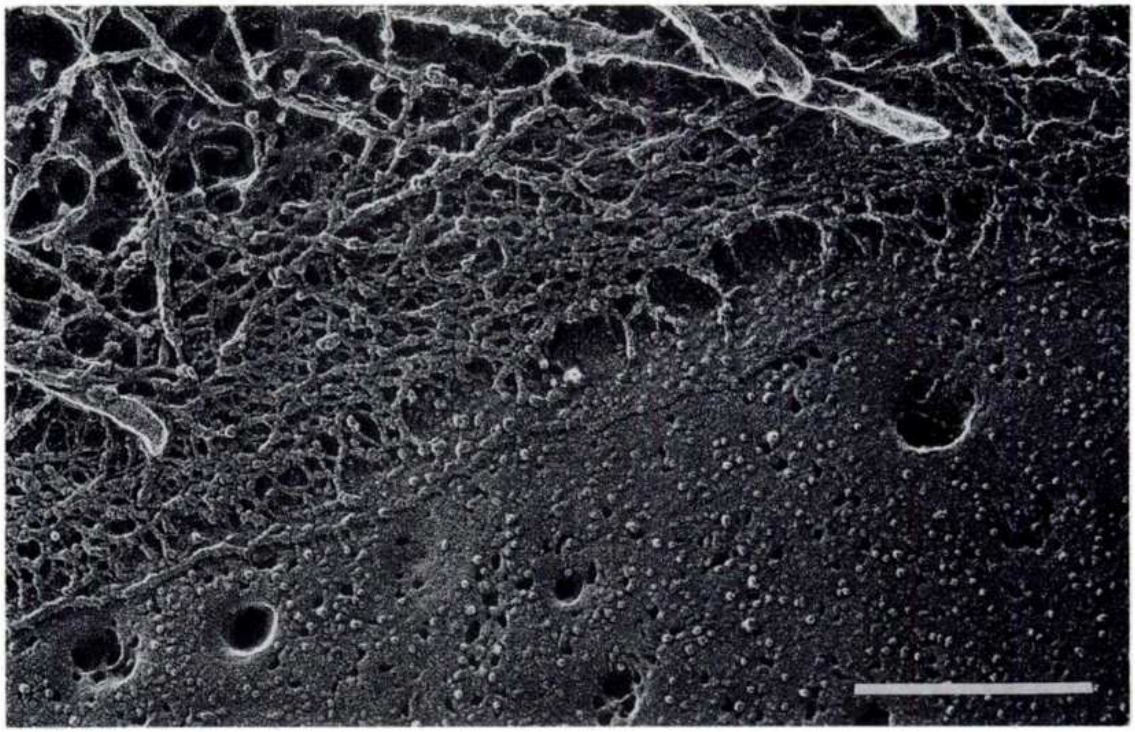

Figure 2.8: Quick-freeze, deep-etch micrograph of a muscle cell with its associated basement membrane. Cell matrix sites, presumably involving receptors for laminin, occur every 10-20nm. At the bottom of the figure, the external face of the membrane bilayer was fractured away. Bar=0.2 um. Adapted from [109].

Collagen also shows topographical and spatial cues that influence cell response such as adhesion and migration. *In vitro* studies on collagen determined self assembly conditions that mimic native collagen type I with its characteristic D-periodicity into fibers. Under specific pH conditions collagen self assembles onto atomically flat mica, possibly exposing collagen binding sites periodically and spatially distributed. Experiments have shown that fibroblast REF-52 cells migrate on these aligned collagen fibers when the surface displays D-periodicity (figure 2.9). In the absence of the 67nm structure the fibroblast do not migrate [143]. Further nanoscale details of such fibers reveal several sub nano-structures below 67nm in the collagen fibril [31].

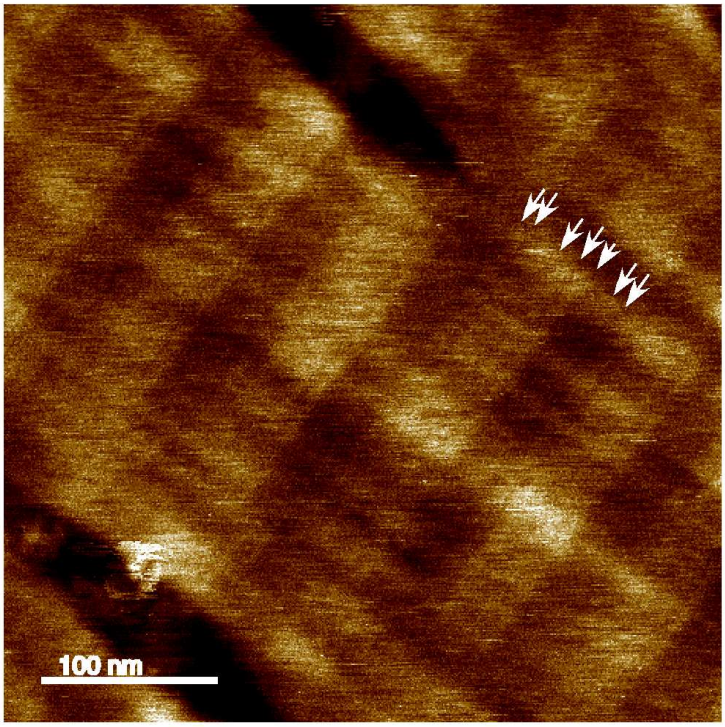

Figure 2.9: Atomic force microscopy (AFM) showing collagen type I with its characteristic 67 nm periodicity. Nanoscale details reveal several sub nano-structures below 67 nm in the collagen fibril. Adapted from master thesis: Carlos Hung 2005.

2.3.2 Engineered cellular environments

Much effort has been invested to engineer surfaces that mimic and contain native ECM proteins. However, an adsorbed mixture of proteins with random unfolding, orientation and conformational states presents a divergence from natural, intentionally arranged protein layers. Immobilization of entire native proteins to surfaces can provide many functions because of the various domains within the molecule [100].

An alternative approach is using peptides instead of complete proteins. Peptides based on the primary structure of the receptor binding domain of an entire protein such as RGD from fibronectin (FN), aim to target specific cellular interactions [100]. Displaying short peptides appeared to enhance the availability and activity of receptor binding domains as compared with presenting the entire native protein [102].

These peptides, whether linear or cyclic, can posses similar functionalities, for example, receptor specificity, binding affinity, and signaling of cell responses, as compared to their native proteins [68, 69].

Standard quantitative cell adhesion assays consist in the preparation of an adhesive substrate with extra cellular matrix ligands immobilized onto a solid support, plus non-adhesive molecules to block nonspecific interactions.

Most small protein fragments and synthetic peptides either do not absorb well to plastic or may not retain cell adhesion activity when absorbed [2][124] and therefore require covalent linkage to the surface to keep functionality.

One strategy is to bind peptides to glass via NH2-terminal primary amine [101] . Another widely used model with defined surface chemistries for studying adsorption of proteins and patterning of cells at surfaces is the self assembled monolayer (SAM's) [144] [78]. When sulfhydryl terminated hydrocarbons called alkanethiols are exposed to a surface of gold, they coordinate to the gold through the sulfur atom and self assemble in a molecular coating. In this way, molecules and peptides decorated with a thiol group can be easily bound to gold.

To prevent nonspecific components of adhesion, the non-adhesive protein (BSA) is a well established blocking method. Heat denatured BSA (1%), usually should allow attachment of 2-3% of most cells and 50-60% on the highest concentration of matrix protein in plastic cultures. Recent studies have shown that BSA works well in plastic, but in gold substrates thiol-PEGs methods are a better option [147].

The peptide surface concentration affects the adhesion. The more peptide you add in the buffer, the more peptide will be adsorbed in the substrate. This behavior is linear at low matrix protein concentrations and then reaches a plateau of maximal cell adhesion at high concentrations. Exaggerating the density of peptides on a surface can dramatically affect cell motility or inhibit cell adhesion. It is usually the best to select the lowest possible concentration of matrix protein that still yields maximal cell adhesion. Standard protocols dictate that the concetration dependence of adhesion should be determined experimentally for each cell type and each extracellular matrix protein ([3].

Most studies on immobilization of peptides in plain substrates not only assume that there is a linear peptide surface concentration, but also an equal and homogenous ligand distribution on the surface. Previous studies suggest peptide-to-peptide spacing of 440nm is required for $\alpha_V\beta_3$ mediated fibroblast cellular spreading, and 140 nm for focal contact (FC) and stress fiber formation [101, 102]. The results are based on various RGD surface densities obtained by controlling the concentration of peptide in the reaction buffer during the surface immobilization process.

Requirements

The design of engineered environments, requires a better strategy to control the peptide density. This imply the ability to create surfaces with define (i) patterned adhesive and non-adhesive regions such that placement and spreading of cells can be restricted and (ii) surface chemistry to control spatial and local physical cues. The clustering of integrins plays a pivotal role in cell behavior.

Over the last decade, several methods from micro to nanometer sized adhesive islands have been proposed to overcome unequal distribution of molecules onto surfaces [25]. For example, a method in the micrometer scale consist of coated islands in the range from 0.3-3 sq um and separated by 1-30 um are obtained by micro-contact printing. Protein adsorbs exclusively to the hydrophobic zones while the spaces in between are blocked with a protein resistant hydrophilic mono-layer [90].

Patterning methods at the micrometer scale do not allow exploring the relationships of integrin between adhesion site, size and distribution with control of integrin receptor clustering, while substrates patterned with ligands at the nanoscale level are suitable for addressing this aspect of cell interactions [25].

Nanotechnology aims to increase control over material structures of nanoscale size in at least one dimension (x,y,z)[175]. Nanoscale structures can be produced starting from a higher scale structures (top-down, miniaturization) or assembly of smaller structures (bottom-up).

Nanoscale bottom-up methods to address spatial organization and lateral distances of adhesive peptides upon cell adhesion and behavior include: star polymers [98], comb-shaped copolymers and [84] and nano-scale pattern islands using dip-pen nanolithography [89]. Such studies lead to the hypothesis that cell spreading might be dependent on critical densities of submicron integrin clusters to begin the recruitment of FA and cytoskeletal proteins in order to develop well formed actin stress fibers and mature FAs [25].

Nanopatterns

The role of local integrin density, which is critical for the initiation of mature and stable FA assembly was addressed for first time using a peptide pattern method based on diblock copolymer micellar lithography technology [53] [7] [166] [51]. This method allows the control of ligand density and spatial distribution, as well as the formation of non adhesive regions.

In these studies, dots coated with c(RGDfk) thiol peptides were positioned with high precision at 28, 58, 73 and 85nm distance from each other. The glass space between the gold dots was covered with poly(ethylene glycol) PEG via NH2 to glass

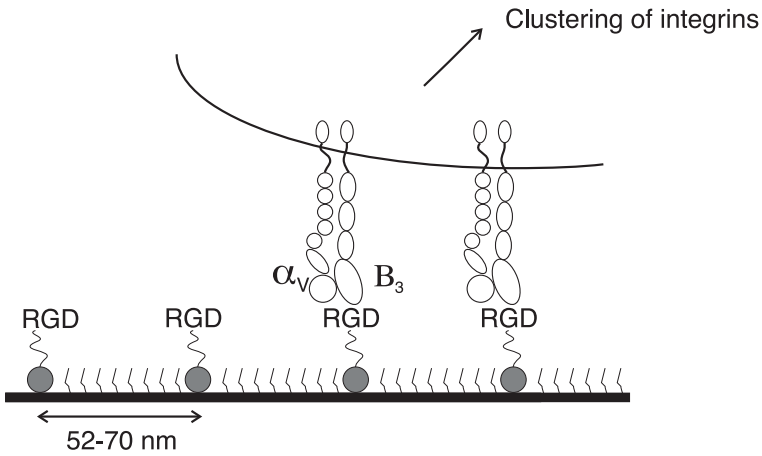

Figure 2.10: Spatial confinement and restriction of integrin clustering via $\alpha_V\beta_3$ receptor crucial for proper cell attachment and spreading. Adapted from [51].

to avoid unspecific protein interactions [16]. The size of the nanodots (< 8 nm) is small enough that only one integrin can bind to one gold dot. According to crystallography studies, the size of a single integrin receptors range from 9 to 12 nm [192]. RGD nanopatterns have been shown to promote cell adhesion via $\alpha_V\beta_3$ [24].

Earlier global density studies [101, 102] suggested that the critical separation for FA formation was 140 nm. In these studies however, a critical separation lenght of 73 nm between the adhesive dots is shown to dramatically reduce cell adhesion and spreading as well as the formation of focal adhesions in fibroblast REF52 cells [7].

This feature is not due to an insufficient number of ligand molecules, and not the total number of RGD functionalized nanoparticles, but rather the spatial confinement and the restriction of integrin clustering via $\alpha_V\beta_3$ receptors was crucial for proper cell attachment and spreading [7]. Figure 2.10 illustrate this finding.

Above the threshold of 73 nm, cells still form lamellipodia and spike-like structures but they lose the stability of their contacts to the surface and undergo major changes in shape and polarity [25]. Figure 2.11 plots the cell spreading dependence with ligand spacing. To form lamellipodia is not influenced by the distance between ECM ligands but the formation of stable contacts, and the maintenance of cell shape [26] and cell adhesion force [160].

The phenomena has been observed for a variety of cell lines: MC3T3-osteoblast, B16 melanocytes, REF52 fibroblasts, 3T3 fibroblasts. The range between 58-73nm is proposed to be the universal lenght scale for integrin clustering and activation.

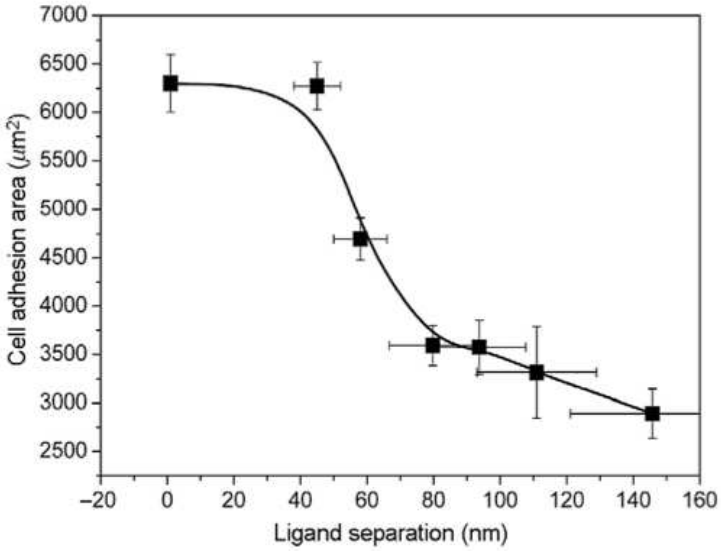

Figure 2.11: Cell spreading dependence with ligand spacing. Adapted from [166].

2.4 Stem cell niche

Two properties are required for a cell to be consider stem cell: self renewal and differentiation. Stem cells must be able to divide "indefinitely" keeping their undifferentiated state. And also, differentiate into specialize cells following a hierarchical and limited manner. According to their potency there are totipotent cells (fertilized egg), pluripotent cells (derived from the blastocyst embryo) and multipotent (adult stem cells in tissue, for example muscle satellite cells, hematopoietic stem cells and mesenchymal stem cells with the potential to give rise to cells from multiple, but a limited number of lineages).

Stem cell behaviour, in particular the balance between self-renewal and differentiation, is ultimately controlled by the integration of intrinsic factors with extrinsic cues supplied by the surrounding microenvironment, known as the stem cell niche [76]. Self-renewal and differentiation depends on restrictive niches [168] in which cells reside, which regulate differentiation and are as variable as the cells themselves.

The niche represents a defined anatomical compartment that provides signals to cells in the form of secreted and cell surface molecules to control the rate of proliferation, determine the fate of stem cell daughters, and protect the stem cells from exhaustion or death [156] [76].

The niches are specific to the tissue where the stem cells are located. For example, skeletal muscle stem cells, are found along the length of the myofibre, in close contact with the myofibre plasma membrane and beneath its basement membrane [76] [35][104].

One of the features of stem cell niches that are important for controlling stem cell behavior is cell-extracellular matrix adhesion. The ECM anchors stem cells within the niche in close proximity to self renewal and survival signals [76], maintain the niche architecture and control the frequency and nature of stem cell divisions [146].

2.5 Muscle skeletal tissue

There are three types of contractile muscle cells in the human body. Skeletal, cardial and smooth muscle cells. Skeletal muscle cells are associated with voluntary movements of the body. Muscles pull on bone to produce movement.

Skeletal muscle is a well organized tissue. It is composed of connective tissue (epimysium) and bundles of individual muscle cell fasciles. Each fascile is separated by a connective tissue layer referred to as perimysium. Within each fascile the muscle cells (also called muscle fibers) appear elongated, multinucleated and striated. The muscle fibers may contain 1000 myonuclei within the cytoplasm called sarcolema.

A third connective tissue layer (endomysium) is between muscles fibers, and electrically insulates the muscle cells from each other. The muscle cells are constituted of bundles of retractive filaments, so called myofibrils. Each myofibril subunit consists of myofibril actin and myosin heavy chain (MHC). Figure 2.12 illustrates the architecture and organisation of skeletal muscle.

All three connective tissue layers (epimysium, perimysium and endomysium) bind the muscle cells together, providing strength and support to the entire muscle. The connective tissue associated with skeletal muscle is merged at the end of the muscles, and prolonged to the tendons. The connective tissue associated with skeletal muscle is composed of ECM proteins and besides its structural role, the ECM plays a role in formation and regeneration of the skeletal muscle.

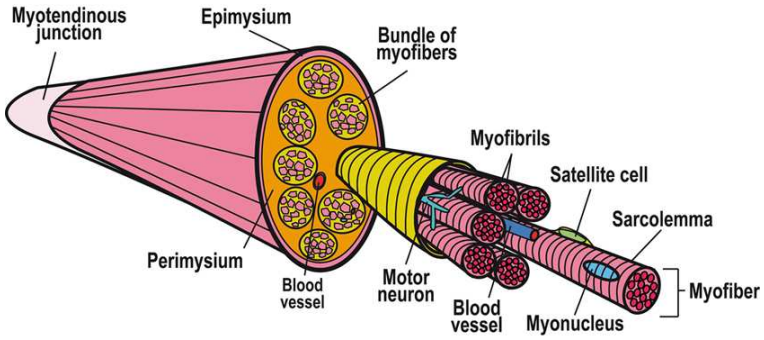

Figure 2.12: The anatomy of the skeletal muscle. The connective tissue layers (epimysium, perimysium and endomysium) bind the muscle cells together, providing strength and support to the entire muscle. The connective tissue is (i) merged at the end of the muscles, and prolonged to the tendons, (ii) composed of ECM proteins and besides its structural role, the ECM plays a role in formation and regeneration of the skeletal muscle. Adapted from [158].

2.5.1 Muscle satellite cells and tissue specific stem cells

Muscle is normally a stable tissue but, after injury regeneration occurs via the activation and proliferation of satellite cells to form a pool of myoblasts, which differentiate and fuse to replace or repair damaged myofibers [120] [162]. Satellite cells anatomically located beneath the basal lamina of myofibers [104], function as myogenic precursors for muscle growth and repair. However, when isolated from muscle and

grafted into injured tissue the myogenic activity was shown disappointing in early studies, perfoming poorly in comparison with true hematopoietic stem cell [136].

Recent studies hypothesized that the satellite cells population might consist of both true stem cells from the sub-laminal niche and other less proliferative progenitor cells from the interstitium. It has been shown that only a proportion of satellite cells with the marker Pax7 are "true" stem cells, and when transplanted they are capable of expanding their population (self-renewing) [36, 35]. Merely this small population function as stem cells, with the archetypal stem cell properties of (i) self-renewal and (ii) differentiation. These muscle adult stem cells eventually give rise to a pool of competent progeny (MPC's muscles progenitor cells or myoblasts) that fuse extensively to form myotubes and generate new myofibers repopulating irradiated damaged muscle.

2.5.2 Progenitor cells and multipotency

Skeletal muscle development and regeneration occurs via the activation and proliferation of muscle satellite stem cells to form a pool of myoblasts. When mononucleated myoblasts touch each other, they exit the cell cycle and multinucleated myotubes are formed. The process known as fusion is followed by the activation of several (MRF) myogenic regulatory transcription factors of the MyoD family: MyoD1, myogenin, My5 and Mrf4 ([43][129] [187]).

Primary human progenitor myoblast and the immortalized mouse cell line C2 (originated from satellite cells) were believed to only posses the ability to form myotubes. But studies in the last 10 years have shown that myoblasts cells are not exclusively committed to myogenesis [80, 197][185].

Bone morphogenetic proteins (BMP) and multipotency

When demineralized bone matrix is implanted into muscle tissues, it triggers new bone formation at the implantation site [181]. The active compound in bone matrix was called bone morphogenetic protein (BMP) [182]. Bone morphogenetic proteins (BMP's) belong to a large family of structurally related proteins, known as the transforming growth factor-beta (TGF-beta). BMP's activate several combinations of typeI / type II (serine/ threonine) kinase receptors and their nuclear effector termed Smads [174].

Recombinant human BMP-2 stimulates the maturation of committed osteoblast progenitors, but also induced trans-differentiation of non-osteogenic cells into osteoblasts. Studies have shown the conversion of myogenic C2 myoblasts into the osteoblastic lineage. BMP suppress myogenin mRNA, inhibit the expression of MyoD

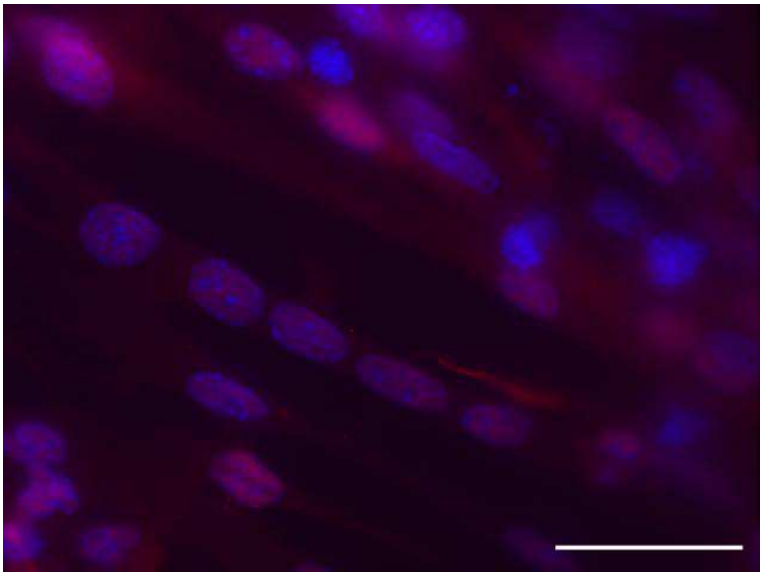

Figure 2.13: Multinucleated myotube. Red stain for (MHC) Myosin Heavy Chain and Dapi-blue the nucleous. Progenitor C2 cells after 4 days of culture differentiate into myotubes. The process is accelerated by adding horse serum and insulin, but also under standard serum conditions differentiation takes place. The scale bar is 50 um.

mRNA, stimulates expression of Id-1 and reduces the ALP activity [80]. Furthermore BMP activates the RunX2 gene (or Cbfa1), specific for osteogenic differentiation[185].

Moreover, under specific conditions myoblasts can differentiate into adipocytes [173][185]. And more recently it was found that certain myoblast progenitor cells have the potential to differentiate into neurons [1],[153],[154].

Multipotency is open to progenitor cells in a "Stock" options model ([185]) and it is not exclusive to adult muscle satellite stem cells or mesenchymal stem cells with higher hierarchy.

The classic definition of a stem cell also implies limited differentiation. However potentials and hierarchy are "options" rather than specific gene expression patterns. Several states of existence, such as proliferation, differentiation and "stem state" have been recently discussed [112][208, 209, 210, 211].

2.5.3 Microenvironment cues (ECM) upon cell differentiation

The stable cell line named C2 progenitor cell or C2C12 is a well documented model for studying cell fate and differentiation [193] [80] [197] [185]. They are muscleskeletal tissue myoblast with the potential to differentiate into bone or muscle. Differentiation of skeletal muscle occurs via a multistep process characterized by a cell cycle withdrawal, expression of muscle specific genes, fusion into multinucleated cells, and assembly of the contractile apparatus [187, 151, 87].

It is yet unclear how the myogenic regulatory factors themselves are activated during myogenesis, but it is well established that a set of environmental signals, including soluble factors, cell-cell and cell-ECM interactions may influence myoblast decision to differentiate [21],[105], [130].

The critical role of signaling through adhesion sites on myoblast proliferation and differentiation is indicated by the influence of diverse isoforms of integrins in the initial signaling and in the later morphogenic processes such as cell fusion and maintenance of myotube integrity [105]. For example, addition of RGD peptides or blocking antibodies in solution to integrin receptors inhibits myoblast fusion and differentiation [111][130].

Another extracellular matrix protein that influence myoblast differentiation is collagen. Inhibition of collagen synthesis blocks myoblast differentiation [125][152].

Further studies have shown that inhibition of proteoglycans synthesis in C2C12 myoblasts causes changes in the ECM self assembly, preventing skeletal muscle differentiation [130] [110]. Proteoglycans play a role in ECM organization and composition since they bind to many ECM proteins. As a receptor heparan sulfate proteoglycans bind, via their sulfated glycosaminoglycans chains, to ECM proteins such as fibronectin, laminin, collagen, and trombospondin. As matrix protein with multiple side chains, proteoglycans serve as multivalent cross-linkers in the ECM. The addition of GAGs to proteoglycans can be perturbed by (i) β-D-xyloside, whereas the sulfation of proteoglycans can be specifically inhibit by (ii) sodium chlorate. The inhibition of proteoglycan synthesis, by any of this inhibitors leads to a decrease in the number and length of the myotubes that are induced to differentiate. The differentiation can be recovered by adding exogenous laminin-rich ECM. Interestingly, the presence or absence of an organized ECM does not affect the expression of muscle specific transcription factors. The gene expression of myogenin is independent. The studies conclude that an organize ECM is not required for activating the myogenic regulatory gene (myogenin), in the initial phase of muscle cell differentiation, but is necessary for achieving terminal differentiation of skeletal muscle cells [130] [110].

Later studies with a similar approach, explore the signals arising from the ECM in the osteogenic commitment of C2C12 cells[131]. Inhibition of proteoglycans (using sodium chlorate) induces the expression of alkaline phosphatase (ALP, osteogenic lineage marker) in myoblasts. The expression of the osteogenic marker can be reverted by adding exogenous ECM. Interestingly, the study found [131] that the expression of the ALP marker didnt affect the expression of muscle commitment MRF (myogenic regulatory factors e.g MyoD) or osteogenic determination Cbfa-1 genes. It is proposed that the osteogenic cell fate by inhibitors of proteoglycans sulfation is BMP-2 independent. But when adding ECM produced by myoblast induced to transdifferentiate into osteoblasts by BMP-2 treatment (ECM different in composition), the ALP marker is also induced in C2C12 cells under normal skeletal differentiation conditions.

The experiments conclude that the composition of extra-cellular matrix induced expression of ALP, by a mechanism independent of BMP-2 and without affecting the expression of key muscle or osteogenic determination genes [131]. Proteoglycan population within the ECM obtained from BMP-2 treated myoblasts is different in composition ([61]) but changes in other ECM constituents may also have a role. Changes in the absence of some type of signals between the ECM and the cells, presumably through integrins, are sufficient to trigger an osteoblastic phenotype [131].

Such studies have revealed that ECM assembly and composition have an epigenetic role in differentiation and cell commitment. However the specific ECM ligands and receptors involved are unknown. The downstream mechanisms that mediate the effects of integrins are unexplored.

2.5.4 Receptors in Muscle Skeletal Development

In vitro studies in avian and rodent species imply that the α_4 integrins, (containing either the β_1 or β_7 subunit), and α_v, $\alpha_5\beta_1$, $\alpha_6\beta_1$ and $\alpha_7\beta_1$ integrins are the major players in muscle differentiation. Whereas $\alpha_5\beta_1$ is the classical fibronectin receptor, both $\alpha_6\beta_1$ and $\alpha_7\beta_1$ are exclusive laminin receptors. $\alpha_5\beta_1$ and $\alpha_6\beta_1$ are widely expressed and down-regulated after myotube formation ([19],[17]), whereas $\alpha_7\beta_1$ is mainly restricted to skeletal and cardiac muscle and strongly up-regulated upon myoblast fusion ([163], [198]). The role of $\alpha_5\beta_1$ and $\alpha_6\beta_1$ in muscle development and the reason they coexist at the myoblast stage as ligand-opposing receptors is not yet well defined [105].

Muscle fibers are surrounded by a basement membrane, composed of the main constituents laminin, collagen IV, the heparan sulfate proteoglycan perlecan, and

nidogen-1 [177][105]. Most likely, cell-matrix contact is predominantly maintained through the interaction of muscle cell transmembrane receptors and laminin, the major cell-adhesive protein found in basement membranes. In skeletal muscle the α_2, α_4, and α_5 chains have been identified ([138],[148] [164] [105]).

Laminin-2 ($\alpha_2\beta_1\gamma1$) and laminin-4 ($\alpha_2\beta_2\gamma1$) are the major laminin isoforms present throughout muscle development and in the adult, providing the intimate contact between basement membranes and the muscle fibers [60]. Accordingly, laminin receptors are thought to play pivotal roles for skeletal muscle function and integrity.

All laminin isoforms detected in skeletal muscle are recognized by $\alpha_3\beta_1$, $\alpha_6\beta_1$, and $\alpha_7\beta_1$ ([47][82][183][105]). $\alpha_7\beta_1$ integrin is the major if not the exclusive integrin receptor found in adult skeletal muscle [105].

Integrins mediate signal transduction across the plasma membrane by activating several intracellular molecules, including focal adhesion kinase (FAK), which plays a prominent role in integrin signaling [77, 20]. Studies have shown a complex and crucial role of FAK in myogenesis. C2C12 cells differentiation is dependent on a transient reduction of FAK signaling but, in contrast, terminal differentiation, with formation of myotubes, is critically dependent on FAK phosphorylation and presumably its activation [34].

Chapter 3

Materials and methods

3.1 Nanopattern substrates

3.1.1 Diblock copolymer micellar nanolithography

Nanopatterns were created by diblock copolymer micellar lithography described in [165, 167, 53]. This approach is based on the self-assembly of diblock copolymers of polystyrene-block-poly (2-vinylpyridine) (PS-b-P2VP) into reverse micelles in toluene. The core of the micelle consists of the P2VP block complexed with a metal precursor ($HAuCl_4$), which is added to the micellar solution during preparation. Glass coverslips were cleaned in a 3:1 H_2SO_4:H_2O_2 solution and dried. Dipping and retracting the cover-slips from such a solution results in uniform and extended monomicellar films on the substrate, and subsequent treatment of these films with oxygen or hydrogen gas plasma, removes the polymer and reduces the salt, leaving the gold "dots" in a nearly perfect hexagonal pattern. A preparation scheme is presented in Fig. 3.1.

The size of the Au nanoparticles may be varied between 1 and 20 nm by adjusting the amount of $HAuC_4$ added to the micellar solution. The spacing between Au nanoparticles may also be adjusted from 15 to 250 nm, by choosing the appropriate molecular weight of PS-b-P2VP and by changing the retraction speed [166].

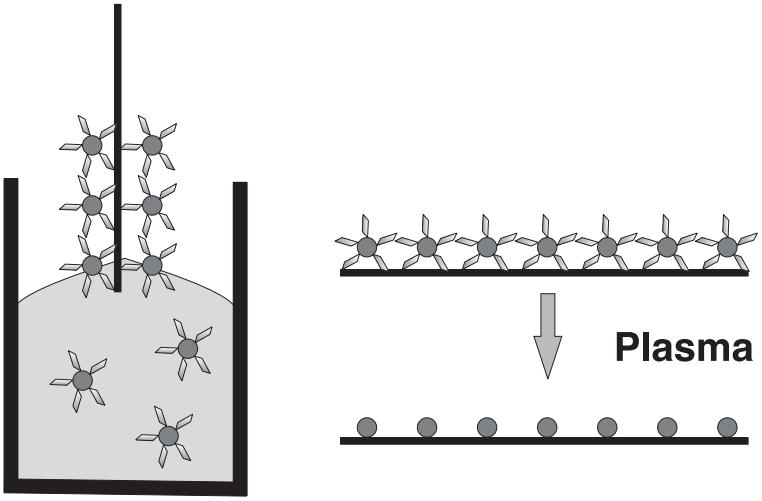

Figure 3.1: Micelles of copolymers containing gold nanoparticles are depos- ited on glass coverslips; after treatment with hydrogen gas plasma, only the polymers are removed from the surface, leaving gold nanoparticles of 8 nm diameter.

3.1.2 Biofunctionalization and passivation

Passivation of the interface entails the binding of polyethylenglycol (PEG 2000) layer to the glass substrate. Covering the surface between the Au nanodots, avoid protein adsorption or interaction of the surface with the cell membrane [7].

Previous to the passivation, the glass surface containing the nanogold dots is kept at 200C for 24h. The annealing process remove the internal stress in the glass and enforced the gold dots attachment the surface. Then the surface is reactivated (negatively charged) applying anisotropic oxigen plasma (150 watt, 0,4 mbar). Both faces of the surface are active.

In a low water atmosphere (under nitrogen flow) the passivation reaction takes place. The absence of water in the system and dry-toluene solvent is important in order to obtain a monolayer polymer coating. The PEG layer thickness correlated with the size of gold nanoparticles, approximately 5 nm [16]. A small spatula amount of polymer per 10ml of dry-tolulene is recommend it. After 20 hours at 80C, the reaction is stopped. The substrates are rinsed with etlyacetate and methanol in order to remove the traces of non-reactive polymer. The solvent are applied with a glass syringe.

For the biofunctionalization, there are wide choices of ligands to link to the Au dots and different immobilization procedures are applicable for different ligands [166]. A forward strategy to couple the peptide ligands to Au nanoparticles is with a thiol (SH) group, through a cysteine residue (C aminoacid). Ligands bind selectively to the Au nanoparticle [7]. All the peptides used in these research, were customized with a linker (CGGG). The triple guanine aminoacid works as a spacer, making accessible the ligand to the cell. A preparation scheme is presented in Fig. 3.2, confluent progenitor muscles cells are observed in the RGD functionalized area, the polyethylenglycol layer prevents unspecific adhesion.

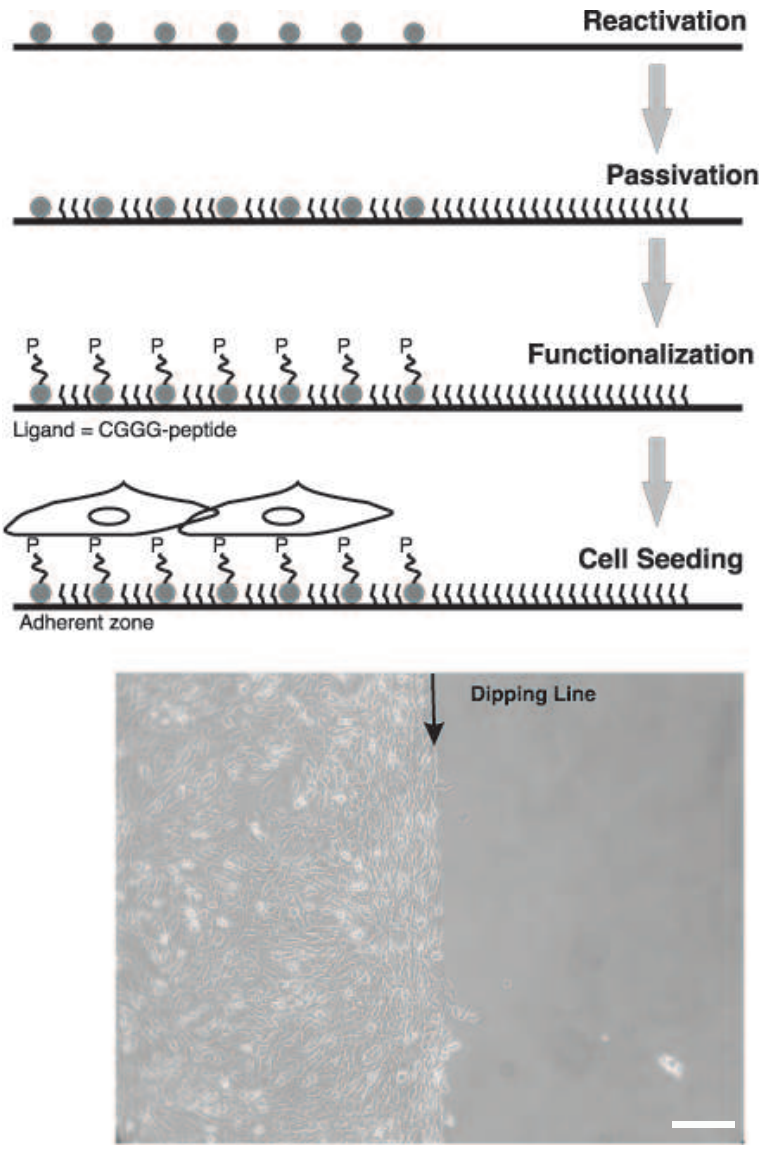

Figure 3.2: Biofunctionalization of nanopatterned surfaces with peptides based on the method for the preparation of RGD surfaces [7]. Confluent progenitor muscles cells are observed in the RGD functionalized area, the polyethylenglycol layer prevents unspecific adhesion. The scale bar is 200 um.

3.2 Cell culture

C2 progenitor muscle cells were suspended in DMEM High Glucose (+ 4500 ml/L Glucose, + Glutamin, - Pyruvate Invitrogen Co.) + 10% Foetal Bovine Serum (Gibco REF 10500-064), and penicillin (100 units/ml)-streptomycin (0.1 mg/ml). The cells were amplified in culture, split before reaching confluence, counted and replated on their corresponding substrates to a density of 6.000 cells / sq cm for 12h at 37C with 5% CO2.

3.2.1 Paxillin focal adhesions

In order to study the focal adhesion matrix formation, C2 progenitor cells were retrovirally infected with yellow fluorescence protein (YFP)-tagged human paxillin in pBabe vector (provided by Dr. Irena Lavelin, Weizmann Institute of Science). The duration of this procedure was 6 days. The work was done with safety virus precautions under the directions of Dr. Lavellin.

The procedure consisted in (i) transfecting the packing cells (293T or phonix cells) with vector Pax-YFP and Helper pCLEco mouse using a lipofactor, (ii) producing the virus on packing cells 293T, (iii) using the medium from the packing cells to infect the target cells (progenitor C2 cells), (iv) selecting with puromycin the positive target C2 cells that express fluorescent paxillin.

Figure 3.3(A) shows bright focal complexes and focal adhesions of C2 cells plated on polystrene dish coated with gelatin, in comparison the control (B) without paxillin shows a diffuse background. No single cloning was used but rather the heterogeneous population.

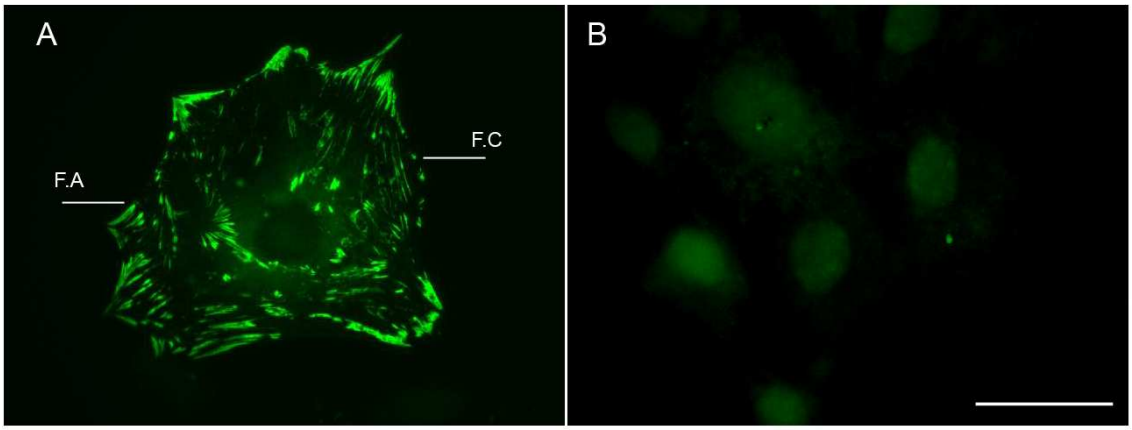

Figure 3.3: A. Retrovirus infected cell with PaxYFP vector was used to highlight focal adhesions. Lines points focal complexes (FC) and stable focal adhesion (FA) B. Control C2 cells. Transition from nascent focal complexes to mature FA creates a symetry break in the FA structure. An elongated polar structure with a distal tip (toe) and proximal end (heel) associated with the growing actin bundle, emerges [190]. The scale bar is 15 um.

Chapter 4

Design of a high-throughput screening (HTPS) system for cell adhesion on defined biofunctionalized nanostructures

4.1 Introduction

System biology studies require large data sets on multiple conditions with profiling of many samples. To investigate questions in cellular adhesion down to the nanoscale level, the use of a "lab-on a chip" technology is proposed. This chapter will focus on the design of high-troughtput screening (HTPS) for cell adhesion. The pipeline analysis consist on the quantification of multiple subcellular features (for example structure and organization of focal adhesions) and statistical comparisons of their distributions in treated vs. control cells [134]. This platform take advantage of nanotechnology techniques to create environments suitable for physical and biochemical stimulation of cells.

4.1.1 Cell based screening

Molecular biology has become a regular tool for research in medicine and therapeutic methods, with specific perturbations at the molecular level. High Throughput Screening (HTPS) as it is known today is a consequence of this development. The complete decoding of the human genome and the ongoing sequencing of animal, plant and microbial genomes has unleashed new analytical possibilities and tech-

niques. Principal applications of HTPS in biomedicine include: Genetic Diseases, Cancer [86], Tissue Typing[44], Infectious Diseases[99], and Drug Discovery.

Cell based screening is an emerging methodology that monitors cellular phenotypes as the read out and is widely used because they produce data sets that are rich in information [135] [42]. Information about cells which is attainable by microscopy includes: cell morphology, intracellular substructures such as cytoskeletal fibers, endoplasmic reticulum, golgi and mitochondria, monitoring gene expression (with promotor reporters), localization of proteins [135]. These kinds of biological screen are referred to as "high content" or "multi-parametric" because many cellular parameters are scored in a single assay [205].

Cell based screening allows cellular processes and their modulation to be explored by (i) chemical or (ii) genetic perturbations [135]. Chemical compound screens aim to discover novel drugs that might interfere with cellular functions by screening chemical libraries. For genetic perturbations, for example, using siRNA technology is a potent method that provides a direct causal link between gene sequence and functional data in the form of targetted loss of function (LOF) phenotype [37] [42].

Screens can provide valuable information on (i) functional genomics: by characterization of the cellular action of multiple genes, (ii) system biology: by elucidating the complex action of multiple biological networks and (iii) drug discovery [135]. Examples included, screening proteosome inhibitors effective for cancer therapy [88], cDNA screening for identifying novel structural cellular proteins based on localization of YFP fusion proteins, discovery of cell migration-related genes [123], phenotypic screening techniques to identify novel therapeutic agents for the treatment of cardiovascular disease [45], and perturbations of cell adhesions [134] [189].

Cell based screening is challenged by technical issues, including image quality, processing time and reproducibility [42]. Development of screening systems requires a multidisciplinary effort: (i) biological input: screening of large libraries (ii) development of a suitable "reporter cell" (iii) microscopy know how, preferably automated microscope readouts for highthrouput (iv) advanced imaging processing using algorithms for image analysis and interpretation linked to a high level of bioinformatics [62] [135].

4.1.2 Chemical and genetic RNAi perturbations on focal adhesion screens

Focal adhesions (FA) are multiprotein complexes involved in the anchoring of cells to their surroundings as well as in the transduction of adhesion-induced signals and regulation of actin cytoskeleton organization within cells. They play a central role in a variety of cellular processes, including tissue morphogenesis, differentiation, cytoskeletal organization, cell migration and transmembrane signalling.

Such parameters unleashed valuable information on cell structure, dynamics and function. Due to their importance these adhesion structures are atractive targets for a variety of drugs [139] and functional genomics studies.

Perturbations in cell based adhesion screen target F.A in culture cells and overall effect on cell spreading and elongation. FA features include abundance, size, shape, molecular composition, distribution and localization within the cell [135]. Cell lines usually express fluorescently targeted paxillin as a prominent component in the FA complex.

Chemical perturbation screens aim to discover novel drugs that might interfere with cellular functions by screening chemical libraries. Recent work explores cytoskeletal and cell adhesion sites as morphological parameters from high-throuput experiments using a chemical library of 2200 combinatorial natural products [134] [126].

Genetic perturbation screens using RNA interference technology have revolutionized the field of functional genomics. The discovery of RNAi allows genome scale screening in cultured cells. The method for gene knock down (not knock out) provides a direct causal link between gene sequence and functional data in the form of targeted loss of function (LOF) phenotype [42].

Small interfering RNAs (siRNAs) technology [157] can be used in (a) direct loss function screen, by (a.1) systematic targeting and identifying the function of each gene individually or (a.2) selecting based screen using pool libraries of shRNAs (short hairpin) to target many genes at once. This approach is effective to many gene types including encoding (structural components, cell surface receptors, transcription factors, enzymes). The second modality is called (b) versus modifier screens. In this approach RNAi is used to identify genes and pathways that, when silenced can either enhance or supress a given initial phenotype of interest. The phenotype can be result of (b.1) initial drug treatment (b.2) combination of drug treatment with/plus siRNA, in which the screen will potentially yield insights into both the mechanism of drug action and the drug-targetted molecular pathways. The details of siRNA technology are available on excellent reviews [42].

A high-throughput microscopy-based screen can be combined with RNAi-mediated gene knockdown to explore molecular pathway function in the assembly of focal adhesions (FAs). In recent work siRNAs [157] was used to target human kinases, phosphatases, and migration- and adhesion-related genes. Multiparametric image analysis of control and of siRNA-treated cells, revealed correlations between distinct morphological FA features or "phenotype signature" [189].

To date cell based focal adhesion screens have been explored by (i) chemical compound perturbations as soluble factors and (ii) knocking down genes by siRNA. However, a library of ligand-receptor perturbations have not been explored as input variables to study the epigenetic variables in FA formation, cell adhesion behavior or signaling.

4.1.3 High throughput and miniaturization

The goal of high throughput screening (HTPS) remains the fabrication of miniaturized laboratory reactors, called micro-arrays that can work in parallel and be compatible with high sensitivity detection systems to monitor their outputs. Complex analyses can be performed within a few hours with the help of microarrays or "biochips" [5].

Classic solid phase substrates such as microscopic slides used in biotesting inspired the development of micro arrays [100]. Present flat substrates can be modified to posses multiple (often hundreds or thousands) probe sites. Each site holds a ligand which, when detected by an imaging technology, most often fluorescence, can indicate the interaction both quantitatively and qualitatively [100]. Those probe spots are micro- to nanometer sized. Examples of flat surface microarrays include: DNA microarrays [64], Protein Arrays [63], Antibody Arrays, Affinity Capture Arrays, Carbohydrate Arrays, Cell Arrays, Tissue Micro Arrays, Automated Ligand Identification System.

The manufacture of microarrrays and biochips benefit from the use of a great number of nanofabrication tools. Surface molecular modification techniques include: self-assembled mono-layers, surface spin coating with polymers or colloids) to control properties of the array interface at the molecular level (adhesion, hydrophobicity, friction). And as shown in this research, the Diblock Copolymer Micelle Nanolithography (BCML) technique.

In addition, HTPS approaches must fullfill certain criteria in order to be useful in a research diagnostic laboratory. They must be able to perform a large number of assays rapidly and simultaneously in a user friendly manner and be small in format. They must be configured to provide robust and reproducible results that allow

standardization and comparison of experiments performed in different laboratories. Because biological samples and reagents are usually small and costly to generate, HTPS methods should be capable of handling small volumes and detecting low concentrations of analytes in order to reduce cost. Preferably, they should be capable of many reuses [5][100].

Finally, data handling, collection, and interpretation generated by HTPS including comparison and storage of databases is necessary to take full advantage of HTPS. Therefore bioinformatics is a component of future HTPS developments.

4.2 Platform design

4.2.1 Choosing the substrate platform for the screening and preparation of adhesive substrate

Quantitative cell adhesion assays require the preparation of an adhesive substratum consisting extra-cellular matrix peptides immobilize onto a solid support. To address the question whether a plain gold substrate or the nano-pattern is an appropriate surface to evaluate a library of thiol adhesive peptides, preliminary cell adhesion experiments were done. Here it is experimentally show why the nano-patterns were the method chosen for the cell based adhesion screen.

In order to evaluate the adhesion performance of a library of peptides, an effective negative control that blocks non specific adhesion to the surface must be established in order to attribute the cell adhesion response to the peptide in question. Cells seed on plain gold substrates are compared with surfaces coated with BSA as negative control. Bovine serum albumin (BSA) is an effective blocking agent for most cells, used at 10 mg/ml heat denatured which usually should allow attachment of $<$ 2-3% of most cells. And should block 50 to 60% on the highest concentration of matrix protein when cultured in plastic [3]. Figure 4.1 illustrate the preliminary experiments.

Glass coverslips were cleaned in a 3:1 H_2SO_4:H_2O_2 solution and dried. The substrates were first coated with 10nm of Titanium, followed by a 20nm of gold (figure A 4.1). The additional titanium layer is a strong inter-phase for gold attachment. A single layer of gold directly onto glass easily detach during the cell culture (picture not shown).

The substrates were incubated with fibronectin (1x40 in PBS for 2 hour at room temperature) or RGD (25um x 3 hours at room temperature), figure 4.1C and 4.1E illustrate the prepared surfaces respectively. Negative controls were further incubated with bovine serum albumin (1 % in BSA) to block non-specific adsorption 4.1 (B, D,F). Progenitor C2 cells were cultured for 24 hours in serum containing medium. Figure 4.2 resume the phase contrast results.

The plain gold sample (figure 4.2A) and the sample incubated with RGD (figure 4.2E) do not show much difference. This address the question of equal distribution of peptides on the gold surfaces or whether the working concentration of peptide of 25um is unsufficient. The sample with the entire fibronectin protein looks remarkably confluent (figure 4.2C). On the other hand, the negative controls with BSA (figure 4.2B, D, F).showed no significant reduction of adhesion.

From these experiments, it can be inferred that BSA did not block efficiently on uniform gold surfaces unspecific adhesion. This could be attributed to several

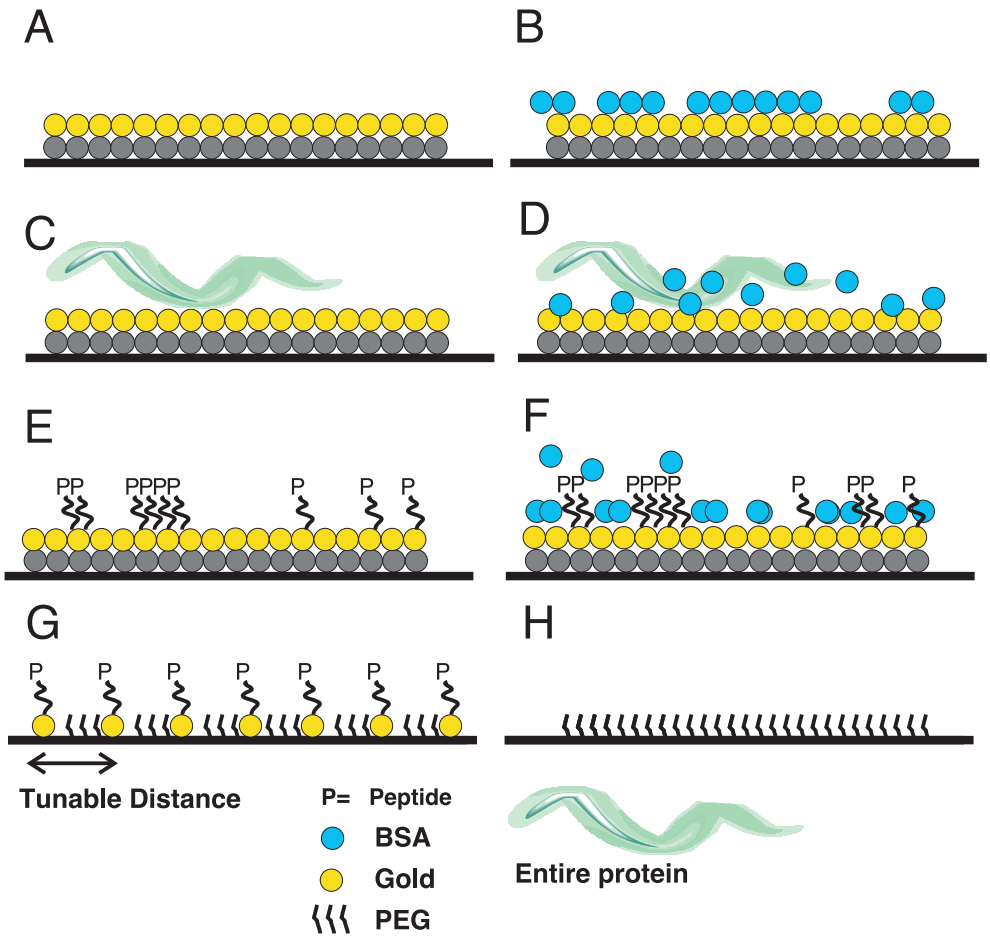

Figure 4.1: Illustration showing preliminary cell adhesion experiments. (A) Gold (B) Gold + BSA (C) Gold and Fibronectin (D) Gold and Fibronectin + BSA (E) Gold and RGD peptide (F) Gold and RGD peptide + BSA (G) Gold-nanodots with RGD passivated with PEG 2000 (H) Glass surface passivated with PEG 2000.

reasons, (i) non-uniform coating of BSA leaving uncovered gold parts and (ii) protein exchange from the serum in the medium. This last effect is known as Vroman effect [46, 127] , and fibronectin present in the medium serum might replace the BSA molecules leading to unwanted adhesion. Additionally, recent studies have demonstrated that on pure flat coated gold surfaces, PEG-thiols are superior to the other blocking molecules. While on polystyrene surfaces blocking with BSA gave best results [147].

Furthermore plain gold doesnt ensure homogenous coating, and the density is variable on the peptide concentration [25][3]. The method doesn't allow control over the spatial cues (inter-distance between ligands) to explore clustering of receptors, and activation of FA in cell adhesion signaling. A suitable surface that facilitate the availability of ligands instead of a flat gold surface (i), with well define anchoring points (i) to controlled density and homogeneous distribution of ligands (iii) with a better repellent molecule to prevent non-specific cell adhesion (iv) is required. Recent studies on attachment and neuronal differentiation have used nano-patterns for gaining unbiased, interpretable data [75]. Figure 4.2H, G illustrate the nanopatterns as an alternative platform in the screening.

Nanopatterns [7] and effective PEG passivation to glass to prevent deposition of proteins shed by cells during culture period [16][18][54] controls unspecific and uncontrollablle protein deposition. Figure 4.3 shows no adherent cells on the passivated area, where non-specific adhesion occurs.

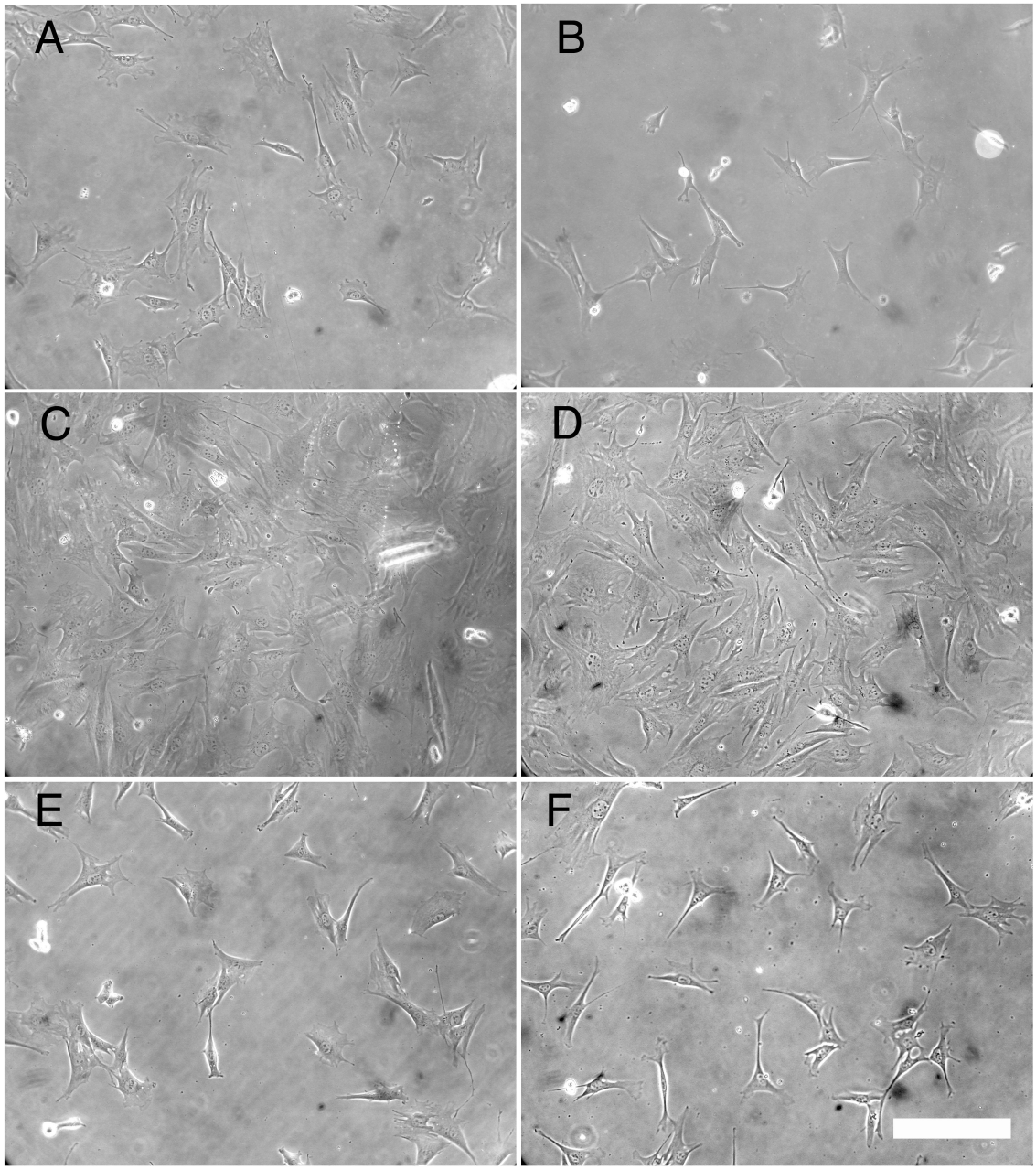

Figure 4.2: Cell adhesion experiments. (A) Gold (B) Gold + BSA (C) Gold and Fibronectin (D) Gold and Fibronectin + BSA (E) Gold and RGD peptide (F) Gold and RGD peptide + BSA (G) Gold-nanodots with RGD passivated with PEG 2000 (H) Glass surface passivated with PEG 2000. The scale bar is 100 um.

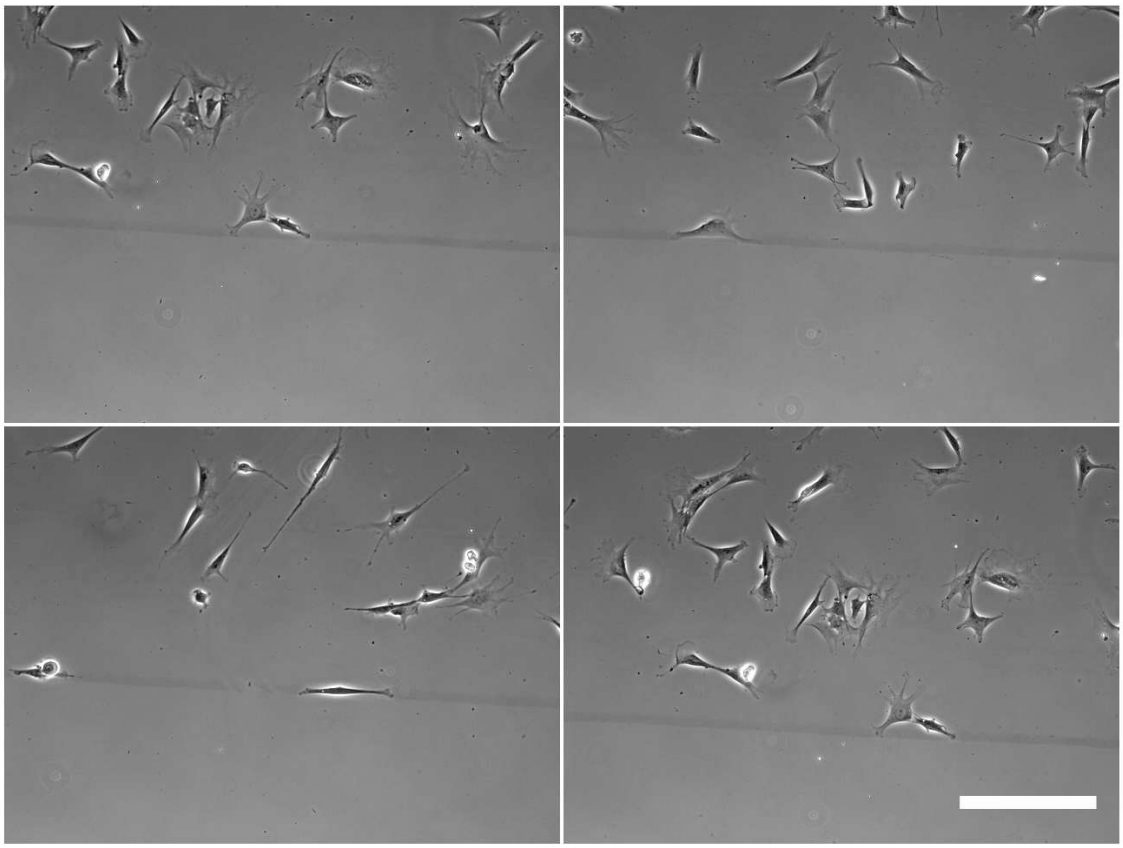

Figure 4.3: Set of 4 cell adhesion experiments on nanopatterns The upper part of each image shows cells cultured on gold-nanodots, decorated with RGD and passivated with PEG 2000. The lower part of each image shows the dipping line and the glass portion of the surface passivated with PEG 2000. The scale bar is 100 um.

4.2.2 First prototype

In academic research, "high density microarrays" samples are investigated for thousands of parameters. Parallel comparison and automation play a decisive role in biochip technology. A new high throughput platform is here described for use in cell adhesion.

The strategy is to use a re-usable culture vessel in combination with a standard glass substrate with the nano-structures. Figure 4.4 illustrate a grid of 4x 12 wells designed to fit into a glass coverslip 25x75 um format. Dimensions and adaptations were made considering a 384 well plate. Polydimetil silohexane (PDMS) was the chosen material to cast such mask. The prototype is envisioned to work with a biomek automatic workstation.

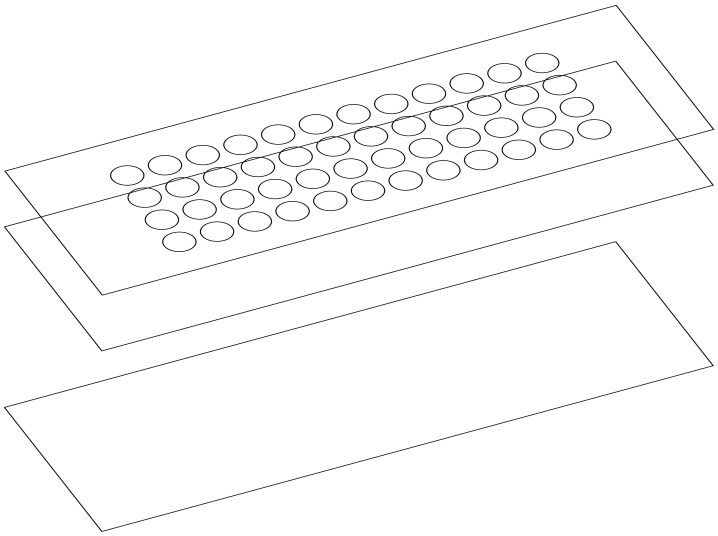

Figure 4.4: PDMS prototype consisting of 4x12 wells. Dimensions and adaptations refer to a 384 well plate. The PDMS mask is mounted and pressed against to glass substrate of 25 mm x 75 mm and 0,7 mm thick. Immobility of the substrate is further achieve with an aluminum chamber. The slide with the passivated PEG 2000 layer and nano-gold dots constitutes its bottom.

The material is flexible, transparent and well known to be biocompatible with cells, making it ideal for cell culture purposes. To prepare the PDMS (Sylgard 184), the crosslinker and silicon base is mixed 1:10 ratio. The viscous liquid is then cast into a mold consisting of 48 round pins screwed to a metal holder. Figure 4.5 shows

removeable pins for easy cleaning and detaching of the polymer. All metal pieces are cleaned with acetone / ethanol and sprayed with silicon to facilitate desmolding prior use. The mold is let to rest for one hour, to let the air bubbles come out of the polymer. Curing takes place overnight at 60C (hot air oven). The casted sample is carefully remove pushing out the pins. The PDMS is rinse with with ethanol 70%, wrapped in aluminium foil and sterilize in the autoclave.All metals parts can be clean with xylene after use.

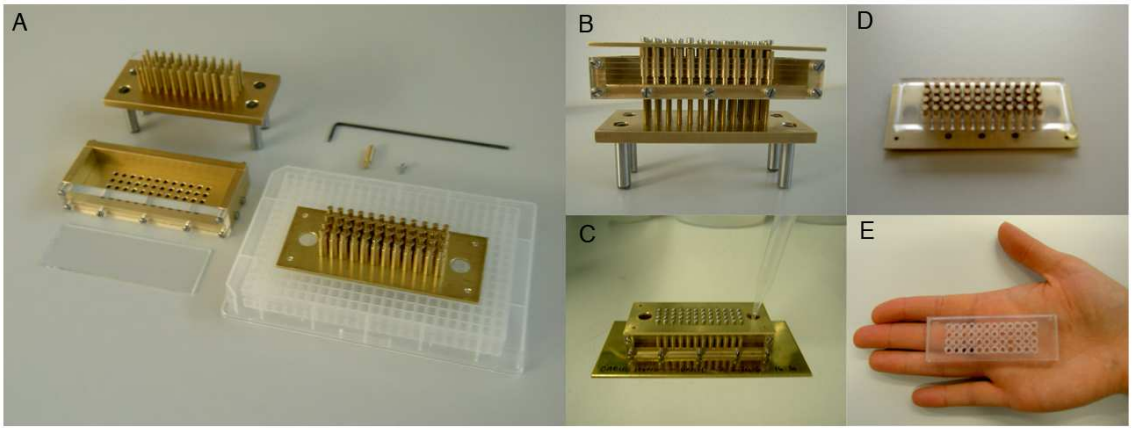

Figure 4.5: A. Tools and component to cast a PDMS culture mask. B. Ejecting pin system C. Casting liquid PDMS D. Removing PDMS after hardening E. Final mask with 48 wells.

The PDMS mask is mounted and pressed against to glass substrate of 25 mm x 75 mm and 0,7 mm thick. immobility of the substrate is further achieve with an aluminum chamber, figure 4.7. Screws in 8 points are used to secure the whole system. After proceeding with the cell culture, the chamber is covered with an adhesive film (that allows Co2 exchange and contamination protection). After use, remove screws and dissemble all parts. Clean all aluminum parts with ethanol and Autoclave.

In this first prototype the PDMS doesnt seal effectively the contact space between the wells. Figure 4.6 shows cultured and stained C2 cells with the PDMS mask. Either the area and dimension are too small for a good contact or the material smooth and adhesive enough. Leaking fluid was observed from one well to another. Sealing is essential to evaluate different peptide conditions on each well. The pressing chamber helps to keep the slide and the silicon together, but the final result is not appropriate for the screening tests.

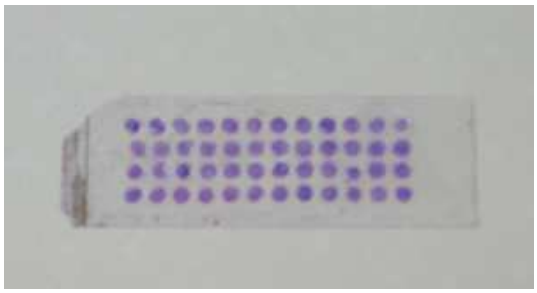

Figure 4.6: Cultured C2 cells, stained with comasin blue.

4.2.3 Working prototype

To overcome the sealing problems in the prototype, a commercial reusable silicon culture vessel is used. The mask (flexiPERM) constitutes the walls of a block of 12 tissue culture wells; the slide with the passivated PEG 2000 layer and nano-gold dots constitutes its bottom. Dimensions resemble a 96 well plate. The silicon mask is not toxic to tissues. It is insensitive to heat, cold and most of all laboratory chemicals.

The smooth lower side of the flexiPERM adheres to the dry slide when slightly pressed against it. In this way 12 wells are formed which are isolated from each other. Adherence can be checked, from below, in the reflected light. Further pressing and immobility of the substrate is achieve with the aluminum chamber, figure 4.7 shows the mechanical parts . Rubber bands instead of screws are use to secure the whole system. Figure 4.8 shows a clean sealing using the commercial silicon mask.

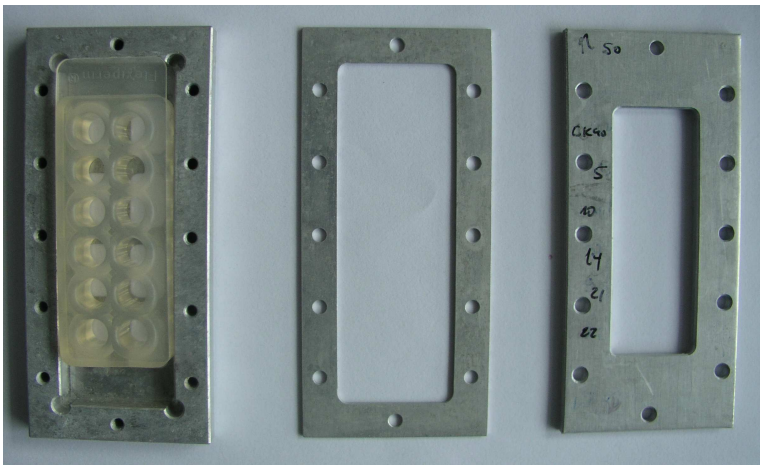

Figure 4.7: Chamber aluminum parts and commercial silicon mask.

It was advantageous to passivate a higher number of glass coverslips in a batch. This enable the same surface quality for the screening. This was possible using in a vertical holder made of glass, with a capacity of 10 surfaces. The device fits into a customed glass set up, with a nitrogen influx plug and a closing lid as shown in 4.9. The passivation procedure is described in section 3.1.2.

The assembly and working with the chamber should be done under the cell culture. All components such as aluminum parts and the silicon vessel should be previously sterilized. Autoclave is recommended.

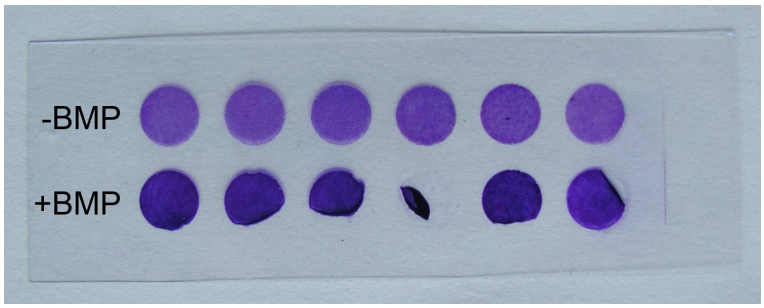

Figure 4.8: Comasin blue staining on cultured cells proves the system is not leeking.

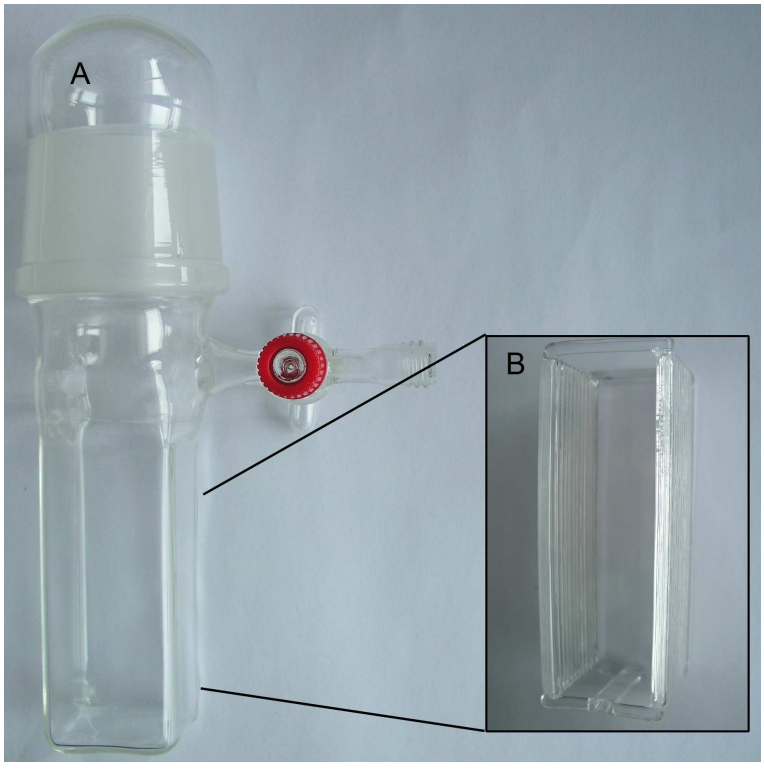

Figure 4.9: A. Glass device to perform the passivation B. Coverslip vertical holder x 10 samples.

4.2.4 Peptide library review and strategy for dissolving large set of peptides

The extra cellular matrix (ECM) and cell adhesion molecules library consisted of 33 ligands or peptides (Fibrinogen, Tenascin, Collagen, Fibronectin, CAM, Laminin). The control peptide is the cyclic RGDfK which specifically recognise $\alpha_v\beta_3$ integrins [24].

The sequences reported in literature for adhesive behavior, were synthesized by GL Biochem (Shanghai) Ltd. China and Invitrogen, Germany with an additional THIOL group attached (C-cisteine for gold binding) plus "GGG" as the spacer. Figure 4.10 summarize the compounds with its associated known receptors and its location within the protein.

Peptides were supplied as lyophilized solids in polypropylene tubes. In these cases, the only practical method was to apply one solvent to all peptides and use the solutions obtained without trying to optimize for each peptide.

As suggested by commercial recommendations the peptides were resuspend in solvent comprising 0.1M HEPES buffer pH7.4 in a 40% acetonitrile/water. They were then aliquoted in 200ul of such buffer, frozen at –70C and lyophilized overnight. After lyophilization peptides are stable at room temperature and can be store at –20C.

Prior peptide immobilization. They the aliquot is resuspended in 50% DMSO / DDW (double distilled water). Then a small working aliquot was taken and further diluted in 20mM HEPES, ph 7.4 to maintain pH. The remaining peptides in DMSO-DWW should be kept at –70C.

Fibrinogen

Amino Acid Sequence	Receptor	Site	Screening Code	References
GWTVFQKRLDGSV or P1	$\alpha_v\beta_3$	Gamma 190-202	Fibrinogen CV-17	A, B, H, S
YSMKKITMKITPFNRLTIC or P2	$\alpha_v\beta_3$	Gamma 377-395	Fibrinogen CG-23	B, H, S
TMKIIPFNRLTIG or P2C	$\alpha_v\beta_3$	Gamma 383-395	Fibrinogen CG-17	H, I
HHLGGAKQAGDV	$\alpha_{IIb}\beta_3$	Gamma chain	Fibrinogen CV-16	B
GPR	$\alpha_4\beta_2$	Alfa chain	Fibrinogen CR-7	B

Tenascin

Amino Acid Sequence	Receptor	Site	Screening Code	References
AEIDGIEL	$\alpha_9\beta_1$	*	Tenascin CL-12	B

VCAM-1

Amino Acid Sequence	Receptor	Site	Screening Code	References
QIDS	$\alpha_4\beta_1$	*	VCAM-1 CS-8	B

MadCAM-1

Amino Acid Sequence	Receptor	Site	Screening Code	References
LDT	$\alpha_4\beta_7$	*	MadCAM-1 CT-7	B

Collagen

Amino acid sequence	Receptor		Site	Screening Code	References
GFOGER	$\alpha_1\beta_1$	$\alpha_2\beta_1$	*	Collagen CR-10	B

RGD's

Amino acid sequence	Receptor		Site	Screening Code	References
RGD cyclic c(RGDFK)	$\alpha_v\beta_3$		FN repeat III 10	RGD cyclic CK-9 (0)	T, U, V
RGD linear	$\alpha_{IIb}\beta_3$	$\alpha_5\beta_1$	FN repeat III 10	RGD linear CD-7	B

Fibronectin

Amino Acid Sequence	Receptor		Site	Screening Code	References
YRVRVTPKEKTGPMKEM	$\alpha_4\beta_1$		COOH-terminal heparin-binding domain	Fibronectin 1	D
YEKPGSPPREVVPRPRPRV	$\alpha_4\beta_1$	proteoglycans	COOH-terminal heparin-binding domain	Fibronectin 2	D
KNNQKSEPLIGRKKT	$\alpha_4\beta_1$		COOH-terminal heparin-binding domain	Fibronectin 3	D
DELPQLVTLPHPNLHGPEILTUPST	$\alpha_4\beta_1$		IIICS, CS1	Fibronectin 4	B, D, E
GEEIQIGHIPRETUDYHLYP	$\alpha_4\beta_1$		IIICS, CS5	Fibronectin 5	B, D, E
IDAPS	$\alpha_4\beta_1$		III14	Fibronectin 6	B, D, E
LDVPS	$\alpha_4\beta_1$	$\alpha_4\beta_7$	IIICS	Fibronectin 7	D, E
WQPPRARI	$\alpha_9\beta_1$		COOH-terminal heparin-binding domain	Fibronectin 8	D
HSRNSI	$\alpha_{IIb}\beta_3$		Cell binding Domain	Fibronectin 9	D
ATECTITISWCTKTE	$\alpha_{IIb}\beta_3$		COOH-terminal heparin-binding domain	Fibronectin 10	D
PHSRN	$\alpha_5\beta_1$		Repeat III 9	Fibronectin 11	E
KLDAPT	$\alpha_4\beta_1$	$\alpha_4\beta_7$	Repeat III5	Fibronectin 12	E
EDGIHEL	$\alpha_4\beta_1$	$\alpha_9\beta_1$	EDA split	Fibronectin 13	E

Laminin

Amino Acid Sequence	Receptor	Site	Screening Code	References
DYAULQLHGCRLHFMFDLG	$\alpha_2\beta_1$	LG4 domain, laminin alfa1 chain hEF-1	Laminin 14	C
KNSFMALYLSKGRLUFALG	Syndecan 2	LG4 domain, laminin alfa 3	Laminin 15	C
PPFLMLLKGSTR	$\alpha_3\beta_1$	LG3 domain, laminin 5, alfa 3 chain	Laminin 16	G
SIYITRF	$\alpha_6\beta_1$	LG1 domain, laminin alfa 1 chain	Laminin 17	G
IAFQRN	$\alpha_3\beta_1$	LG2 domain, laminin alfa 1 chain	Laminin 18	G
YIGSR	67 kd receptor	Beta 1 (old nomenclature, B1 chain)	Laminin 19	F, N, O, P
LGTIPG	67 kd receptor	Beta 1 (old nomenclature, B1 chain)	Laminin 20	F
CSRADKCAASIKAWVSADR	67 kd receptor	Alfa 1 chain (old nomenclature, A chain)	Laminin 21	F, K, L
RYVDLPRPWCFEKCGMNVTR	Heparin Sulfate Proteoglycan	Beta 1, inner globule (F-9)	Laminin 22	F, J, Q, R

Figure 4.10: Peptide library: adhesive ligands compounds with its associated known receptors and its location within the protein. The given screening code identifies the ECM peptide and the associated number is not related to any nomenclature, but simplicity to cite the sequence in the screen.References A, B, C, D, E, F, G, H, I, J, K, L, M, N, O, P, Q, R, S, T, U, V correspond to [118], [142], [199], [114], [133], [108], [83], [180], [194], [27], [184], [172], [155], [57], [56], [33], [161] [94], [140], [66], [79], [95] respectively.

4.2.5 High throughput experimental method

The surface biofunctionalization is an important step that requires skillful preparation and attention. After assembly of the chamber under the cell culture hood, 50ul of the diluted peptide (25 uM) in buffer are applied individually to the wells. Five peptides and one RGD control are tested in duplicates. It is important to keep track on the chamber orientation and identify the wells in each experiment. Peptides are incubated for 3 hours, at room temperature. All the wells are washed with 100 ul of double destilled water (DDW) x 3 times (20 minutes each) with a multipippet. For sterilization of the substrate, 100 ul of ethanol is used for 10-15 minutes. The wells are washed again with sterile DDW x 3 times. A final wash with sterile PBS is applied before cell seeding. Cells are plated at a density 6.000 cell/cm2 in a volume of 100ul. The chambers are placed in a big sterile petri dish with some PBS to preserved humidity. The petri dishes are kept for 12h in the incubator and then transfer to the bench for disassemble, figure 5.1.

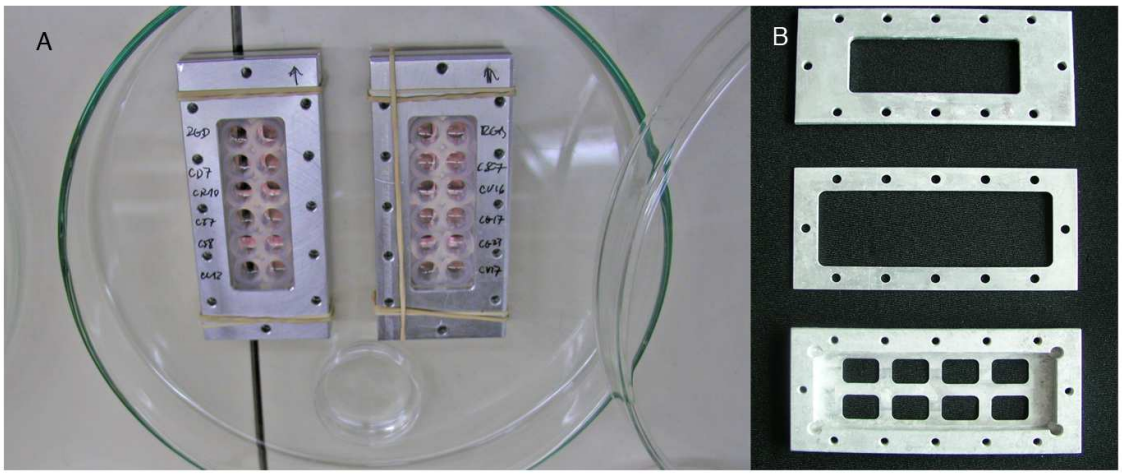

Figure 4.11: A. Chamber in glass petri dish with cultured media B. Chamber aluminum parts.

4.2.6 Cell fixation and final preparation

After culturing, the chamber is disassemble, the silicon mask is removed and the substrate is gently washed with at 37C PBS. The cells are fixed in 3% paraformaldehyde (PFA) for 20min at 37C and then washed with PBS. The slides with fixed cells were mounted upside down with ELVANOL on a glass object 26mmx76 mm. After 2 days of letting the samples dry in a dark place, the slides were ready to the microscope stage for screening. An adhesive film helps to locate the wells position as shown in figure 4.12.

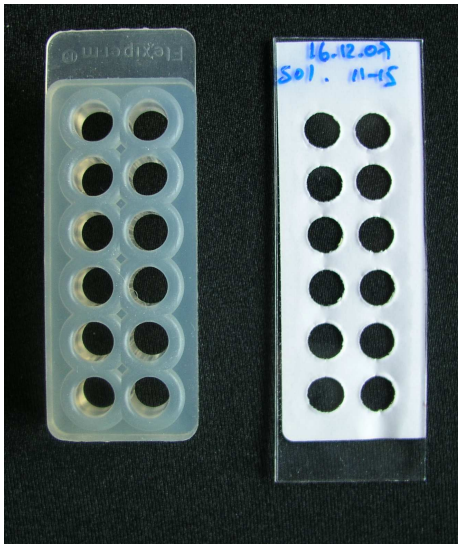

Figure 4.12: Mounted high content screen slide in a 25 x 75 mm format.

The flexiPERM and aluminium parts are reusable. Immediately after culturing the cells rinsed in flowing water, rubbing it slightly. Then kept it in a bowl with 70% ethanol solution for 20 min. After drying in air, the flexiPERM and aluminum parts can be autoclaved. Autoclaving in the foil bag has proved to be the best method. The flexiPERM and chamber parts wrapped in aluminum foil should remain in the bag until it is used again. In this way it is protected against contamination.

The biochip platform for the parallel analysis and validation of samples, can be extrapolated using other ligand-receptor systems of interest. A much higher sample throughput is potentially possible by designing a chamber to the format of a full microplate platform. A multi-chamber able to hold several standard 1x3 inches substrates, producing and processing up to 96 conditions.

4.3 Image acquisition and data analysis

4.3.1 Contrast phase microscopy and cell counting

Cell attachment assays quantitate the fraction of cells that attach to matrix-coated surfaces and are resistant to gentle washing. A PBS solution at 37 C must be added gently to the culture in order to minimize turbulent flow which could dislodge even well attach cells. Attached cells can be quantified by labelling cells with radioactivity, by staining attached cells, by using metabolic assays, by prelabelling cells with fluorescent dyes or directly counting the attached cells in a microspic field.

Transmitted light microscope Axiovert 200, in phase contrast mode, was the instrument used for monitoring the morphologic cell adhesion response, and also to count the cells. The thin mounted slide 0.17 mm thick, with the cultured cells on the nano-structures must face down the objective. Unwanted dirt and elvanol traces can be removed by gently cleaning the surface with ethanol. The quality of the phase contrast image is affected by the cleanness of the microscope slide.

A set of 8 pictures are taken per condition, see figure 4.13. Image J, Cell Counter plugin was the software application use to count cells within a field at 10x magnification. Note that at any time you can add types or remove them. Select the type you want to count (1 to 8), and count by clicking on the feature in the image. A colored number corresponding to the type you are counting will be displayed on the image every time you click, and the corresponding counter is updated. The counter shows the results in the ImageJ results table. The counts per picture and the totals are displayed. Exports the marker data to an XML file. Export the Image image with the markers written on it.

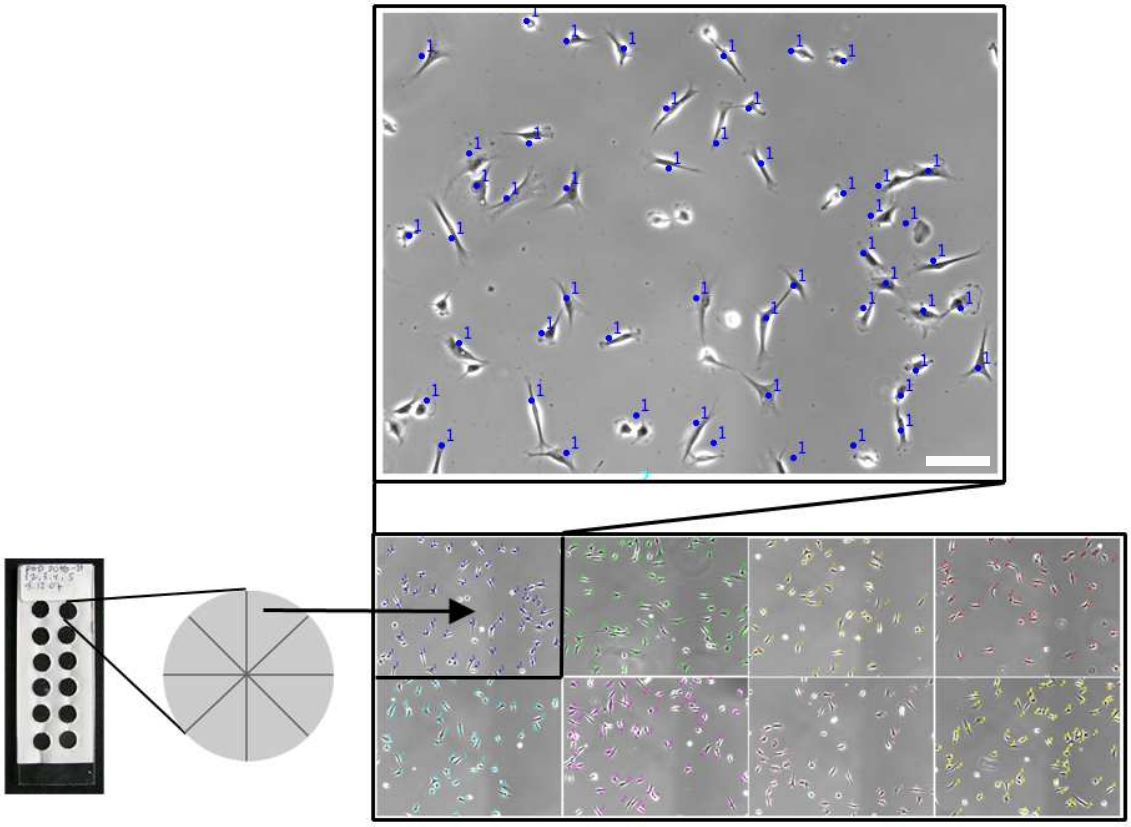

Figure 4.13: Set of 8 pictures are selected per condition. The enlarged picture shows scale bar=100 um. A colored number corresponds to the image that is counted.

4.3.2 Cell segmentation analysis, area and elongation

Adhesion cell area and elongation was calculated from phase contrast images acquired with the transmitted light microscope. The same 8 pictures used for cell counting were analyzed for manual segmentation. ROI Manager on Image J was the plugin software used to individually segment each cell adhere to the substrate in a field of 10x magnification. The set measurement to analyze the polygons correlates to 0.65 micrometer/ pixel in a 10x picture. Figure 4.14 illustrate the procedure.

For quantification the polygon fit to an ellipse. The cell area output is report in square micrometers. And the major axis and minor axis in micrometers. The elongation is report without units as it the ratio between major/minor axis. The data is export to a XML file.

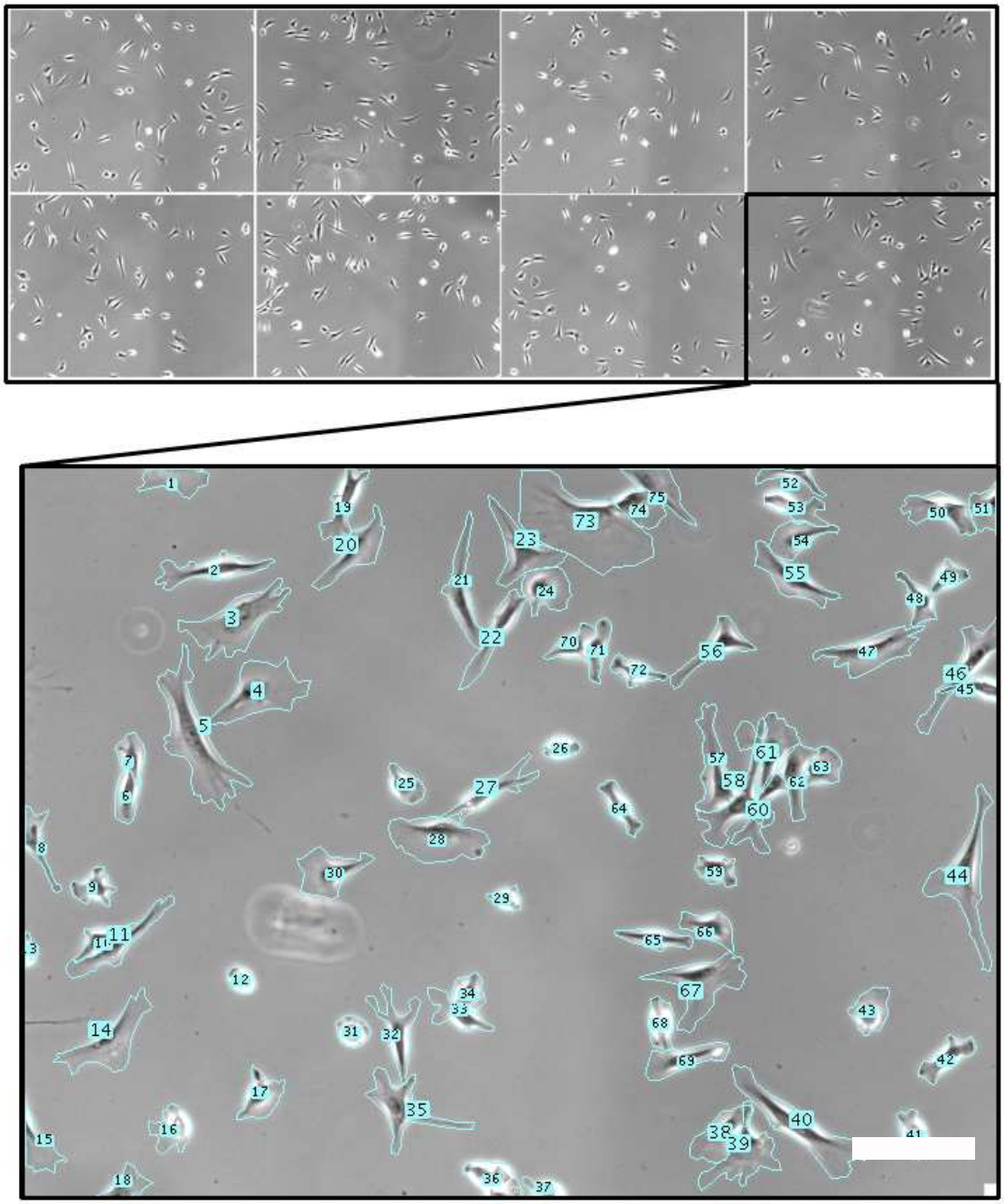

Figure 4.14: Set of 8 pictures are selected per condition. The enlarged image shows the scale bar =100 um. Cell are is segmented using polygons. For quantification the polygon fit to ellipses.

4.3.3 Fluorescent microscopy

In fluorescence microscopy, also called epifluorescence microscopy, the image is not the result of direct transmission of visible light as in light microscopy. In this case, the investigated specimen itself emits light. Fluorescence probes within a complex biological object can be selectively excited and detected. The possibility to stain or genetically express interesting structures with fluorescent probes enables the localization and identification of specific structures.

The fluorophores in the sample are excited by light of define wavelength. In the Jablonski diagram (shown in figure 4.15) the excitation into the S2-state (A) as well as the subsequent fluorescence emission (F) is indicated (blue and green, respectively). The difference between the energies of excitation and emission results from different interactions between the excited state and the solvent at the time of excitation and at the time of emission, respectively. This energy gap is expressed as "STOKES shift", i.e the difference between the excitation and emission wavelength maxima. Owing to the lower S1-state, the emission occurs at a longer wavelength maximum than the excitation.

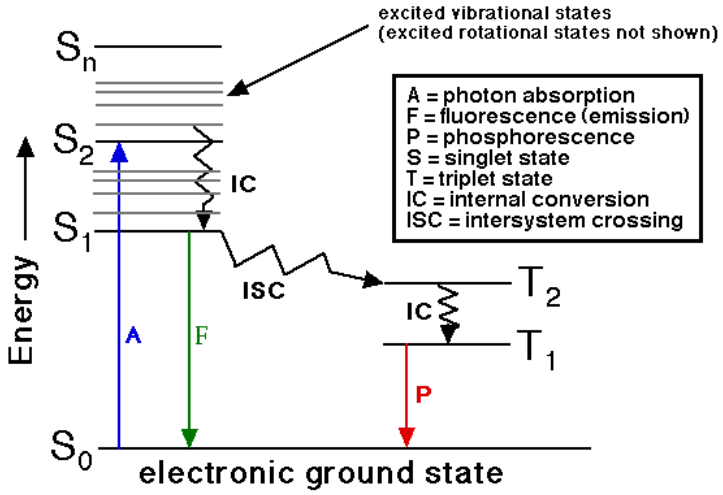

Figure 4.15: Jablonski diagram: the excitation into the S2-state (A) as well as the subsequent fluorescence emission (F) is indicated (blue and green, respectively).

In the microscope, the incident light supplied by a mercury arc lamp (1) reaches the excitation filter (A), letting pass excitation light of a suitable wavelength (2). A

chromatic beam splitter (B) reflects this light on the specimen via the objective.The specimen absorbs the excitation light and then emits long wave fluorescence (3) which is collected by the objective and transmitted again by the chromatic beam splitter (B). A final emission filter (C), transmit only light with the emitted wavelength (3) to the eye piece, the camera o the detector. Diagram 4.16 illustrate the principle.

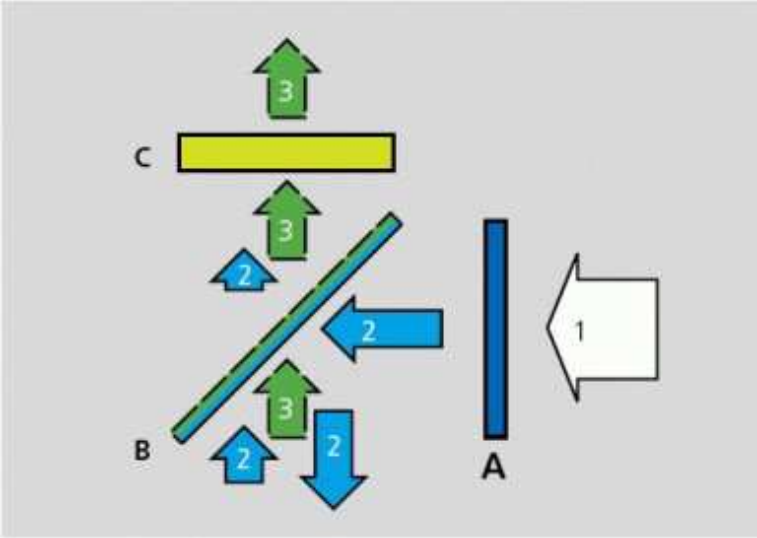

Figure 4.16: Epifluorescence microscopy principle: Incident light (1). Excitation filter (A). Excitation specific wavelength (2). Chromatic beam splitter (B). Long wave fluorescence (3). Emission filter (C).

4.3.4 Quantitative fluorescent microscopy: data collection

Biological image data collection was performed with the microscope system DeltaVision RT, in combination with the softWoRx image analysis software. The inverted epifluorescence microscope allows precise control of stage motion and is used for quantitative microscopy.

Retrovirally infected C2 cells self express Pax-YFP to localize punctate focal adhesion structures at the interphase between cells and the ECM components. The chosen filter for detecting paxillin focal adhesion expressing YFP (Yellow Fluorescent Protein) was the FITC filter. The filter is called FITC because its used for detecting Fluoresce in Iso Thio Cyanate with excitation wavelength 490 nm, and emission wavelength =526 nm. Digital images were collected in 40x oil immersion objective

+ Aux magnification. All pictures were made at the same time exposure, as close as possible to the saturation point, and at the same percentage of light transmission. Standarized conditions set in relation to the RGD control.

4.3.5 Focal adhesion analysis, number, area and elongation

The paxilin-YFP focal adhesion analysis was performed using with a mathematical algorithm under MatLab (acknowledgement to Dr. Alex deBeer). Raw cell images often contain diffuse background, which is especially prominent in thick regions of the cell like the nucleus. Subtraction of the average image intensity flattens this background (high pass filtered) and facilitates interactive determination of a uniform threshold level that is below the staining intensity for all matrix adhesion patches. Image segments corresponding to individual matrix adhesion (patches) are then define by the algorithm and approximate to ellipses as shown in figure 4.17. Such ellipses are then count, and measured (elongation ratio and area). The smallest paxillin structure correspond to 20 sq pixels, which equals an area of 0.5 sq um. The conversion in the delta vision system equipment is 6.25 pixels to 1 um. Parameters were optimized for 52nm RGD control, and used to all the screened data, aiming to get a lower systematic error. However, when plotting the results high amount of artifacts were found in the 70nm and 110nm data (objects such as vesicles close to the nucleous and bright cell-cell borders were identified by the algorithm). Because such artifacts did not correspond to the qualitative observations, where no visual focals are identified at 70nm and 110nm, with the except of few ones on P22. New parameters were re-adjusted to 70nm and 110nm, allowing a proper signal to noisy/systematic error.

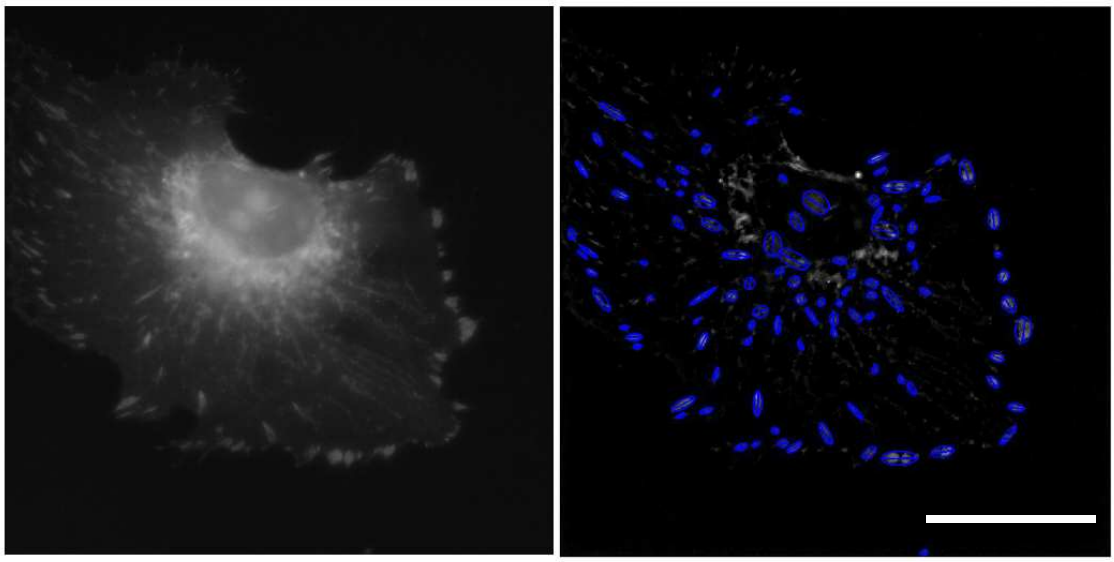

Figure 4.17: Left: Raw cell images often contain diffuse background. Right: Individual matrix adhesion (patches) are defined by the algorithm and approximate to ellipses. The scale bar is 25 um.

4.3.6 Statistical representation of large image stacks

Experimental biologists are often unsure how error bars should be interpreted. Error bars could describe the number of measurements, replicates or independent experiments [39]. For the quantification of cell area, cell elongation, focal adhesion (size, area and number), and myotube (area and elongation), the mean or average values and standard deviation is report. In this work the standard deviation describes how the data is spread in relation to the number of measurements = n.

The distribution of data values can be further be represented as a histogram. The distribution helps to identified populations within in the data set, and aims to explain high standard deviation values in some experiments.

The histogram's x-axis reflects the range of values in Y. The histogram's Y-axis shows the number of elements that fall within the groups; therefore, the Y axis ranges from 0 to the greates number of elements deposited in any bin.

To plot a histogram, the measurement values are organized in a mathematical matrix Hist (y,x) and plotted in MatLab. Where x is a vector, returns the distribution of y among length (x) bins with centers specified by x. In addition, data is normalized to the total number of measurements in order to compared different conditions.

For example, cell area values are in a range from 0 to 5500 square micrometers. We define bins of 50 square micrometers size.

$$x = [0:50:5500]; (min, bin, max).$$

The histogram function hist(y,x), distribute the y values into the 110 bins. For the experiment 70nm and RGD cells we have the follow values,

$$\begin{aligned} y &= [13, 8, 10, 12, 11, 19, 5, 16, 25, 8, 23, 12, 45, 27, 24, 15, 8, 49, 19, 7, 4795, 2136, \\ &\quad 1066, 79, 118, 189, 63, 70, 149, 78, 366, 57, 31, 126, 103, 2065, 917, 1960, \\ &\quad 2326, 61, 28, 41, 26, 44, 14, 60, 38, 21, 41, 11, 592, 741, 488, 555, 487, 259, 383, \\ &\quad 1252, 1160, 819, 16, 2093, 1675, 902, 1178, 2019, 2085, 173, 102, 2511, 1778, \\ &\quad 901, 214, 1058, 1706, 1502, 837, 2571, 678, 2019, 3164, 940, 572, 2519, 207, \\ &\quad 1456, 2607, 1308, 321] \\ [a1, b1] &= hist(y, x) \\ c1 &= [(a1/numel(y)) * 100]; \text{ where } n = numel(y) = 43 \end{aligned}$$

The histogram is plot in figure 4.18. In addition, data is normalized to the total number of measurements in order to compared with other conditions (figure 4.19).

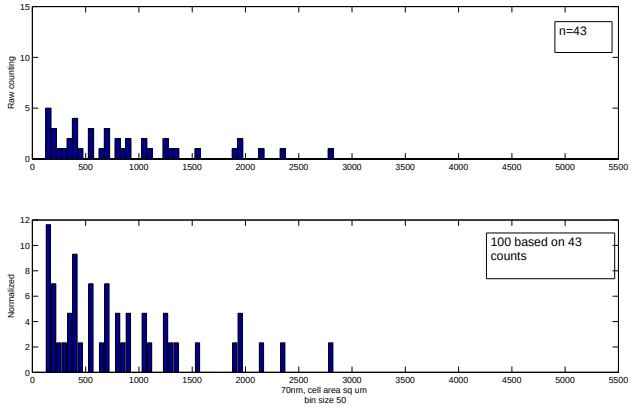

Figure 4.18: Histogram example, cell area distribution at 70nm for RGD control. The image at the bottom is normalized.

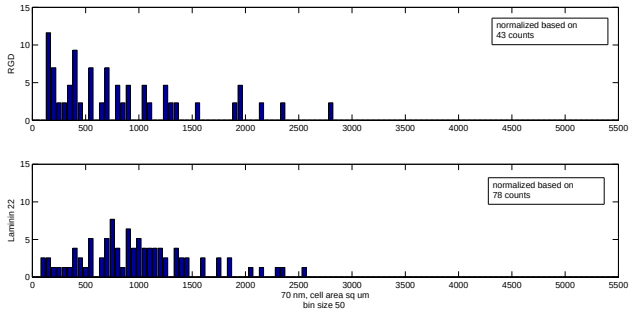

Figure 4.19: Comparison of two histograms normalized by their number of measurements. Cell area distribution at 70nm is shown for RGD control and Laminin 22.

4.4 Closing remarks

Quantitative cell adhesion assays require the preparation of an adhesive substratum consisting extra-cellular matrix peptides immobilize onto a solid support. Nanopattern substrates allow to investigate questions in cellular adhesion down to the nanoscale level. The homogeneous ligand distribution, controlled distance between ligands, and effective passivation against non-specific adhesion of nanopatter susbtrates allows to study ligand-receptors interaction [7][166] [51] [75].

The working "lab on chip" platform, consist of a commercial mask (flexiPERM) with 12 culture wells; on top of a 1x3 inches glass slide, with the passivated PEG 2000 layer and nano-gold dots. Immobility of the substrate is further achieved with an aluminum chamber. The dimensions of the wells resemble a 96 well plate.

Cell based screening development requires a multidisciplinary effort: (i) biological input: screening of large libraries (ii) development of a suitable "reporter cell" (iii) microscopy know how, preferably automated microscope readouts for highthrouput (iv) advanced imaging processing using algorithms for image analysis and interpretation linked to a high level of bioinformatics [62] [135].

Chapter 5

Screening adhesive peptides

5.1 Introduction

Perturbation of focal adhesions have been so far explored with (i) chemical compounds screen[134] and (2) siRNA technology [189]. However no ligand-receptor screens have been reported so far as input perturbation to explore cell adhesion mechanisms in specific microenviroments at the nanoscale level. The perturbation variables here presented are extra-cellular matrix ligands, potentially useful to explore such questions at the epigenetic level.

The homogeneous ligand distribution, controlled distance between ligands, and effective passivation against non-specific adhesion in nano-patterns allows to study ligand-receptors interactions, and adhesion-mediated signaling [7][166] [51] [75].

This chapter will illustrate the strategy steps to target adhesive and phenotype specific ECM peptide ligands on C2 reporter cell. Here we present the use of the designed "lab-on a chip" platform, controlling the ligand input (library of peptides as perturbations) and the readout response of the cells (number of adherent cells and phenotypic changes). Further revalidation and a review on such results are presented.

5.2 Results and discussions

5.2.1 Selection of peptides candidates based on adherent cells

Cell attachment assays quantitate the fraction of cells that attach to ligand-imbolized surfaces. The average number of adherent cells in control within a field of 10x, was n=46 out of 168 counts in set of 4 images. Out of 35 ligands, 24 showed adhesion above 40% in relation our control, the cyclic RGDfK which specifically recognise $\alpha_v\beta_3$ integrins [24]. The given screening code identifies the ECM peptide and the associated number is not related to any nomenclature, but simplicity to cite the sequence in the screen.

The experiment was performed in one single batch. All surfaces were biofunctionalized and passivated under the same chemistry conditions at once. The cell culture conditions such as media and time applied to all the evaluated conditions. In other words, all the samples evaluated were subjected to the same systematic error. Figure 5.1 summarizes the adhesion results.

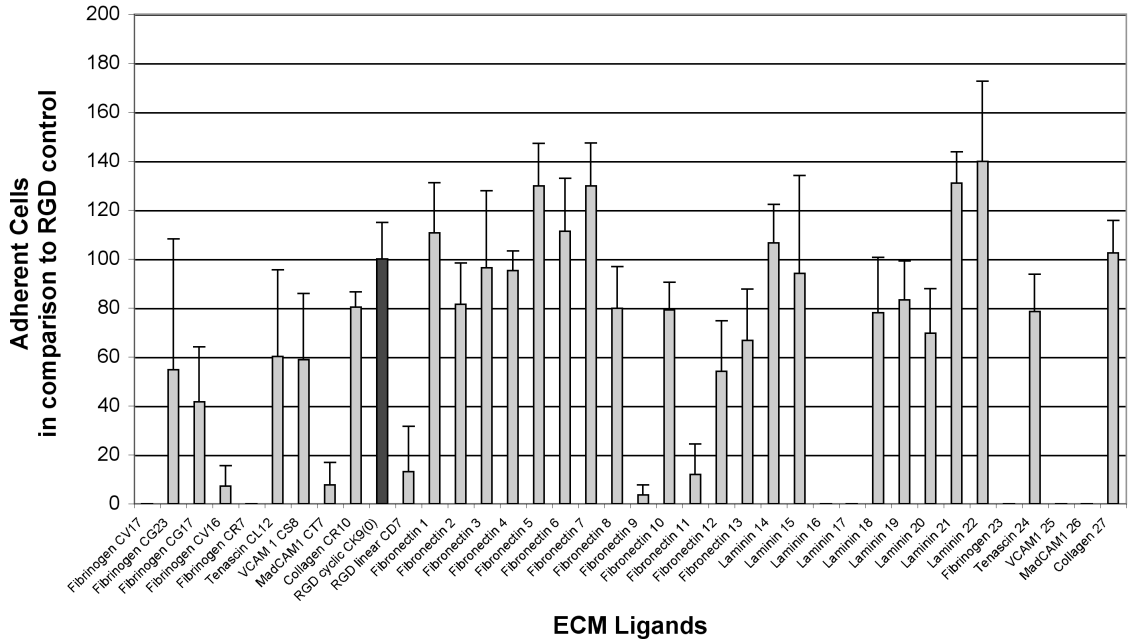

Figure 5.1: The chosen platform substrate for the screening was the gold nanodot surface with 52nm nanodots spacing. The extra cellular matrix (ECM) peptide library consisted of 33 peptides (Fibrinogen, Tenascin, Collagen, Fibronectin, CAM, Laminin). The given screening code identifies the ECM peptide and the associated number is not related to any nomenclature, but simplicity to cite the sequence in the screen. Details on the screen peptides are shown in section 4.2.3. Progenitor C2 reporter cells were cultured for 12h. Note: Fibrinogen 23, Tenascin 24, VCAM 25 and Collagen 27 were synthesized by Invitrogen. The last group corresponds to the same sequences as Fibrinogen CV17, Tenascin CL12, VCAM 1 CS8 and collagen CR10 respectively. Cell Adhesion quantification was based on the average number of adherent cells in comparison to RGD control, n=46 out of 168 counts.

5.2.2 Selection of peptides candidates based on phenotypic behavior

The aim is to target ECM sequences that produce cytoskeletal changes in the C2 progenitor cells. This allows us to further research peptides that are potentially interesting for studying ligand-receptor interactions, adhesive-signaling mediated molecular pathways and adhesive ligands effects upon differentiation.

After quantifying the number of adherent cells in the screen, a further qualitative selection was performed manually and compared with the RDG control. Cell morphology was visually classified as either spread, elongated, or clustered. A scoring system from 1 to 5, 5 being the highest, was established as shown in figure 5.2. Phenotypes that scored above 4 were taken as candidates. A total of 10 out of 24 ligands that induce adhesion were chosen as preliminary candidates. The table in figure 5.2 highlights 3 groups of candidates: cluster (FG CG23, FG CG 17), elongated (FN 1, FN 3, FN 5, LM 14) and spread (FN 10, LM 21, LM 22).

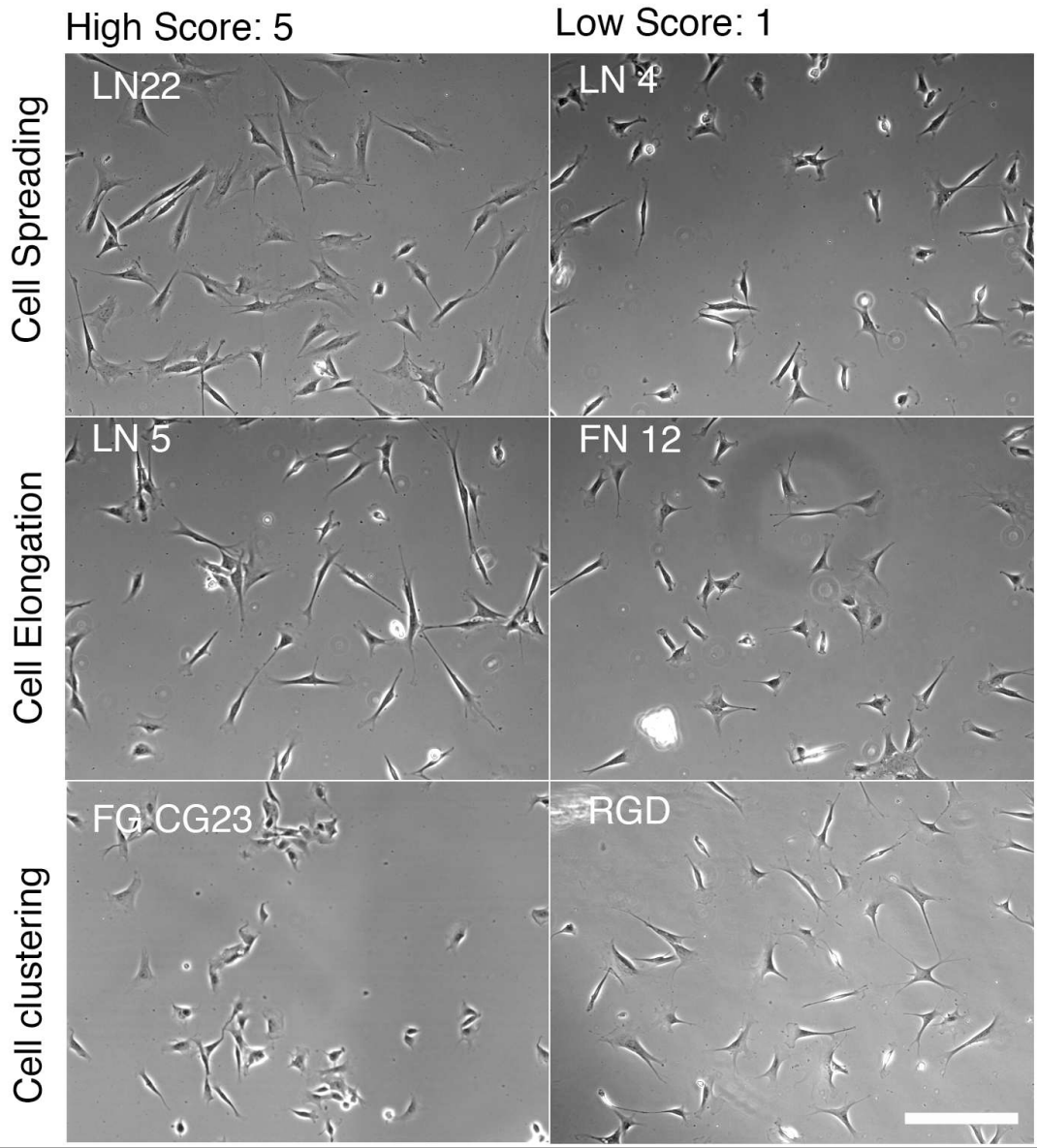

ECM	Amino Acid Sequence	Adhesion		
		Spread	Polarized	Cluster
Fibrinogen CG-23	ganma 377-395 or P2 YSMKKTTMKIIPFNRLTIG	1	1	5
Fibrinogen CG-17	ganma 383-395 or P2C / TMKIIPFNRLTIG	1	1	5
Tenascin CL-12	AEIDGIEL	1	1	1
VCAM 1 CS-8	QIDS	2	3	1
Collagen CR-10	GFOGER	3	2	1
Control CK-9 (0)	**RGD cyclic c (RGDFK)**	**3**	**2**	**1**
Fibronectin #1	YRVRVTPKEKTGPMKEM (C-terminal heparin binding domain)	2	4	1
Fibronectin #2	YEKPGSPPREVVPRPRPGV (C-terminal heparin binding domain)	3	3	1
Fibronectin #3	KNNQKSEPLIGRKKT (C-terminal heparin binding domain)	2	4	1
Fibronectin #4	DELPQLVTLPHPNLHGPEILDVPST (IIICS, CS1)	1	3	2
Fibronectin #5	GEEIQIGHIPREDVDYHLYP (IIICS, CS5)	2	5	2
Fibronectin #6	IDAPS (IIICS)	2	3	2
Fibronectin #7	LDVPS (IIICS)	2	3	2
Fibronectin #8	WQPPRARI	1	2	1
Fibronectin #10	ATETTITISWRTKTE (C-terminal heparin binding domain)	4	2	2
Fibronectin #12	KLDAPT (repeat III5)	1	1	1
Fibronectin #13	EDGIHEL	1	2	1
Laminin #14	DYAVLQLHGGRLHFMFDLG (LG4 Module, laminin alfa1 chain hEF-1)	2	4	1
Laminin #15	KNSFMALYLSKGRLVFALG (LG4 Module, laminin alfa 3	3	2	2
Laminin #18	IAFQRN (LG2 domain, laminin alfa 1 chain)	2	2	3
Laminin #19	YIGSR	2	2	2
Laminin #20	LGTIPG	1	2	2
Laminin #21	CSRARKQAASIKVAVSADR	4	3	1
Laminin #22	RYVVLPRPVCFEKGMNYTVR	5	2	2

Figure 5.2: Images of representative ligands, showing manual high or low scores in spreading, elongation and clustering. The table summarize the scoring assign to the first round of selected peptides. The given screening code identifies the ECM peptide and the associated number is not related to any nomenclature, but simplicity to cite the sequence in the screen. The scale bar is 100 um.

5.2.3 Validation on selected candidates

Adhesive peptide candidates were selected based on their adhesion performance, strong phenotypic changes (high score) and/or rare phenotypes such as clusters. In this manner we identified hits that in visual scoring were significantly different from controls.

Candidates were revalidated twice. In the first round the phenotype in all the screen images was visually examined again. Figure 5.3 summarizes the phenotypic observations. In the validation process, fibronectin (FN) ligands 1, 3 and 5 did not appear elongated and the results were not reproducible. Fibrinogen (FG) peptides CG23 and CG17 looked alike (hetereogeneous clusters) with high standard deviations. Both fibrinogen peptides belong to the same region in the fibrinogen molecule and differ from each other in few aminoacids (see figure 4.10 in section 4.2). The phenotype of Fibronectin 10 is similar and slightly spread in relation to the control. Some cells in the Laminin 14 appeared more elongated. Laminin 21 and Laminin 22 spread above all the most.

In the second verification the number of adherent cells are re-counted. The cell shape in segmented and values of spreading as well as elongation are obtained. FA number, area and elongation are also quantified. Due to the large amount of data and in order to highlight the most relevant features for comparison, the multiparametric plot is reduced to 3 variables (cell area, number of adherent cells, and number of focals) as shown in figure 5.4. A complete statistical quantification and analysis for the second validation are in figure 5.5.

The values are report having as a base line the RGDfk control to visualize the decrease and increase in relation to the control. The reported standard deviations appear high, this is attributed to a wide population of cells, including those that are dividing and starting to spread. The histograms show in the upper right corner the size of the population.

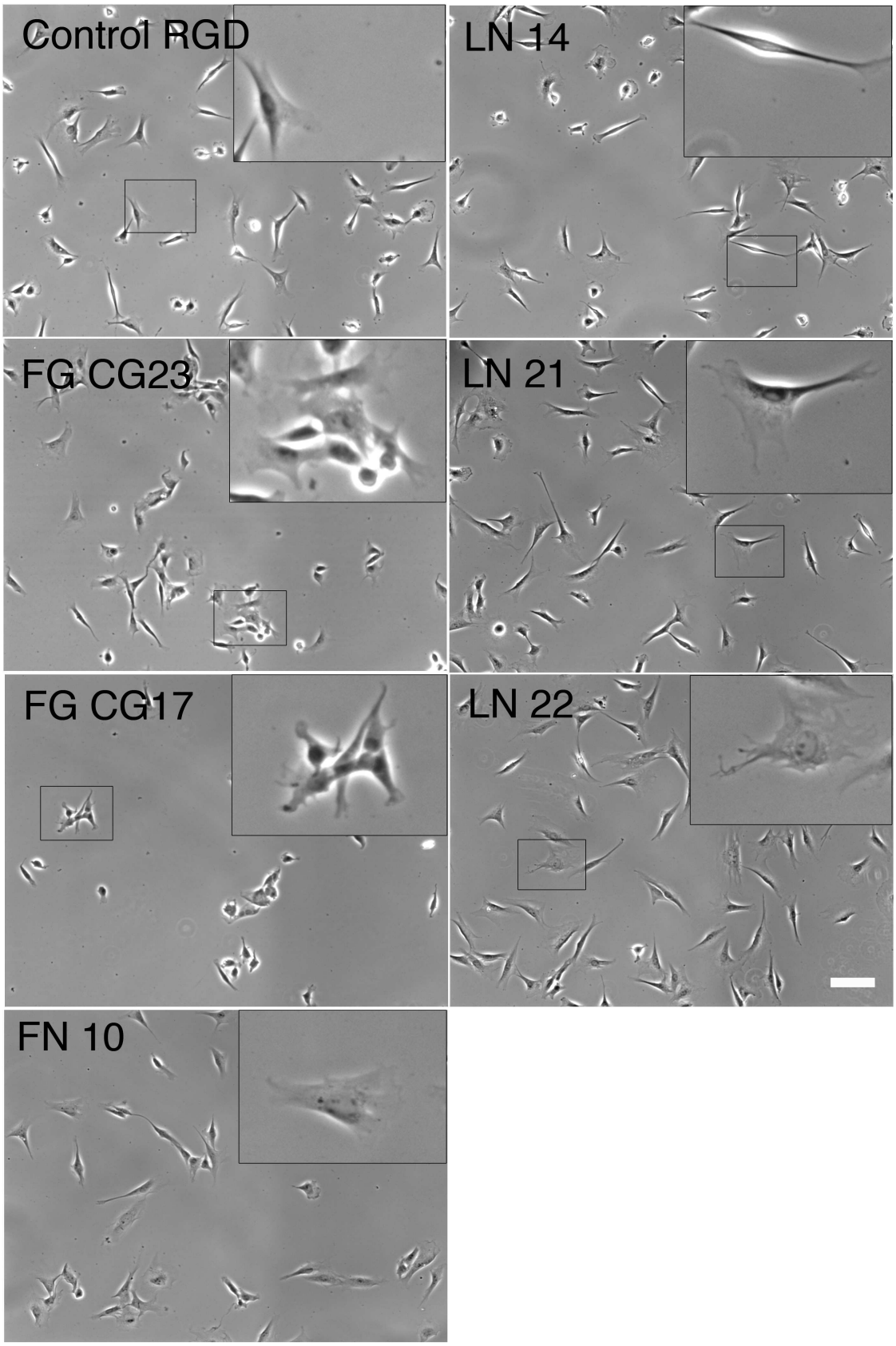

Figure 5.3: Revalidation of phenotypic changes. Fibronectin 10 is similar to the control, Laminin 14 is slightly elongated and Laminin 21 and Laminin 22 spread above all the most. FG CG 23 show a rare phenotypes of cell cluster. The scale bar is 100 um.

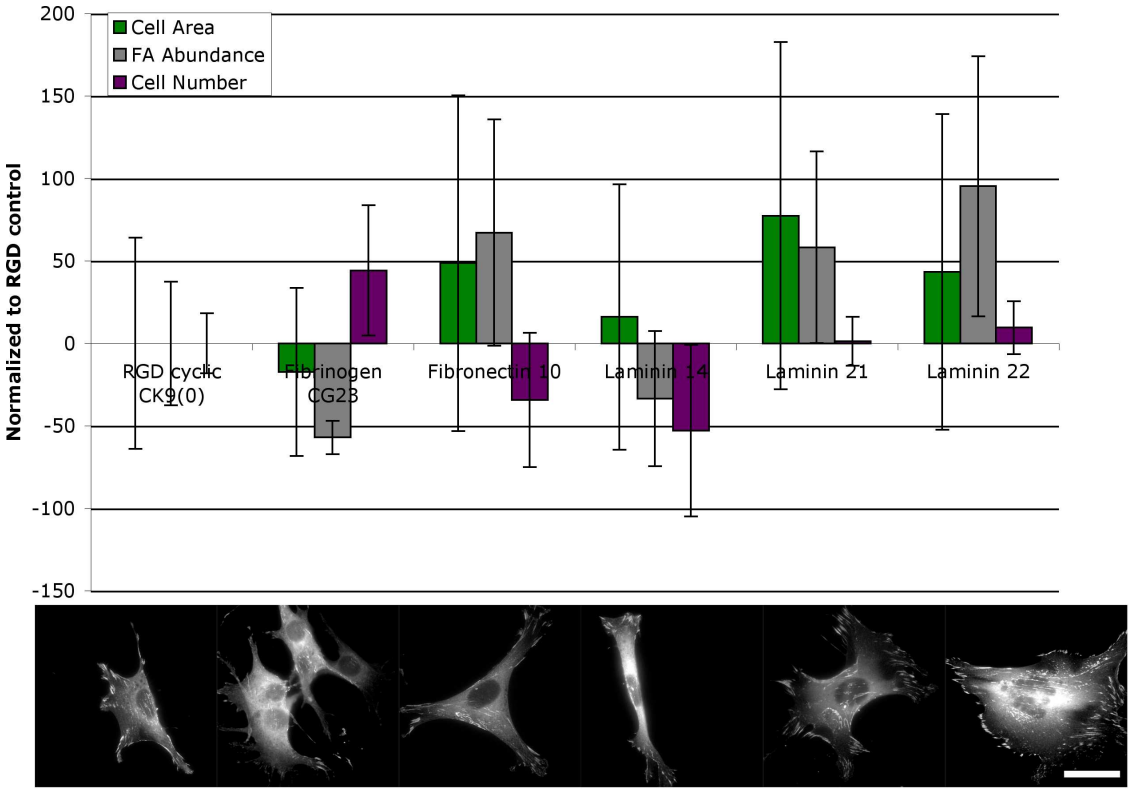

Figure 5.4: Multiparametric plot showing main relative variations among peptides at 52nm. Base line control corresponds to RGDfk (zero). The average cell area n=1631sq um out of 399 counts in a set of 8 images, average FA number n=51 out of 740 counts in 12 pictures, average cell number n=49 out of 399 counts in a set of 8 images. The FA images at the bottom show paxillin adhesive structures, most of them in the periphery. Scale bar is 25 um.

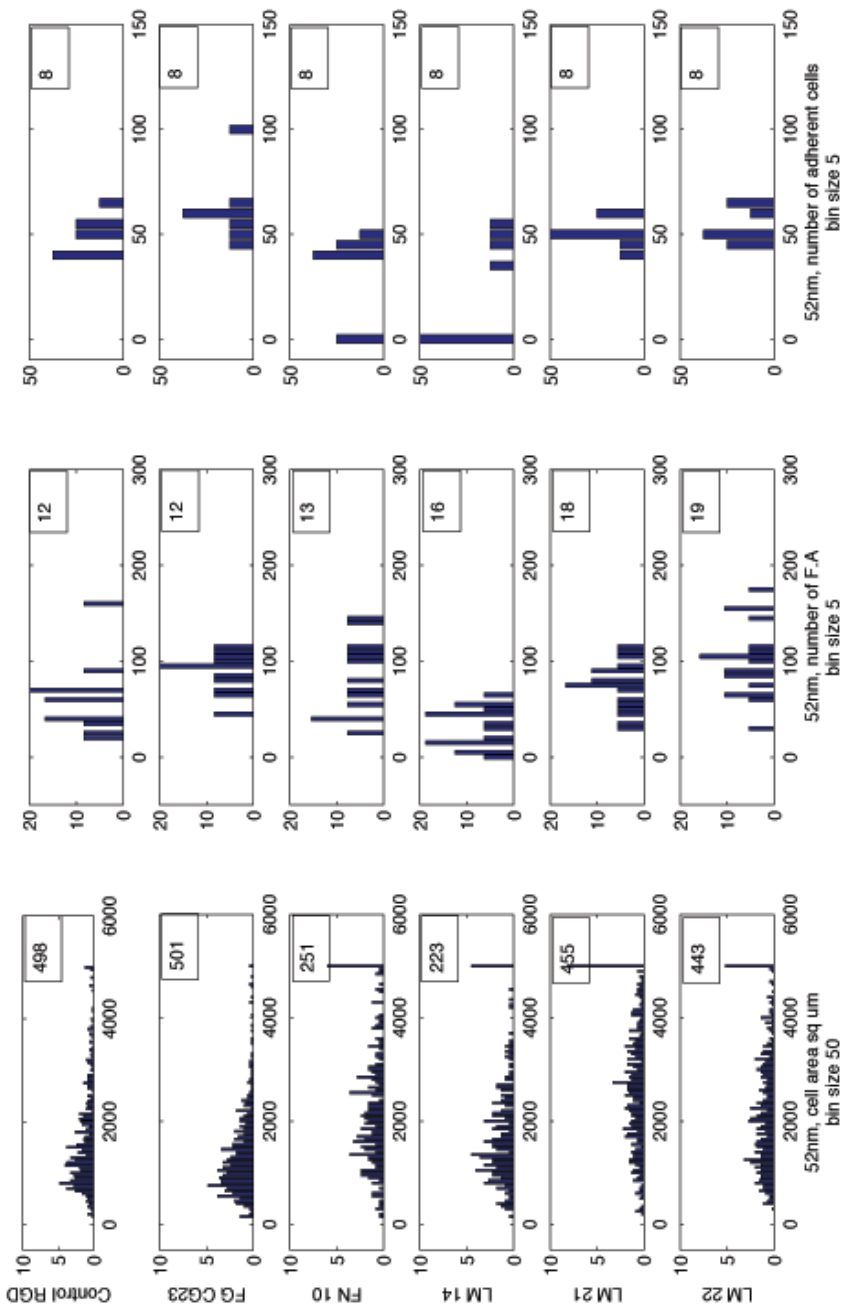

Figure 5.5: Mutiparametric fistogram (cell area, number FA, number of cells) at 52nm.

5.2.4 Adhesion review on selected candidates

The changes in phenotype are an intrinsic property of the adhesive perturbation. The same systematic error in the substrate preparation and cell culture applies to all the evaluated conditions. Under the screen frame conditions and all the inclusive variables (such as ECM self-production), the ligand plays a pivotal role in the adhesion activity here report (figure 5.6).

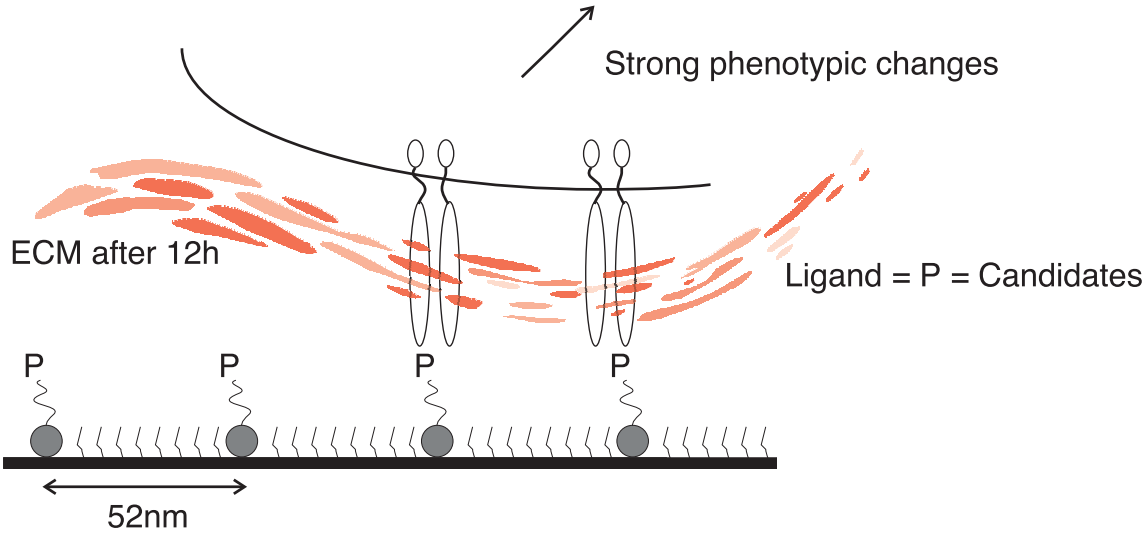

Figure 5.6: The same systematic error in the substrate preparation and cell culture applies to all the evaluated conditions, including self produced ECM.

Figure 5.7 condenses relevant information of the candidates ligands experimentally studied in this research. In the table the associated receptors found in literature are reported. No statements or final conclusions can be made between the ligand-receptors reported in literature and the change in morphology / adhesion observed experimentally. More than one receptor could be involved in recognizing such a sequence. It is not possible to assume that such receptors reported in literature are present in C2 cells. To answer this question, immune fluorescent antibody staining of integrins and proteoglycans is the next step to ensure the presence of the potential receptors. The FACS technique could be potentially used to target this question.

It is observed on the reported C2 cells, a high spreading and high score in adhesion for the laminin 22. The laminin peptide 22, displayed the highest FA abundance from all candidates. Two times more than the RGD fibronectin control alone. This synthetic laminin fragment (20 amino acids long) has been shown to exhibit strong

Reference	Binding Site	Receptor Class or Size	Notes.
RGD Control	RGDfk	$\alpha_V\beta_3$	Well known tripeptide, Arg-Gly-Asp that binds specifically to $\alpha_V\beta_3$ [ref. A, B, C, D]
Fibrinogen CG23	YSMKKITMKITPFNRLTIC Gamma 733-395	$\alpha_M\beta_2$	The sequence correspond to the γ chain of fibrinogen (Fg) and interacts specifically with the integrin $\alpha_M\beta_2$, suggesting it contain identical recognition information. Paradoxically, $\alpha_M\beta_2$ recognize a broad ligand repertoire. [ref. E, F, G]
Fibronectin 10	ATECTITISWCTKTE COOH-terminal heparin binding domain	$\alpha_{IIb}\beta_{3a}$	Fibronectin RGD independent binding site, mimetic from the 29Kd fragment $Ala1^{592}$ to Glu^{1963} [ref. H]
Laminin 14	DYAVLQLHGGRLHFMFDLG LG 4 domain, alfa 1 chain	$\alpha_2\beta_1$, Syndecan 2 (Heparan Sulfate Proteoglycan)	Induces cellular activity through both $\alpha_2\beta_1$, Syndecan 2. The sites contain positively charged amino acid residues, such as Lys and Arg, that are crucial for interaction with negatively charged heparan sulfate chains. [ref. I]
Laminin 21	CSRADKCAASIKAWVSADR Alfa 1 chain	67Kd CAM Receptor	Non integrin laminin binding protein found to interact with the 67Kd receptor. The function of the 67kd laminin receptor, is to stabilize the binding of laminin to cell surface integrins, acting as a integrin accessory molecule. 67 kd protein also binds to elastin with an affinity aaproximately equal to laminin. [ref. J, K, L]
Laminin 22	RYVDLPRPVCFEKGMNYTVR Beta 1	Heparan Sulfate Proteoglycan	Small fragment of laminin (less than $1/300^{th}$ of its molecular mass) potent in promoting cell adhesion in melanoma cells. It is suggest that the binding is not due to exclusively ionic interaction. [ref. J, M, N, O]

Figure 5.7: Summary of selected candidates. The given screening code identifies the ECM peptide and the associated number is not related to any nomenclature, but simplicity to cite the sequence in the screen. References A, B, C, D, E, F, G, H, I, J, K, L, M, N, O correspond respectlively to [140], [66], [79], [95], [142], [180], [94], [114], [199], [108], [184], [172], [27], [33], [161].

heparin binding activity [27]. Many cells exhibit heparin-like structures on their surface [50] [122]. Cell surface heparan sulfate (HS) present in adherent cells, is synthesized on a variety of cells surface proteins but is mainly present on two major families of membrane-bound proteoglycans (PG's), the syndecans and the glypicans [12].

Previous studies have shown that syndecans act as adhesion receptors by engaging with fibronectin, laminin or vitronectin [38]. Syndecans which consists of a protein core with covalently attached heparan sulfate chains [(glycosamiglycans)] also bind to (GF) growth factors (including transforming growth factors TGF such as BMP [12] [150]) that are either dilute or distant from their specific receptors, and essential

co-receptors to GF's and therefore parts of of the integrin-GF receptor system [169].

Overall the interest feature of proteoglycan receptors lies on the glycoamino chain. It modulates the activation of a large number of extracellular ligands. It is reported in literature that such chains, synergistically activate integrin activity [169] [116] [12].

It is established that syndecans can co-operate synergistically with integrins to regulate adhesion-complex formation, cell spreading and directional migration. There is co-operation between syndecans and laminin -binding integrins ($\alpha_2\beta_1$, $\alpha_6\beta_4$), and syndecan-4 synergizes with the FN-specific $\alpha_5\beta_1$ integrin. In addition, syndecans can activate integrins, for example syndecan-1 regulates the migratory function of $\alpha_V\beta_3$ integrin . Thus individual combinations of syndecan–integrin pairs influence the type of signalling proteins recruited at adhesion complexes, and consequently the physiological response elicited [169].

We speculate that adhesion in laminin 22 could be attribute to synergistic effects between syndecans and integrins (figure 5.8). The substrate decorated with the laminin peptide might activate the proteoglycan receptor and the glycoamino chains funtion as (i) ligand for subsequent integrins and/or (ii) binding growth factors that enhance adhesion or cellular response.

An important outlook of this screen is to further explore laminin 22 sequence, and characterize the receptors involved in its activity. This might unleash answers in the combinatorial engagement of syndecan-integrin.

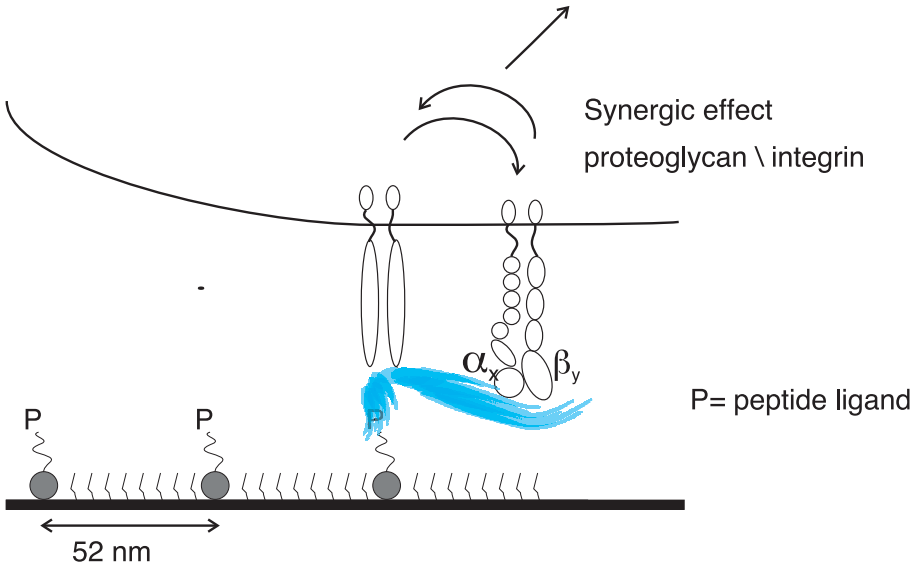

Figure 5.8: This rather speculative model highlight the importance of combinatorial integrin-syndecan interaction and the role glycosamiglycans chains playing as ligands that activate integrins and/or bind soluble growth factors.

5.3 Closing remarks

A library of 33 ECM derived peptides ligands were screened systematically. First, the peptide library is evaluated for cell attachment. Then, a qualitative phenotypic rating system is introduced, and later measurements of significant phenotypic characteristics are performed, figure 5.9 summarize the screening strategy. Out of this library 3 laminins, 1 fibronectin and 1 fibrinogen adhesive peptides-ligands were identified and revalidated that induced a defined phenotype. Figure 5.9 summarizes the strategy used to select peptide-ligands on C2 as reporter cell.

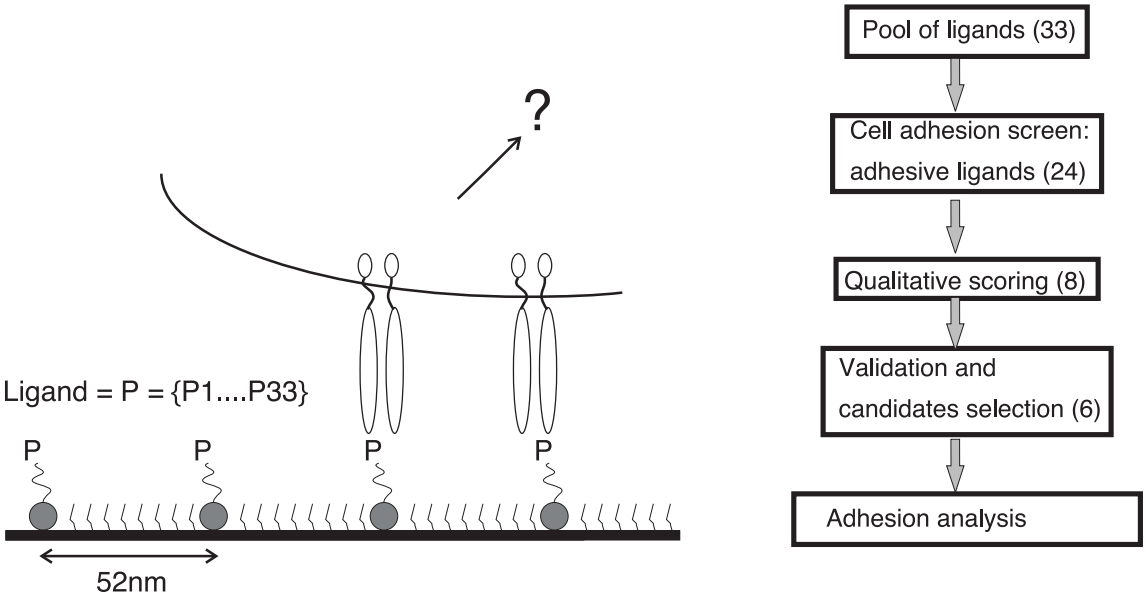

Figure 5.9: The input variable in the system consisted of a library of 33 extra cellular matrix (ECM) peptides. The chosen platform substrate for the screening was the gold nanodot surface with 52nm nanodots spacing.Out of 33 ECM peptide ligands, 24 showed adhesion above 40% in relation to RGDfk control. After quantifying the number of adherent cells in the screen, 8 peptides were qualitatively selected and 6 revalidated (5 candidates + control).

Chapter 6

Screening spatial cues: distance dependency

6.1 Introduction

After screening a library of ECM ligands, as chemical perturbations, we identified 5 candidates that produce accentuated phenotypic differences on well defined nanostructures. Here we explore the spatial cues dependence upon cell adhesion. The ECM candidates were screened on gold nanodots surfaces spaced at 52nm, 70nm and 116 nm. The peptides are linear, up to 20 amino-acid short sequences and non RGD containing. The significant phenotypic characteristics evaluated on this screen were cell shape, which includes spreading and elongation and paxillin FA morphology, which includes FA area; FA length; and FA abundance. Statistical analysis is shown with detail in this chapter. Figure 6.1 shows an overview of the chemical and spatial cues addressed in the screen.

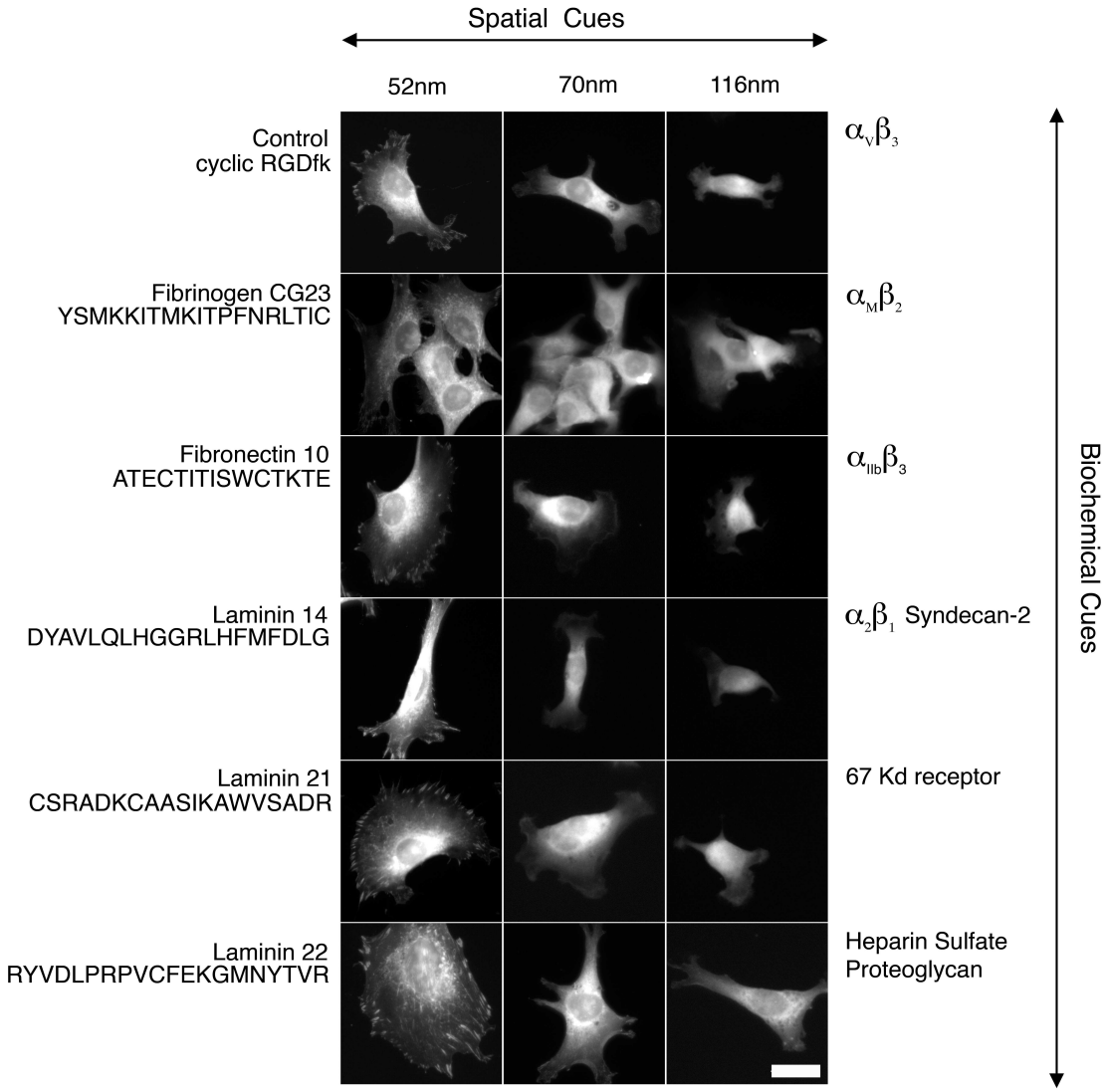

Figure 6.1: Overview of the chemical and spatial cues address in the screen. Chemical cues: The peptides are linear, up to 20 amino-acid short sequences and non RGD containing. The associated receptors known in literature are shown in the right side. Spatial cues: the ECM candidates were screened on gold nanodots surfaces spaced at 52nm, 70nm and 116 nm. The C2 muscle progenitor cells express paxilling-YFP as FA component. The scale bar is 25 um.

6.2 Results and discussions

6.2.1 Cell number and spatial cues

The cell based screening was extended from 52nm to 70nm and 116nm ligand spacing. The number of adherent cells is shown in figure 6.2. The number of adherent cells at 52nm is considerably higher for all ligands. Fibrinogen CG23 induced the highest value of adherent cells (heterogeneous cluster of cells). At 70nm and 110nm values drop to 20-30% in all peptides as compared to the control.

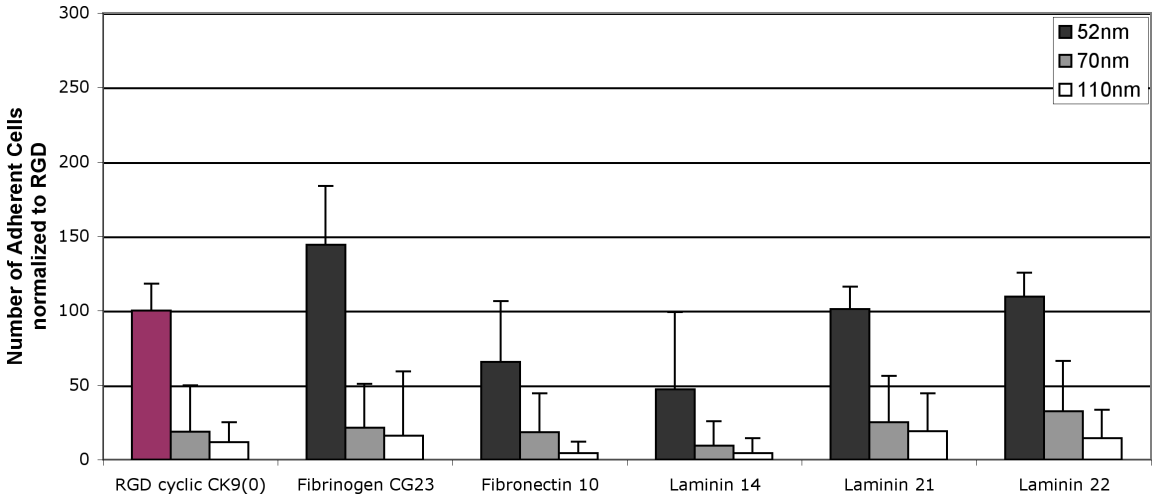

Figure 6.2: Adhesion dependence and spatial cues. The number of adherent cells drop below to 50% and 30% at 70nm and 116nm spaced between gold particles.The average number of adherent cells in control within a field of 10x, was n=49 out of 399 counts in set of 8 images.

6.2.2 Cell shape and spatial cues

Cell segmentation was performed in order to quantify cell spreading and elongation which is shown in figure 6.3. Cell area showed higher spreading with the nanogold dots spaced at 52 nm in peptides Fibronectin 10, and Laminin 21 and 22 (scored above 150% in comparison to the control). At 70 nm and 116 nm ligand spacing, a decreasing cell spreading tendency is observed. Cell area results on Fibrinogen CG23 were more irregular, and the distance seems not to affect the spreading behavior on this peptide condition that shows a rare cluster morphology.

On the other hand, elongation is not significantly affected by the ligand spacing as shown in (bottom figure 6.3). Elongation is reported as the ratio between the two axes of approximated elipses. The result indicates that the shape of such ellipses remains more or less the same, independent of the peptide and distance.

Note that the standard deviation bars in the cell spreading area are large. This is due to a wide population of cells including those that are dividing and starting to spread. A complete histogram with the measured populations are shown in figure 6.4. The wide populations distributions shrink when the distance between ligand is higher. A good example that highlight the distance dependency can be appreciated on peptide laminin 22 in the mentioned histogram.

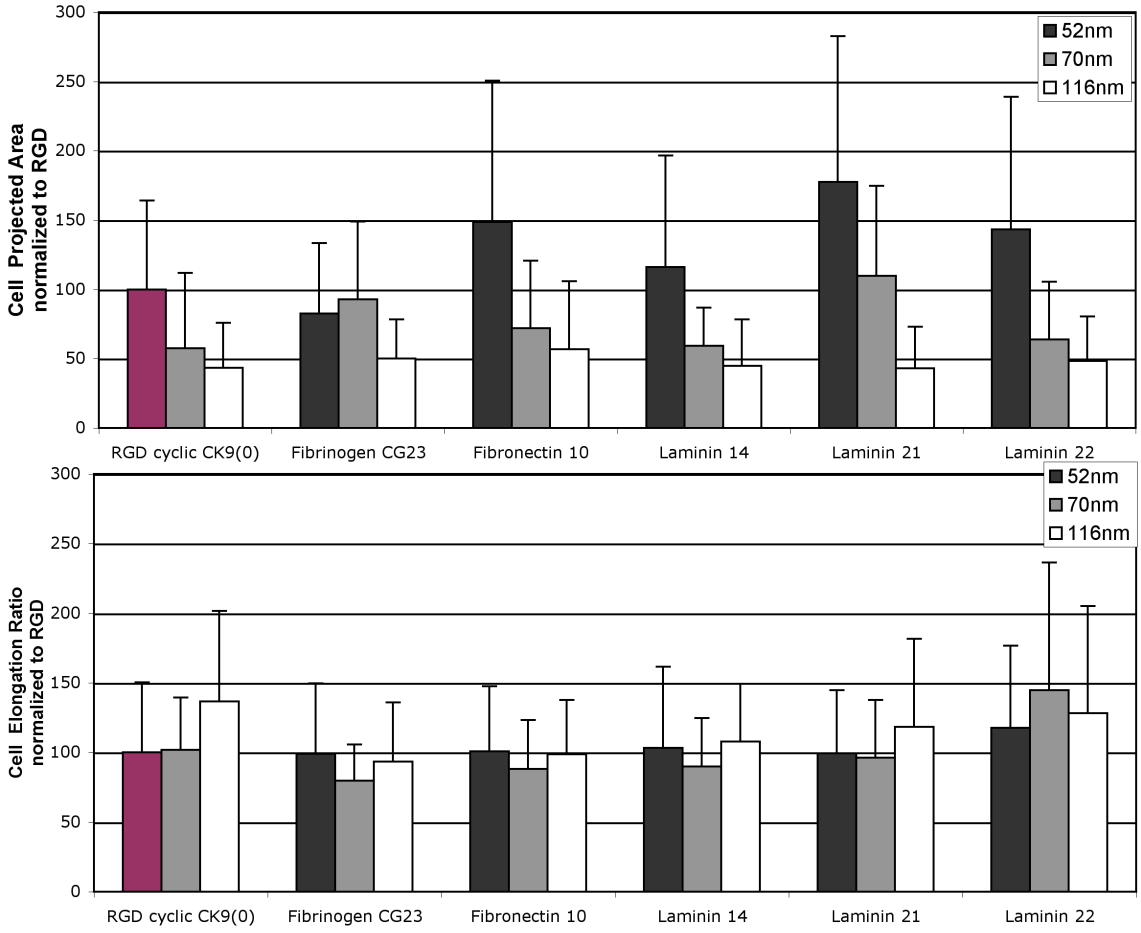

Figure 6.3: Top: Cell area showed higher spreading with the nanogold dots spaced at 52nm in peptides Fibronectin 10, and Laminin 21 and 22 (scored above 150% in comparison to the control). At 70nm and 116nm ligand spacing, a decreasing cell spreading tendency is observed with the exception of Fibrinogen CG23 that shows a rare cluster morphology. The average cell area in control was n=1631 sq um out of 399 counts in set of 8 images. Bottom: Elongation is not significantly affected by the ligand spacing. The average elongation ratio in control was n=2,36 out of counts 399 counts in set of 8 images.

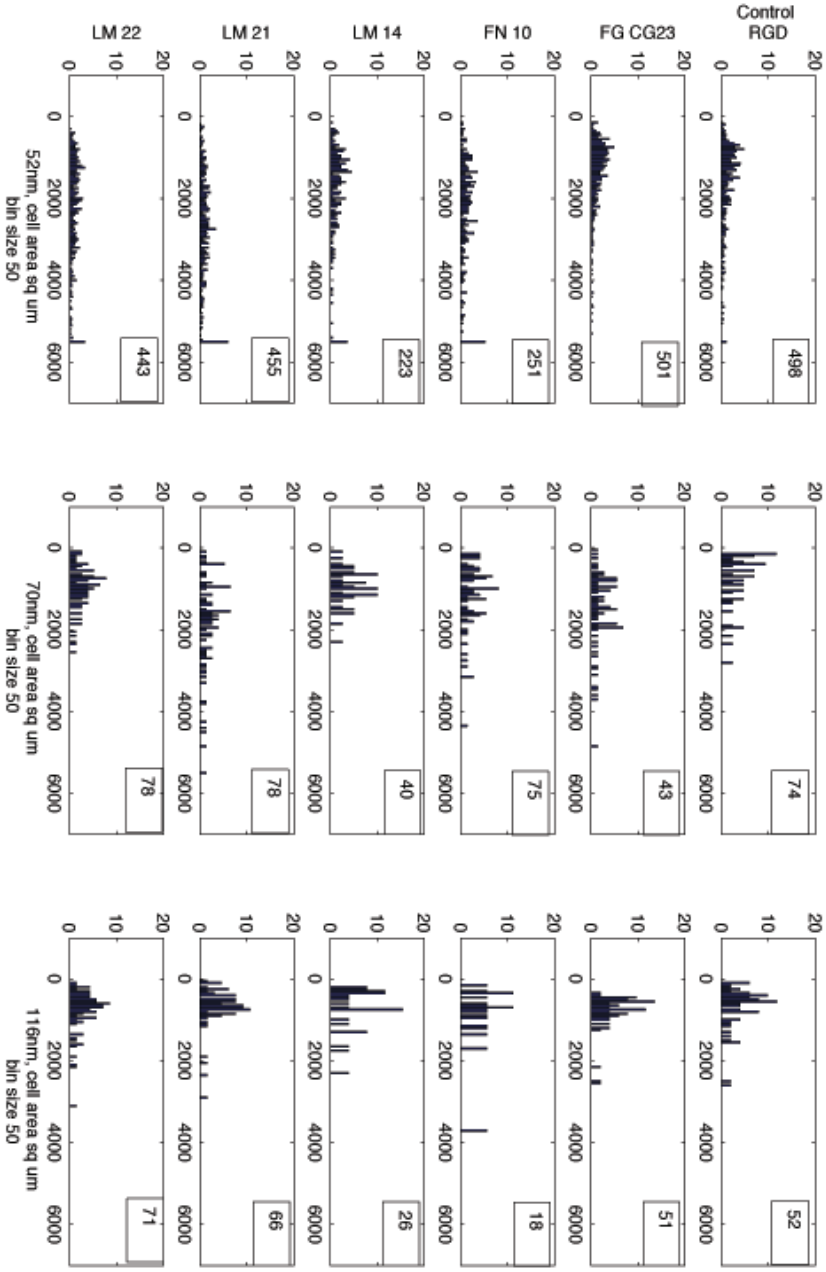

Figure 6.4: Histogram showing cell spreading distribution on gold nanodots spaced at 52 nm, 70 nm and 116 nm. A good example, showing the distance dependency and cell area spreading can be appreciated on peptide Laminin 22.

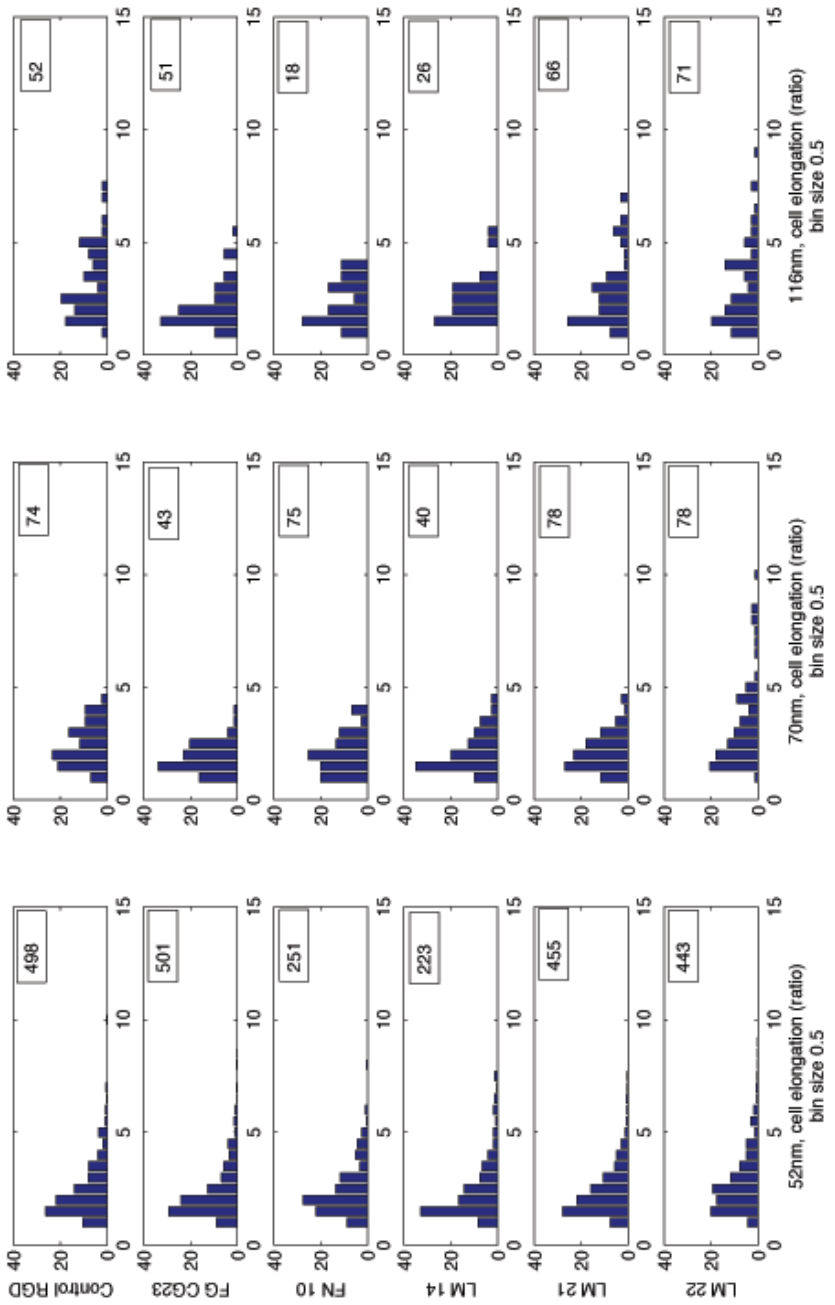

Figure 6.5: Histogram showing cell elongation distribution on gold nanodots spaced at 52 nm, 70 nm and 116 nm.. Cell elongation is not strongly affected.

6.2.3 Focal adhesion and spatial cues

The "sites" of adhesion consist then of focal complexes, focal adhesions and fibrillar adhesions. FA area, number and elongation is quantified in relation to the RGD control and present in figure 6.6. Statistical details are shown as complete histograms in figures 6.7, 6.8 and **??**. In fibrinogen CG23, the number of focals were determined by dividing all the focals in the image field to the average cluster size among the collected data (4-5 cells).

F.A area and number decreases with increased spacing. This tendency is regardless of the peptide studied. The substrate with 52nm of ligand spacing provided a higher number of adhesion sites. Abundant and larger focal adhesions mainly at the cell periphery are reported for the selected candidates at 52nm. F.A area and number decreases with increased spacing. This tendency seem independent and regardless of the peptide studied. The substrate with 52nm of ligand spacing provided a higher number of adhesion sites. Less paxillin containing structures are formed at 70nm. At 110nm,with the exception of ligand laminin 21 and 22, few visible paxillin structures in the collected data.

F.A elongation does not seem to be affected, either by the ligand nature or distance. The elongation is reported as a ratio with no length units. The shape of the elipse representing the paxillin site remains relatively unchanged (Figure 6.6)

The results in section 6.2.1 and 6.2.2 on the C2 muscle cell line, suggest that the distance plays a role in the number of adherent cells and cell spreading (except for FG CG23). At 70nm and 110nm spacing between ligands adhesion performance drop. The FA area and number here presented, also follow the trend, score values decreases to 50% with increased spacing to 70nm.

Whether 70nm is a threshold or barrier where formation of stable contacts and takes place, its a question for further research. More points to describe a curve are neccesary. Additionally, the ligand-receptor for the molecules evaluated in this study required further characterization.

There is also lack of information in the range between 70nm and 116nm. Recent, studies on neuron attachment and growth have shown that anchorage of a cytoskeletal protein (spectrin) to DM-GRASP molecules inmobilized in nanopatterns drop at 70nm. Later adhesion recovers at 80nm and falls again at 110nm [75]. The phenomena is attributed to the geometry and size of the DM-GRASP molecules which is 35 amino-acids long. No detailed information such as the folding and orientation of the linear peptides in this study (20 amino acids long) are known.

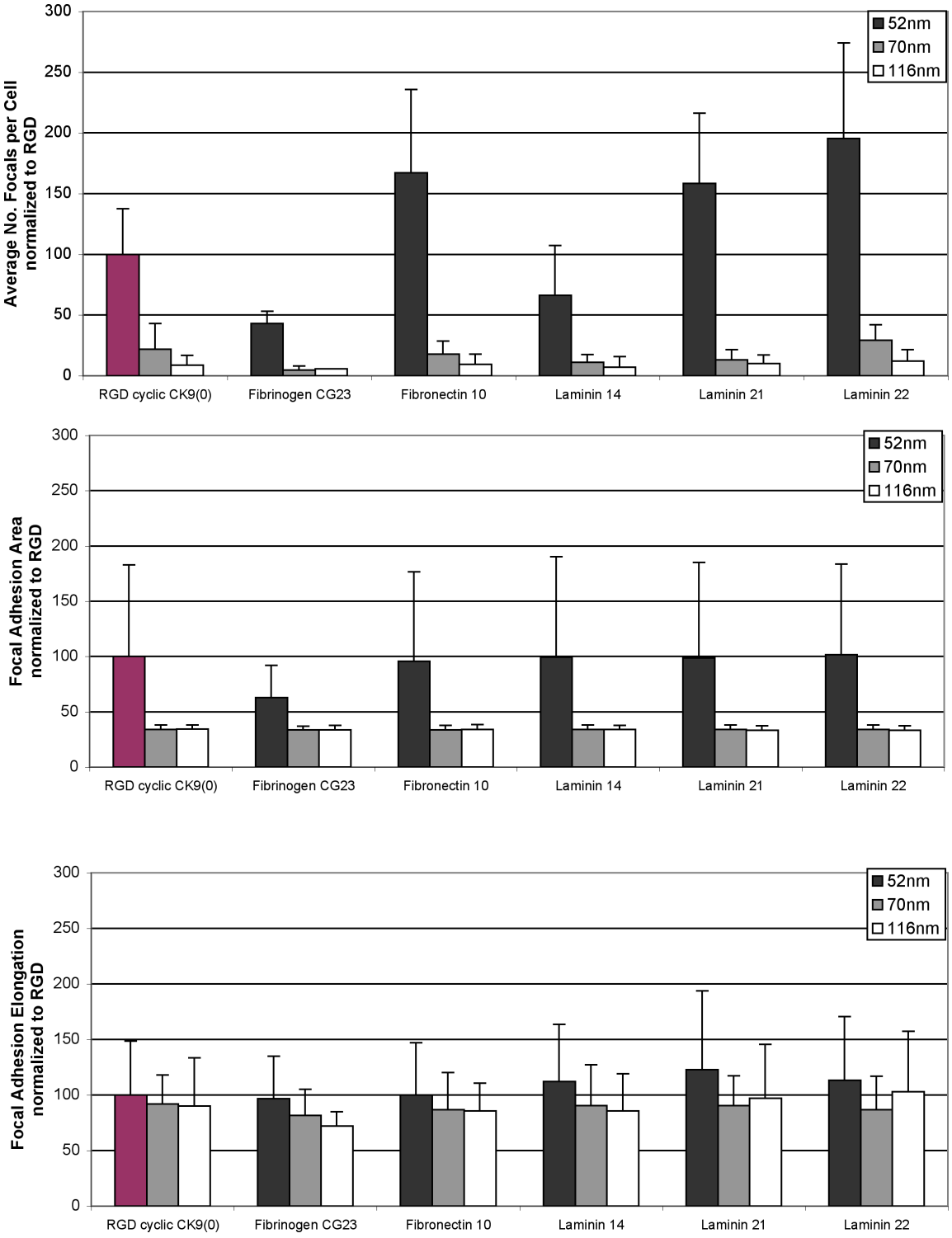

Figure 6.6: Focal adhesion and spatial cues. Top: Laminin 22 scored the highest at 52nm, with two times more FA than the control. FA number values drop below 40% and 20% at 70nm and 116nm. Average number of FA per cell in control n=51,7 out of counts 740 counts in 12 pictures. Middle: The FA area dropped below 50% for the ligands at 70nm and 116nm. Average FA area per cell in control n=70, 7 out of counts 740 in 12 pictures. Bottom: The elongation of FA doesnt appear to be affected by the interspace distance between ligands. Average FA elongation per cell in control n=2,15 out of counts 740 in 12 pictures.

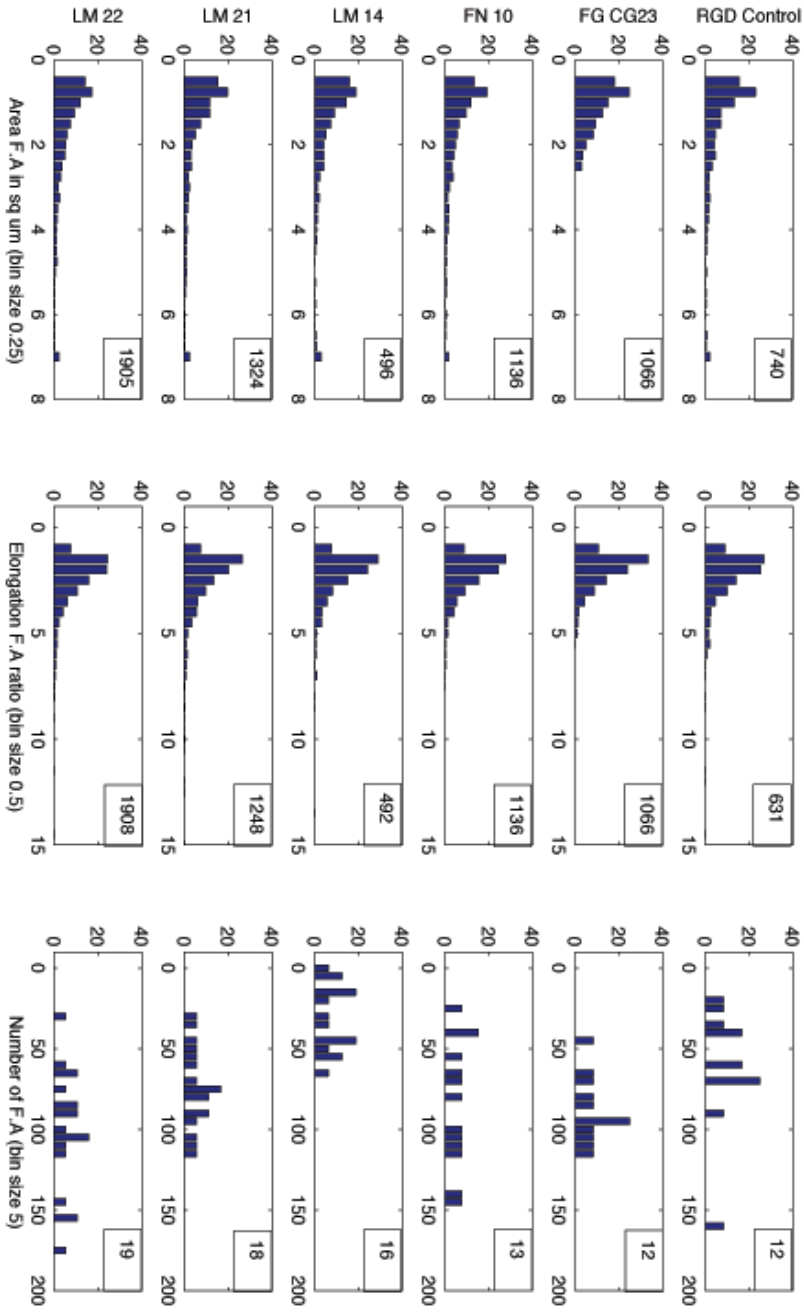

Figure 6.7: Complete histogram showing F.A area, elongation and number for selected candidates in 52nm substrate.

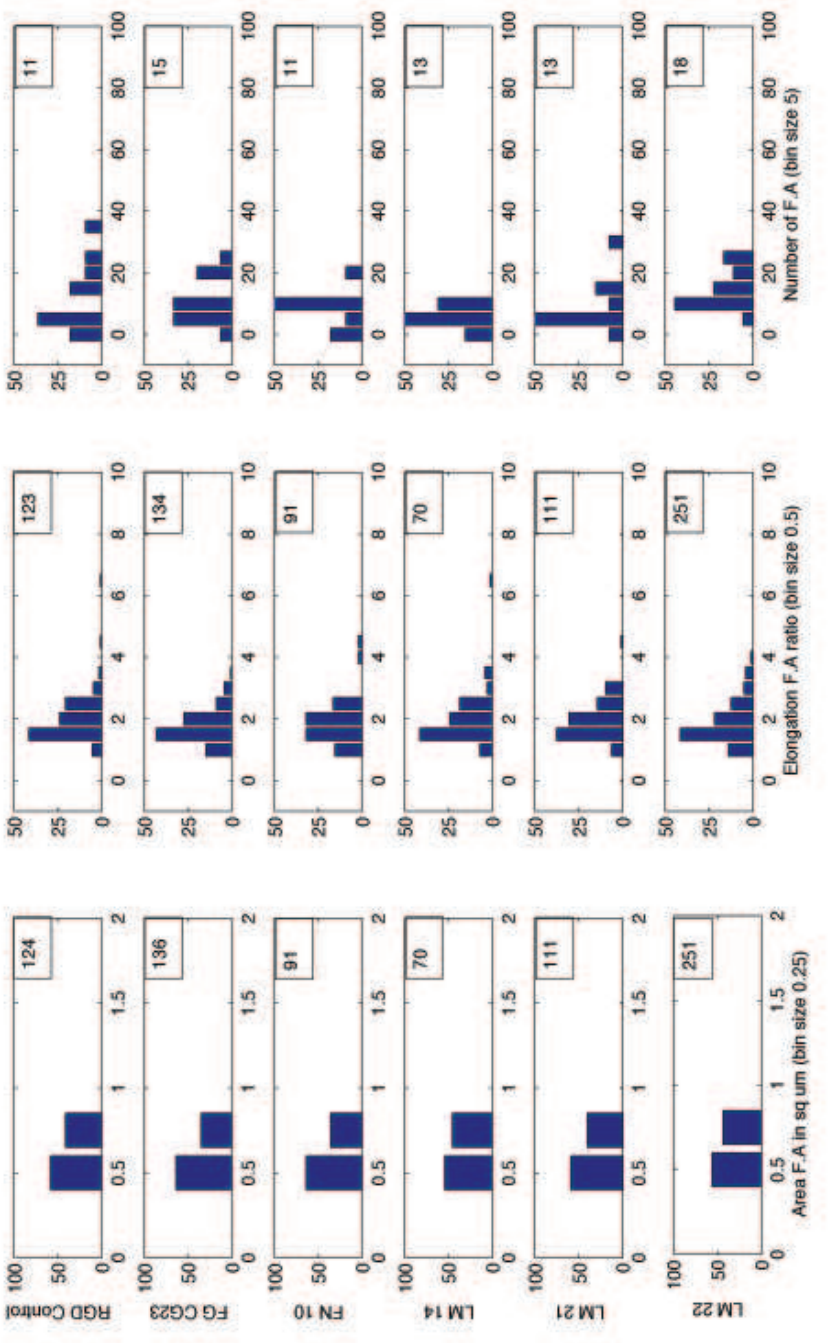

Figure 6.8: Complete histogram showing F.A area, elongation and number for selected candidates in 70nm substrate.

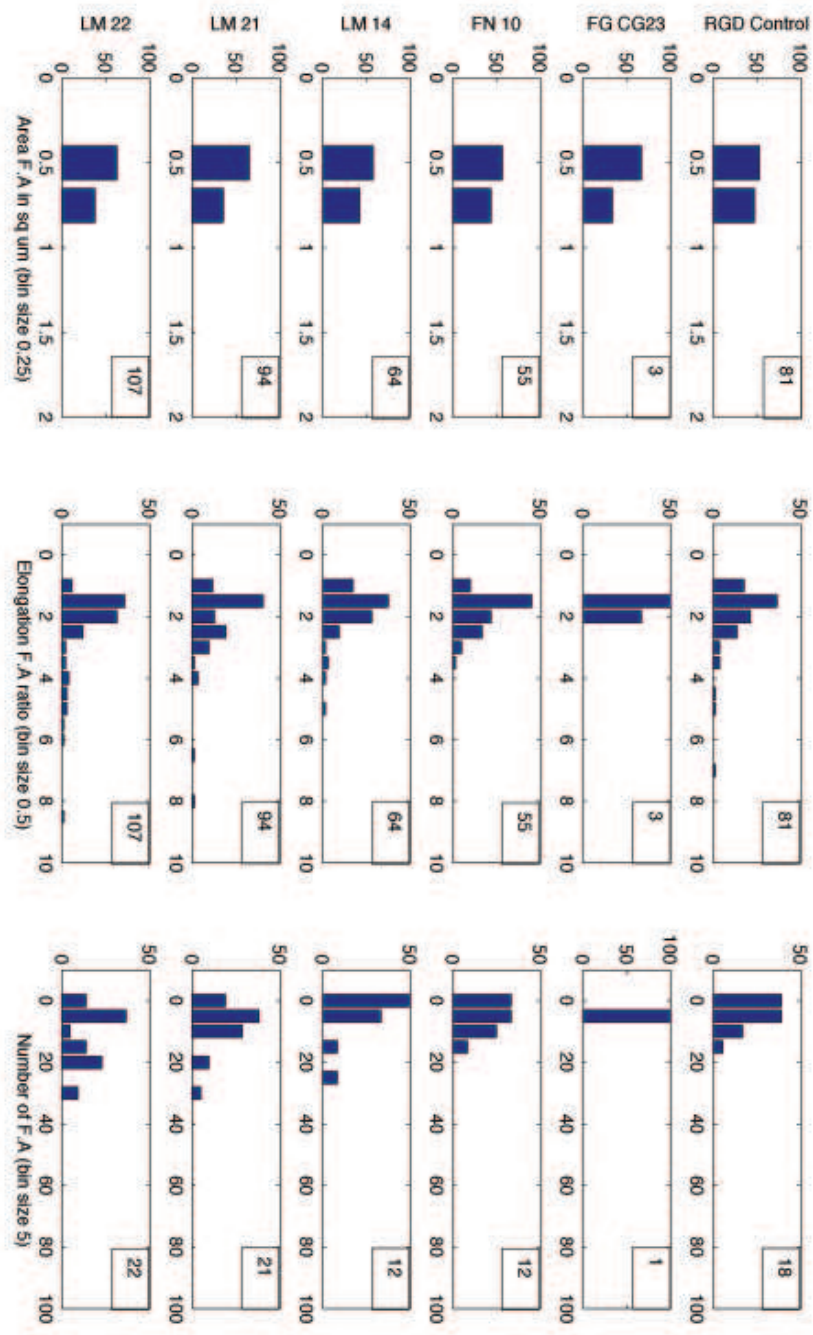

Figure 6.9: Complete histogram showing F.A area, elongation and number for selected candidates in 116nm substrate

6.2.4 Cell specificity: preliminary experiments on REF52

The REF52 fibroblast reporter cell is a well characterized system for RGDfK peptides which specifically recognise $\alpha_v\beta_3$ integrins [24]. The cell adhesion findings on nanopatterns revealed that a distance of less than 58-73 nm between receptor-ligand bonds is necessary to ensure focal adhesion in integrin-mediated cell adhesion on ligand-coated substrates [7]. The formation of stable contacts is fundamental for the maintenance of cell shape [26] and cell adhesion force [160] [25].

The control ECM ligand, in our screen on C2 cells, is also the RGDfk. By comparing FA formation and cell shape between cell lines REF52 and C2, we intent to understand: (a) if the readout phenotype upon ligand perturbation is cell specific (b) if FA activation below 70 nm is independent on the receptor, ligand and the cell type.

When evaluating the selected candidates on the REF52 system. We observe no remarkable intrinsic phenotypic differences when varying the ligands upon (figure 6.10). The selected candidates upon the REF52 cells appear to have a less sensitive response, with no major effects in elongation, cell area spreading, or number of adherent cells. Due to time constrains and the large set of images to process no information on focal adhesion is reported for REF52.

By comparing the REF52 to the previous cell shape C2 results (figure 6.11 normalized to control the RGD peptide on C2), its possible to observe the cell specificity response of the ECM candidates upon C2 cells.

In general the REF52 fibroblast spread more in cell area but the number of adherent cells were lower. Visually REF52 appeared more round in shape (low score in elongation) and spread more than C2 cells regardless of the potential ligand-receptor involved. No rare cluster formations were observed when testing adhesion on fibrinogen FG CG23. The cell shape and the adhesion performance on C2 cells was more heterogeneous as discussed in chapter 5. Interestingly, laminin peptides 21 and 22 scored higher cell spreading area on both C2 and REF52 cell lines. The main information is the cell specific phenotype response of the selected candidates upon C2 progenitor cells. The results on phenotype at 52nm ligand spacing are cell specific.

On the other hand when varying the spatial cues, cell area and the number of adherent cells decreases at 116 nm. However, due to the large amount of data to process and time shortening, no concluding data on focal adhesion formation were collected. So far, preliminary cell shape results are presented it here. Further characterization of FA number, size and shape in REF52, might help to know whether FA matrix formation is specific to the density regardless the ligand, the receptor and the cell type involved.

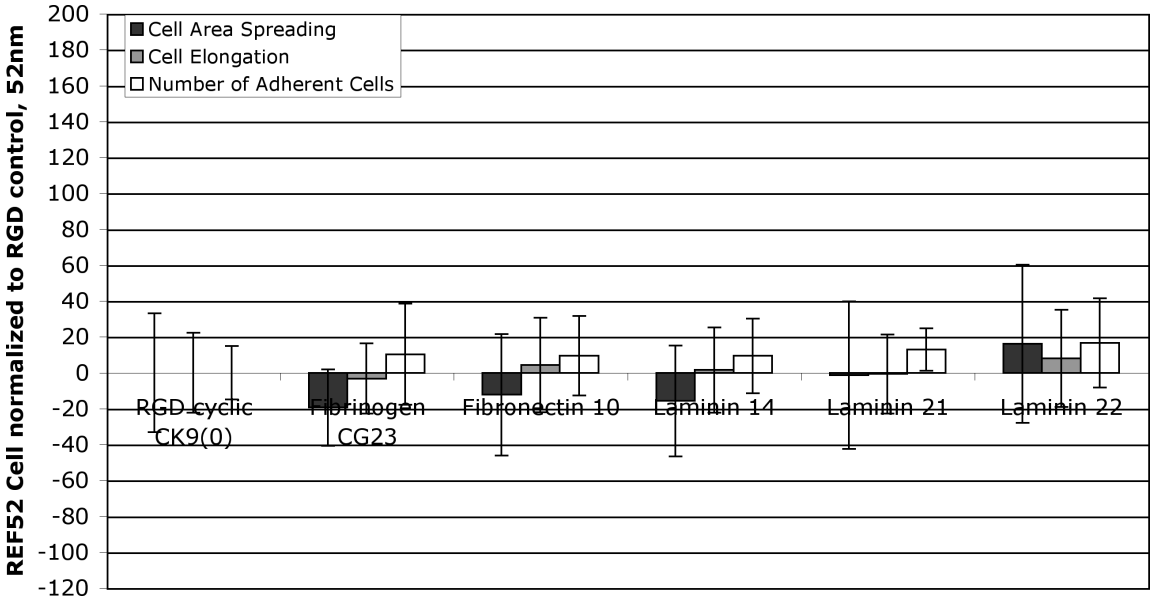

Figure 6.10: Intrinsic phenotypic changes on REF52 cells at 52nm ligand spacing. Base line control corresponds to RGDfk (zero) in REF52. Average cell area n=2457 sq um, average elongation ratio n=1,46 and average no. adherent cells n= 27 out of 223 counts in set of 8 images.

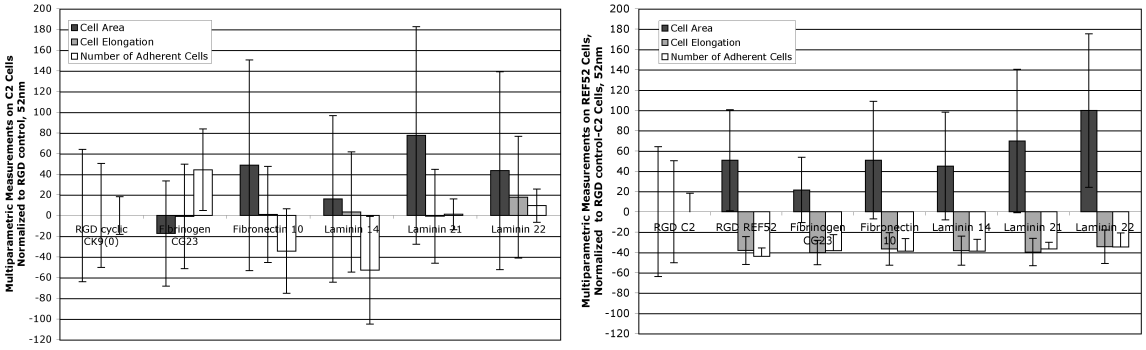

Figure 6.11: Comparative cell adhesion results between REF52 vs C2 cells at 52nm ligand spacing. Base line control corresponds to RGDfk (zero) on C2 cells. Average cell number n=49, average cell area n=1631sq um, average cell elongation n= 2,36 out of 399 counts in set of 8 images.

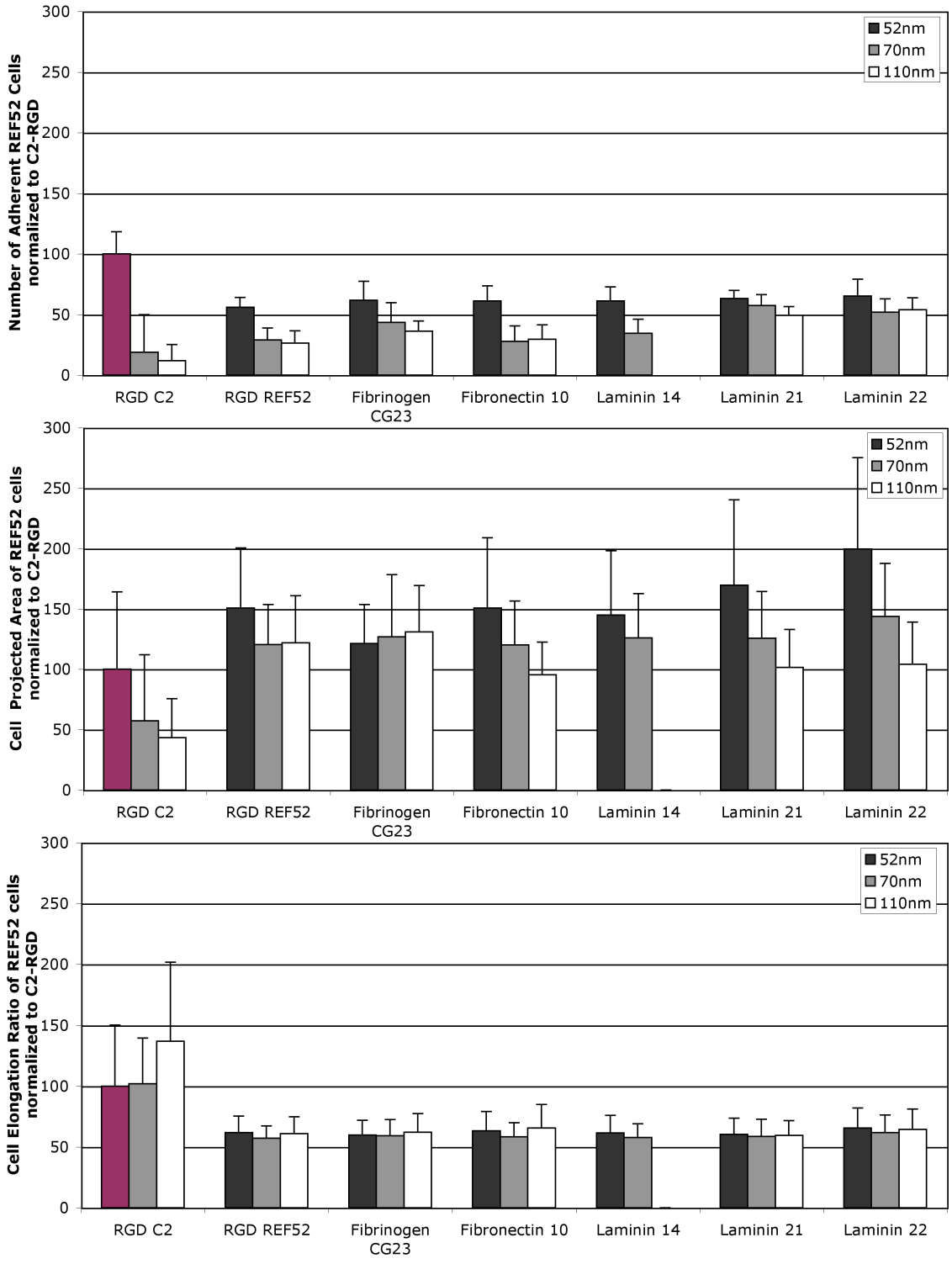

Figure 6.12: Distance dependence upon REF52 cells (number of adherent cells, cell area and elongation). Normalization relative to the RGD peptide on C2 cells. cell number n=49, cell area n=1631sq um, cell elongation n= 2,36 out of 399 counts in set of 8 images.

6.3 Closing remarks

The role of local integrin density, which is critical for the initiation of mature and stable FA assembly was addressed for first time using a peptide pattern method based on diblock copolymer micellar lithography technology [7]. In this study, a critical separation lenght of 73 nm between the adhesive dots is shown to dramatically reduce cell adhesion and spreading as well as the formation of focal adhesions in fibroblast REF52 cells [7].

This feature is not due to an insufficient number of ligand molecules, and not the total number of RGD functionalized nanoparticles, but rather the spatial confinement and the restriction of integrin clustering via $\alpha_V\beta_3$ receptors was crucial for proper cell attachment and spreading [7]. Above the threshold of 73 nm, cells still form lamellipodia and spike-like structures but they lose the stability of their contacts to the surface and undergo major changes in shape and polarity [25]. To form lamellipodia is not influenced by the distance between ECM ligands but the formation of stable contacts, fundamental in the maintenance of cell shape [26] and cell adhesion force [160].

The local generation of mechanical force causes global changes in cell shape (cytoskeleton) and motility, modulating gene expression [23] and producing changes cell proliferation, differentiation and survival. The mechanical force developed by contractile stress fibers within the cell can (i) induce a local Ca+ influx near focal adhesions, (ii) produce the transition of β-integrin subunit from inactive to active conformation [51].

Nascent Focal adhesions normally develop into mature focal adhesions (FA matrix adhesion) as a consequence of the activation of Rho [32] and recruit intermediate proteins such as Vinculin, Paxillin and Talin [204]. In cell based adhesion screens, cell lines usually target fluorescent Paxillin as a prominent component in FA complex [135] [134] [189]. Paxillin phosphorilation has long been associated with the cordinate formation of focal adhesions and stress fibers [149][58].

From the results, obtained in this screen, we observed a tendencies in the adhesion performance, which includes cell spreading and elongation and paxillin FA morphology that is modulated with the (i) peptide ligand and (iii) spatial cue or distance.

The cell area results in this screen showed higher spreading with the nanogold dots spaced at 52nm in peptides Fibronectin 10, and Laminin 21 and 22 (scored 50% more than the control). At 70nm and 116nm between ligand spacing, a decreasing cell spreading tendency is observed. Cell area results on FG CG23 were more irregular, and the distance seems not to affect the spreading behavior on this peptide condition,

that shows a rare cluster morphology.

F.A area and number decreases with increased spacing. This tendency seem independent and regardless of the peptide studied. The substrate with 52nm of ligand spacing provided a higher number of adhesion sites. Abundant and larger focal adhesions at the cell periphery are reported for the selected candidates at 52nm. Few paxillin containing structures are formed at 70nm. Likewise almost no paxillin containing structures are formed at the larger spacing 110nm, with the exception of ligand laminin 21, and 22 with few visible paxillin structures in the collected data.

Receptor clustering below 70nm might not be exclusive for $\alpha_V\beta_3$-RGDfk and it might also be true for other receptors. But this question requires further prove. Elucidating the receptors and formation of integrin adhesions would be a major contribution. We address the importance of ligands as active sites in cellular response producing specific and accentuated changes in cystoskeleton and FA. Moreover, adhesion performance is subjected by the ligand spacing distance.

Beyond monitoring ligand induced phenotypes at the levels of cell morphology and FA behavior, the next step is to examine the presence of integrins in the reporter cell. Controls either by antibodies in combination with FACS or western blots would be a major advance. Another way to prove the binding via specific receptors to the substrates is to pre-block the receptors with the soluble peptide. This can bring robustness and control to further explore receptor-ligand activation mechanism in selected candidates.

Additionally, there is a lack of information in the range between 70nm and 110nm. Studies on neuron attachment and growth have shown that anchorage of a cytoskeletal protein (spectrin) to DM-GRASP molecules inmobilized in nanopatterns drop at 70nm. However later on, adhesion recovers at 80nm and falls again its performance at 110nm [75]. The phenomena is attributed to the geometry and size of the DM-GRASP molecules which is 35 amino-acids long. No detailed information such as the folding and orientation of the linear peptides (20 amino acids long) in this study are known.

To research whether there is an specific range for focal adhesion matrix formation, its another research project. An approach here introduced, to examine the role of spatial cues inducing FA matrix adhesion, is comparing adhesion results between REF52 and C2 cells. The RGDfk peptide which specifically recognize $\alpha_V\beta_3$ integrings is a common control, particularly well characterize for the REF52 fibroblast.

When evaluating the selected candidates on the REF52 system at 52 nm, we observed the cell specificity response of the candidates upon C2 cells. When varying the spatial cues to 116 nm, cell area and the number of adherent cells decreases. We showed preliminary results only in this regard. Further characterization of FA

number, size and shape is required. More data on FA might help to elucidate the role of physical cues, in cell adhesion activation. Is the spacing, the ligand-receptor or the cell type involved? It would be interesting to explore in detail, specificity of density inducing FA Matrix adhesion formation. The results here presented are just the beginning, regarding this interesting question.

6.4 Perspectives and Optimization

Perturbation with ECM ligands can be further explore with new design of peptide motifs, that specifically interacts with key receptors . Sensitivity and ligand specificity using different amino acid lengths and structures can refine adhesive-signaling research.

Multi-parametric cell based screens require the combination of technical skills from informatics to cell culture. As in large pharmacological screens or high throughput RNAi screens [42], automation is desirable to improve the output of the samples. Setting robotic procedures for ligand biofunctionalisation during substrate preparation would be an advantage. A robot could facilitate pipetting the reagents into the wells, coordinating incubation and washing steps.

Recent work has resulted a design for a fully automated high throughput (HT), high resolution multi-well plate scanning microscope platform and its application in several cell-based screening projects [135]. Additionally, a chamber that could adapt to a 96 well plate dimension, with a larger substrate glass bottom could help to standardize its use in a fully automated microscope. Also by increasing the number of wells, the rate of acquisition will be significantly improved and eventually a large data stack, for statistical robustness.

In terms of computing infrastructure, microscopy based screen can generate gigabytes of image data. A professional back up system with large capacity is required. In addition, a laboratory information management system combined with a bar coded labeling tracking can help to organize, store and retrieve all input and output information of an screen. This include peptides, sequences, slide identification numbers, raw experimental data and processed data.

Accurate interpretation and process of complex images can be optimized with better algorithms to segmented the objects of interest [135]. Improvement in readout methods used in phenotypic assays to diversify and scored multi-parametric morphological features will be an important contribution in the future. A main problem encountered in biological imaging is background due to autofluorescence, non-localize difuse labelling or out of focus contributions. Further advancement in

several areas including data exchange, disseminating data sets online, and higher resolution microscopy will particularly have strong effects on HT screening.

Chapter 7

Preliminary cell differentiation studies

The stable cell line named C2 progenitor cell or C2C12 is a well documented model for studying cell differentiation and fate [193] [80] [197] [185]. They are muscle-skeletal tissue myoblast with the potential to differentiate into bone or muscle. Figure 7.2 illustrate the (a) myogenic pathway (b) osteogenic pathway and the main (c) visual and genetic markers.

There are several epigenetic factors affecting differentiation of cells. The one we are dicussing in this thesis are spatial arrangment and adhesive peptides. In this thesis, adhesive peptides that confer different cell shapes have been discussed. Systematically we have identified bio-active ECM adhesive ligands that intrinsically influence cell shape and spreading in myoblast C2 cells. Furthermore, it was determined that 52nm spacing between ligands was the condition that provide strong phenotypic changes.

How is the rate of myogenesis and osteogenesis influenced by define extra-cellular matrix environments is the frame of this chapter. Here it is discuss preliminary experiments with 3 peptides selected from the screening: Fibrinogen FG CG23 that triggered a rare cluster phenotype, the sequence LM 22 that showed high spreading and the cyclic RGD as reference control. Identifying components that enhanced or decreased cell differentiation may help us to understand the mechanism and role of specific ECM components in muscle and bone regeneration.

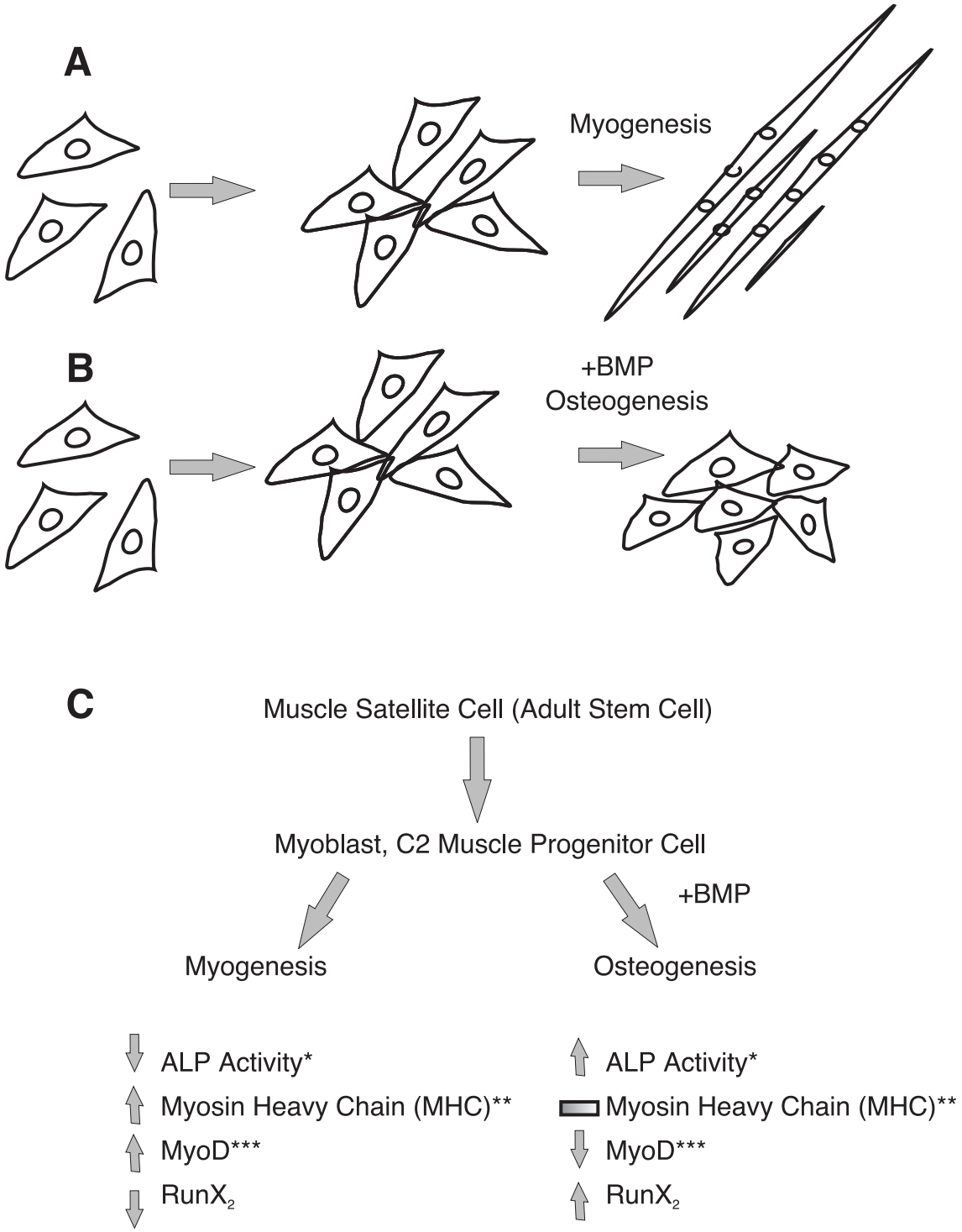

Figure 7.1: Myoblast C2 default differentiation is towards the myogenic pathway. Even without any inducing factor, cell-cell contact in C2 cells induces cessation of proliferation and differentiation into muscle fibers. Transdifferentiation to osteoblast is possible with the bone morphogenetic protein BMP [185].

7.1 Experiment design

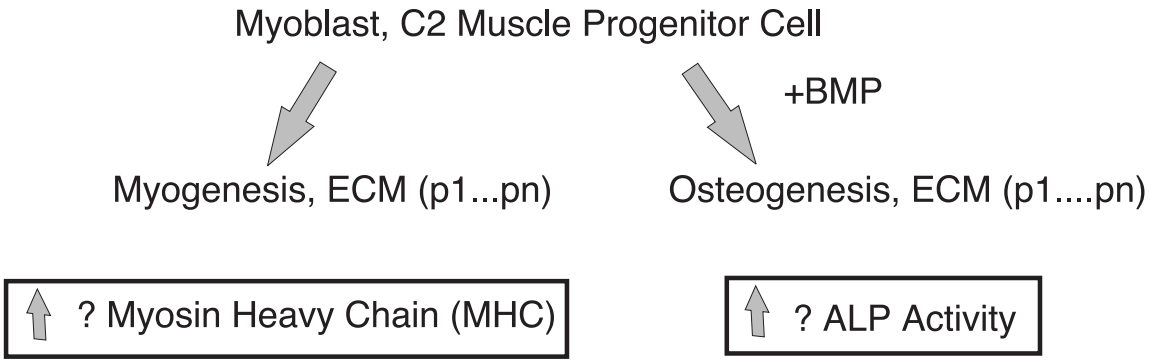

Figure 7.2: Identifying components that enhanced or decreased cell differentiation may help us to understand the mechanism and role of specific ECM components in muscle and bone regeneration. Progenitor C2 cells default differentiation is towards the myogenic pathway, and myosin heavy chain MHC is the main marker. In response to the bone morphogenetic protein (BMP), activation of osteogenic markers such as ALP is detected [110] [131][132].

C2 default differentiation is towards the myogenic pathway. To address the effect of ECM upon muscle skeletal differentiation, myoblast cells were seeded on bio-functionalized substrates (20x20mm) with 52nm gold dot spacing for 12h in 10% FCS. Without any inducing factor, cell-cell contact in C2 cells induces cessation of proliferation and differentiation into muscle fibers. After 96h, differentiated myotubes can be detected by inmuno-staining of myosin heavy chain in the contractile apparatus. The samples were fixed and stained with MHC as the first antibody (serum). As a second antibody, Alexa 568 was used. Image data was collected with an Axiovert Microscope using a Texas Red filter (at 10x magnification). To obtained quantitative data including number, elongation and area of myotubes of the fluorescent objects were segmented in Image J. Data were further processed with MatLab.

To address the effect of ECM upon osteogenesis, first the cells were seeded on bio-functionalized substrates (20x20mm) with 52nm gold dot spacing for 12h in 10% FCS. Afterwards, the medium in the cell culture was replaced by osteogenic medium (10FCS + 500ng/ml BMP-2) and kept for 96h. Recombinant Human BMP-2 (Preprotech GmBH, Catalog 120-02) is a potent osteoinductive cytokine. BMP-2 is a 26 Kda homodimeric disulfide linked protein consisting of two identical 115 amino acid

chains. In addition to its osteogenic activity, BMP-2 appears to play an important role in cardiac morphogenesis, and is expressed in a variety of other tissues including lung, liver, spleen, prostate, ovary, and small intestine.

In response to the bone morphogenetic protein (BMP), activation of osteogenic markers such as ALP is detected. The change in alkaline phosphatase level and activity is implicated in a variety of physiological and pathological events such as bone development [85], bone-related diseases [191]. SensoLyte pNPP Alkaline Phosphatase Assay Kit Colorimetric (Anaspec, Catalog 71230) is optimized to detect alkaline phosphatase activity in biological samples using p-Nitrophenil phosphate (pNPP) as the colorimetric phosphatase substrate. pNPP turn yellow and can be detected at absorbance 405nm (Tekkan).

We report the alkaline phosphatese activity (12h, 96h) in relationship to the total amount of protein. For determining the concentration of protein, we used Bradford Protein Assay (Quick Start BioRad, 500-0201). Brilliant Blue G-250 dye to proteins and its detected at 595 nm in the assay using a spectrometer or mircoplate reader (Tekkan)

7.2 Extracellular matrix ligands effect on Myogenesis

In the examination of myogenesis we found that substrates with 52nm ligand-spacing, functionalized with Fibrinogen CG23, Fibronectin (RGD) and Laminin 22, support the default myogenic differentiation. Cell fusion and differentiation starts 48 h after. And myotubes are visible at 96h as shown in Figure 7.3.

A priori it is observed that myoblasts cultured on laminin 22 and fibrinogen CG23, show a population with larger myofibers in area and length in comparison to the control. To confirm such observation, quantification of the MHC stained structures was performed. The histogram in figure show a myotube population in the area range (2000-3000 sq um) and a population with longer myotubes (major axis, 100-200 um) for Laminin 22 and Fibrinogen CG23.

In order to find a plausible explanation for this phenomena, we correlate the myotube parameters with previous adhesion results. Figure 7.5 top summarizes the scores in cell shape (area, elongation), number of adherent cells and F.A abundance in the initial phase of adhesion (12h). The ordinate axis represents normalized values of the four adhesion parameters (with respect to the RGD control).

After 96 hours in culture (figure 7.5 middle), myogenesis on P-22 (laminin) substrates correlated with higher number of focal adhesions, higher cell spreading area and more myotubes (lenght, area and number) in comparison to RGD control. We speculate that a higher cell spreading and cell coverage on the surface, accelerate the cell-cell contact during proliferation and therefore the cell fusion process. The higher spreading of laminin 22 is an intrinsic property of peptide at 52nm spacing. We speculate that this sequence interacts with proteoglycan receptors. And the GAGs from proteoglycans capture extracellular matrix molecules that additionally favours the adhesion and spreading of myoblast or synergistically activate other integrins.

With Fibrinogen CG23 as substrate molecule, we observed significantly longer and thicker myotubes after 96h, not only in comparison to control RGD but also to Laminin 22 (figure 7.5 middle). The reported standard deviation values are very high. This is due to the wide distribution. While longer and more "mature" myotubes are observed. Some new small myotubes eventually start to appear. Interestingly, the fibrinogen molecule correlates with score high values in cell number, with high deviation standarts which correspond to heterogeneous clusters (Figure 7.5 top). The rare observed phenotype is characterize by cluster formation or compact round structures after 12Hrs. A few small focals are visually observed among 4-5 cells cluster. We suggest that on fibrinogen CG23, the cells exit the cycle at an early stage. We speculate that clusters posses higher initial cell-cell contact, and the

myotube formation higher.

In this section, we have addressed how initial changes in myoblast shape and adhesion, due to the intrinsic ECM ligands act as a cue in the cell-fusion process or muscle skeletal differentiation (Figure 7.5 bottom). We suggest that cell spreading caused by laminin 22 and cluster-formation caused by fibrinogen contribute to longer and thicker myotubes.

The myogenesis results (MHC stained myotubes) were normalized to the control cyclic RGD. It is important to highlight that RGD support myotube formation when inmobilized in the 52 nm substrate as shown in figure 7.3. Previous studies have reported an inhibition effect in fusion by RGD peptides when adding them in solution, suggesting the process of muscle differentiation takes place by an integrin recognition mechanism.

In this experiment, the myotube formation on RGD inmobilized peptides were lower but not totally inhibited. An additional gelatin control, might be useful to comparative illustrate the decreasing modulation of RGD upon muscle skeletal differentiation. The RGD spaced with 52 nm did not inhibit the muscle formation or cell fusion. This might only happen at lower ligand spacings.

We have choosen MHC as the main reporter marker for muscle skeletal differentiation. No additional information regarding the level of expression of myogenin gene, under the ligand and spatial conditions were explore here.

Previous studies conclude that an organize ECM is not required for activating the myogenic regulatory gene (myogenin) in the initial phase of muscle cell differentiation, but its necessary for achieving terminal differentiation of skeletal muscle cells [130] [110]. The composition and spatial cues of the ECM achieving muscle differentiation have not been elucidate it yet. And the mechanism remains unclear.

Here we report that specific ligand Fibrinogen CG23 (sequence) and Laminin 22 (sequence) spaced at 52 nm accelerate the differentiation of myoblast cells in comparison to immobilized RGD. Furthermore we suggest that initial changes in myoblast shape and adhesion, due to intrinsic ECM ligands act as a cue in the cell-fusion process or muscle skeletal differentiation. Cell spreading cause by Laminin 22 and cluster-formation cause by fibrinogen might contribute to longer and thicker myotubes. The receptors involved in the adhesion are not known.

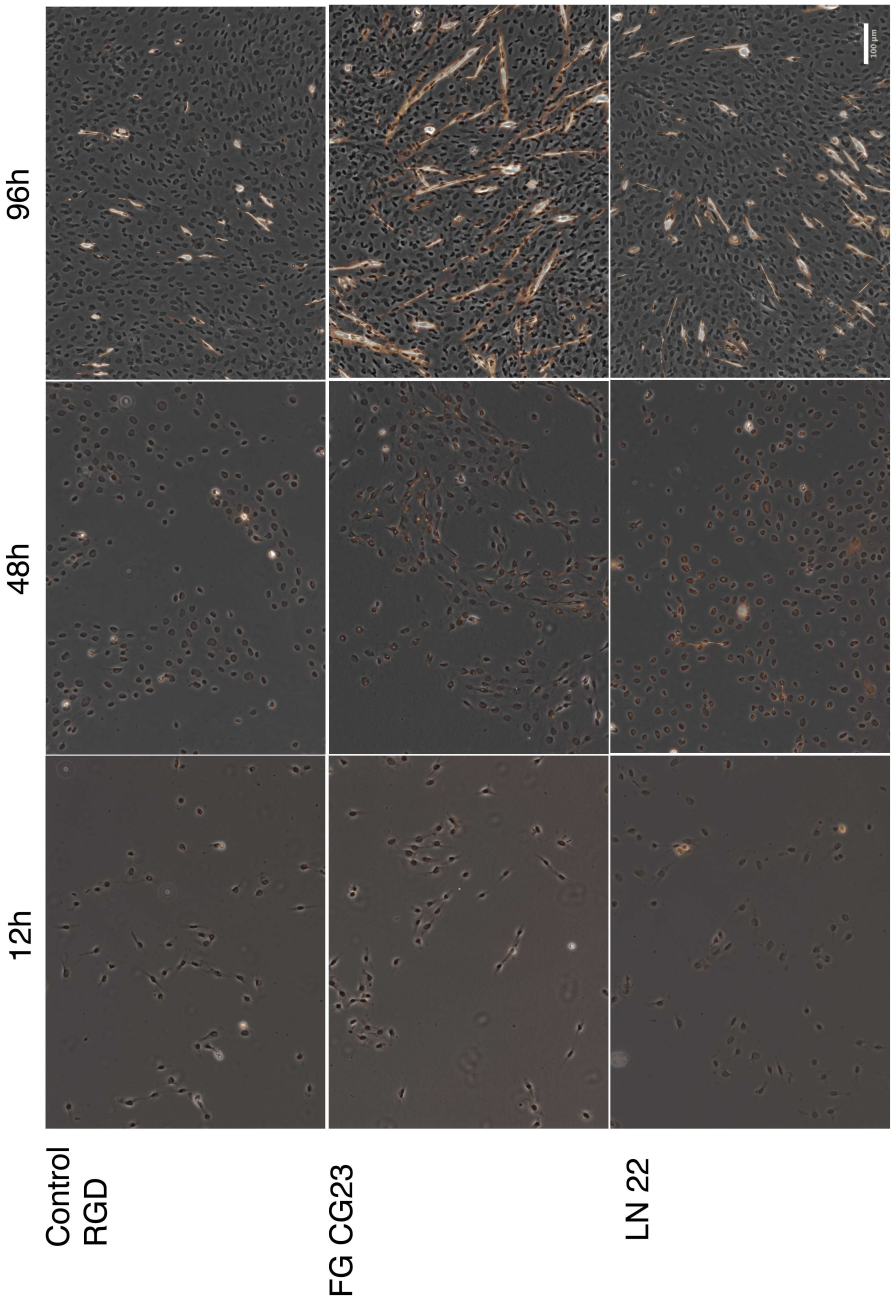

Figure 7.3: Cell fusion and differentiation starts 48 h after culture. Myotubes are visible at 96h. A priori it is observed that myoblasts cultured on laminin 22 and fibrinogen CG23, show a population with larger myofibers in area and length in comparison to the control after 96h. The scale bar is 100 um.

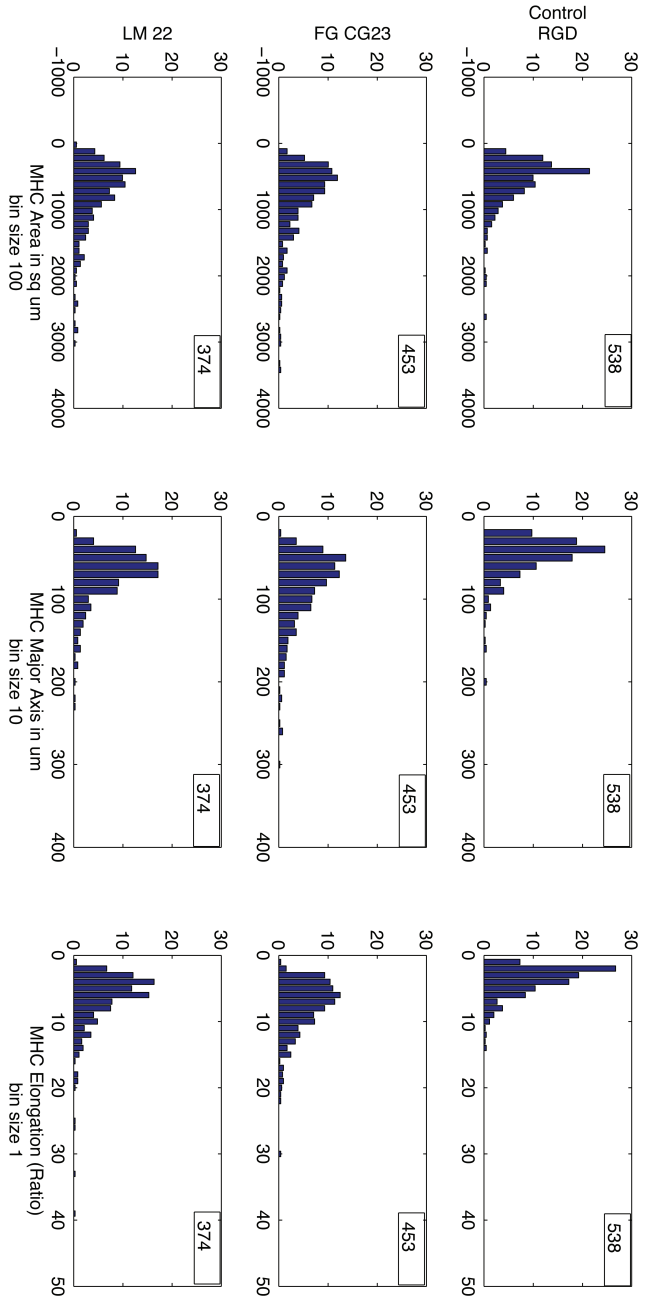

Figure 7.4: The histogram in show a myotube population in the area range (2000-3000 sq um) and a population with longer myotubes (major axis, 100-200 um) for Laminin 22 and Fibrinogen CG23.

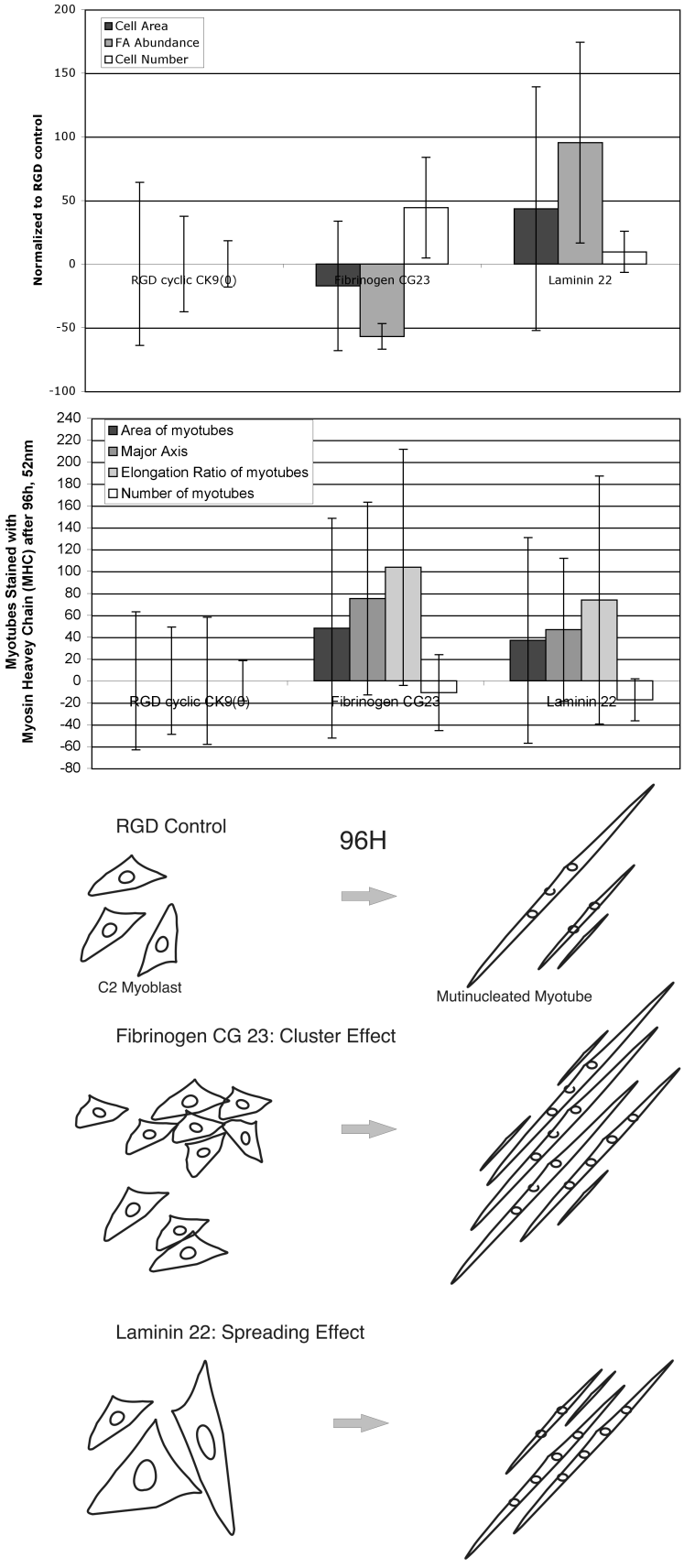

Figure 7.5: Quantification of the MHC stained structures. Cell spreading cause by laminin 22 and cluster-formation cause by fibrinogen might contribute to longer and thicker myotubes. We suggest that on fibrinogen CG23, the cells exit the cycle at an early stage. It speculate that clusters posses higher initial cell-cell contact, and the myotube formation higher.

7.3 Extracellular matrix ligands effect on Osteogenesis

BMP-2 treatment of the muscle progenitor cell C2, inhibits myotube formation and induces the expression of Alkaline Phosphatase (ALP), changing their differentiation pathway into the osteoblastic lineage [80].

In order to understand the effect of individual ECM components upon osteogenesis. We cultured myoblast on the selected candidates for 96h in the presence of -BMP, having as negative control RGD in the absence of BMP-2. Figure 7.6C reports the alkaline phosphatese activity in relationship to the total amount of protein for the selected candidates. At 12h in the absence of BMP, ALP activity was undetectable.

The results show that laminin 22 is an ECM ligand that promotes osteogenesis in the presence of +BMP-2. The ALP activity report for Fibrinogen CG23 and RGD were lower. The negative control showed very low ALP activity for RGD in the absence of BMP-2.

While differentiation may cause changes in cell shape, several studies have shown that changes in cell shape themselves can alter the differentiation of pre-commited mesenchymal lineages. Micropatterned substrates with defined adhesive and non-adhesive islands [171] have been used to control cell shape and spreading. Studies have demonstrated that cell shape and spreading regulate adipocite and osteoblast fate on on human mesenchymal stem cells [106].

From our screening studies, the laminin 22 ligand trigger a phenotype that spread 50% more than the to control. While Fibrinogen spread 20% less than in control. We observed that specific ECM components modulated the rate of osteogenesis.

Previous experiments conclude that the composition of extra-cellular matrix induced expression of ALP, by a mechanism independent of BMP-2 and without affecting the expression of osteogenic determination genes such as Cbfa-1 or RunX2 [131]. However, certain components of ECM, presumably the integrins, are sufficient to trigger an osteoblastic phenotype, but remain unknown.

It would be desirable to complete these studies by measuring the ALP activity of the selected peptides in the absence (-BMP) after 96h. In addition evaluating the expression of Cbfa-1 by RT-PCR, could answer whether the mechanism is actually BMP-2 independent under the conditions here propose. For time constraints, we present preliminary experiments. The result points out that Laminin sequence 22 enhanced slightly the rate osteogenesis.

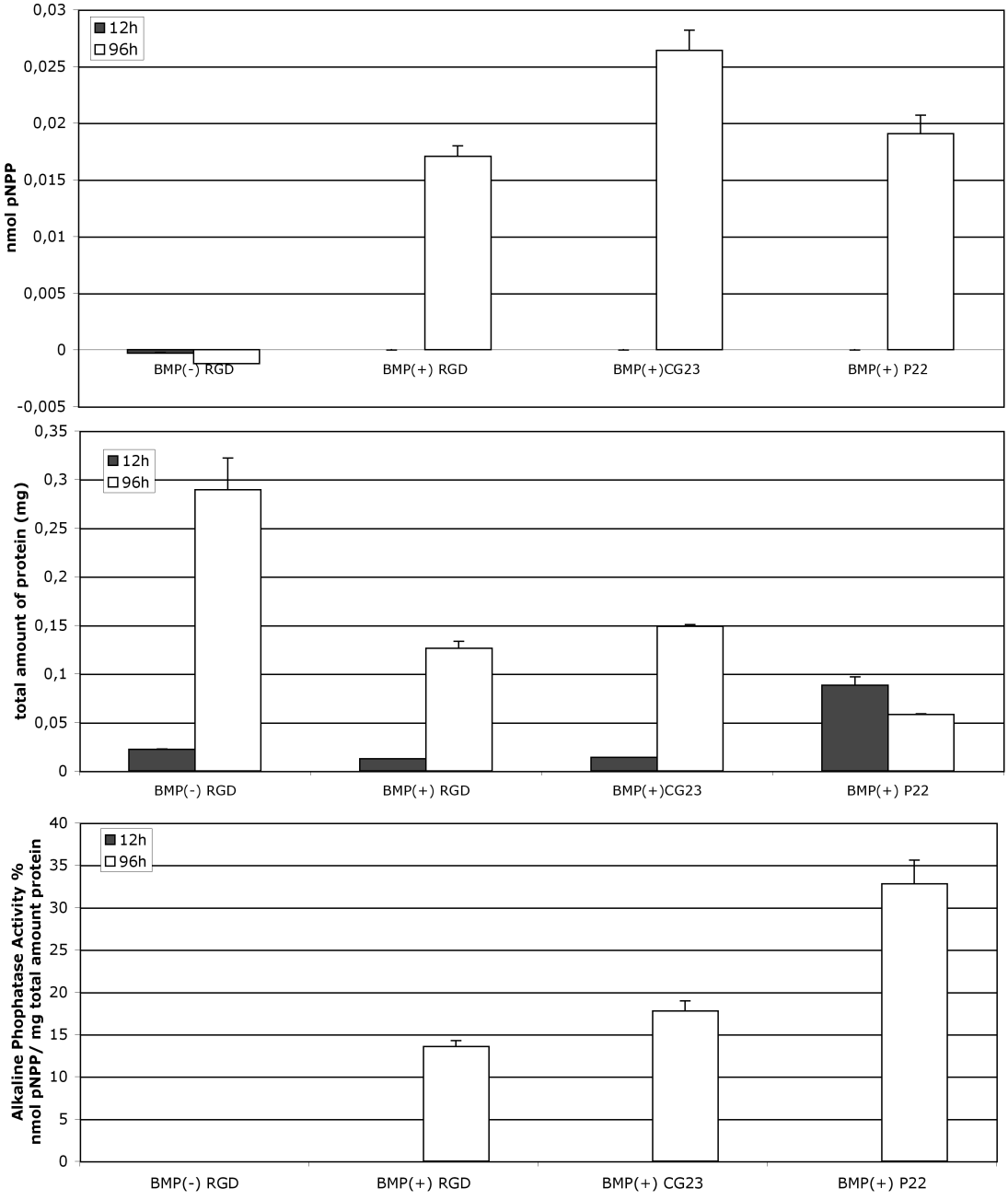

Figure 7.6: The results show that laminin 22 is an ECM ligand that promotes osteogenesis in the presence of +BMP-2. The ALP activity report for Fibrinogen CG23 and RGD were lower.

Chapter 8

Conclusions and Future Outlook

A platform for cell adhesion screennig on nanostructures was here presented. Cell based screening and nano-pattern technologies are emerging experimental methods, that monitor cellular phenotypes as the read out and can generate, multi-parametric data sets that are rich in morphological features. The significant phenotypic characteristics evaluated on this screen were cell shape, which includes spreading and elongation, and paxillin FA morphology, which include FA area; FA length; and FA abundance. This thesis gathered and examined a library of ECM perturbations as input variables to study cell adhesion, FA formation and the epigenetics in C2 differentiation.

Experimentally, cell attachment and phenotype evaluation on nanopatterns spaced at 52 nm [7] was performed. The homogeneous ligand distribution, controlled distance between ligands, and effective passivation against non-specific adhesion allows to study ligand-receptors interaction [7][166] [51] [75].

Out of 33 ECM peptides, 5 peptide candidates (Fibrinogen CG23, Fibronectin 10, Laminin 14, Laminin 21 and Laminin 22) were identified. Figure 5.7 summarizes the results. The given screening code identifies the ECM peptide, and the associated number is not related to any nomenclature, but simply to cite the sequence in the screen. The control peptide is the cyclic RGDfK which specifically recognise $\alpha_v\beta_3$ integrins [24]. The candidates are linear in structure, non RGD containing and with up to 20 amino-acids in their sequence. The observed changes in phenotype are intrinsic to the adhesive perturbation and occurred at 52nm.

It was found that Laminin 22 mediated strong adhesion in C2 cells. This laminin sequence induced an increase in cell spreading (50%) and number of FA structures (100%) as compared to the control RGDfk peptide. Laminin 22 scored the highest in FA abundance from all candidates, two times more than the cyclic RGD control alone.

It is possible that the cell adhesion could be attributed to synergistic effects between syndecans and integrins. This synthetic laminin fragment has been shown in early studies to exhibit strong heparin binding activity [27]. It is worth mentioning that laminin is one of the main component of base membrane essential in muscle and bone development. Another interesting candidate was Fibrinogen CG23, that triggered a rare cluster phenotype. The receptors involved in the phenotypic changes remain to be elucidated. So far we know a priori from the literature few related receptors in other cell systems.

In the next step, adhesion dependence upon the ligand spacing of the candidates were evaluated. It is observed that the number of adherent cells decreased by 50% and 70% at 70nm and 116nm spaced between gold particles. The cell area results showed higher spreading with the nanogold dots spaced at 52nm and at 70nm and 116nm, a decreased in area is observed except for the fibrinogen peptide. Cell area results on the fibrinogen candidate were more irregular, and the distance seems not to affect the spreading behavior on this peptide condition, that shows a rare cluster morphology. The reason is unknown, but the ECM Fibrinogen is known to clot blood cells.

As for the cell elongation, the results don't seem affected by the distance. A decreasing trend was also observed with the FA number, values decreased 60% and 80% at 70nm and 116nm. Less paxillin FA structures are formed at 116nm, with the exception of 2 laminin ligands with few visible paxillin structures in the collected data. The FA area dropped below 50% for the ligands at 70nm and 116nm.

The study address the importance of ligands as active sites in cellular response producing specific and accentuated changes in cystoskeleton and FA. Moreover, adhesion performance is subject to the ligand spacing distance. The results point out anundant and larger FA structures below 70nm. Receptor clustering below this barrier might not be exclusive for $\alpha_V\beta_3$-RGDfk and it might also be true for other receptors, but this question requires further examination.

Beyond monitoring ligand-induced phenotypes at the levels of cell morphology and FA behavior, the next step is to examine the presence of integrins in the reporter cell. Controls either by antibodies in combination with FACS or western blots would be a major advance. Another way to prove the binding via specific receptors to the substrates is to pre-block the receptors with the soluble peptide. This can bring robustness and control to explore specific pathway mechanisms in selected candidates.

It would be interesting to explore in detail, specificity of density inducing FA Matrix adhesion formation. To research whether there is an specific range for focal adhesion matrix formation, regardless ligand-receptor and cell type, its another research project. An approach here introduced to understand spatial cues induction

of FA matrix adhesion, is comparing adhesion results between REF52 and C2 cells. The RGDfk peptide which specifically recognize $\alpha_V\beta_3$ integrings is a common control, particularly well characterize for the REF52 fibroblast. Additional data on FA, for the selected candidates in the REF52 might help to elucidate the role of physical cues, in FA matrix formation. The results here presented are just the beginning, regarding this interesting question.

The identification of these ligands allow us to explore preliminary relationships between ECM and cell myogenesis and osteogenesis. Progenitor C2 cell default differentiation is towards the myogenic pathway. It is known that without any inducing factor, cell-cell contact in C2 cells induces cessation of proliferation and differentiation into muscle fibers. 3 out of 5 candidates were preliminarily analyzed for myogenesis. It is observed that myoblasts cultured on Laminin 22 and Fibrinogen CG23, show a population with myofibers larger in area and length in comparison to the RGD control after 96h. High cell spreading caused by laminin 22 and cell cluster-formation cause by fibrinogen might contribute to longer and thicker myotubes. On the other hand, in response to the bone morphogenetic protein (BMP), osteogenic differentiation is induced and markers such as alkaline phosphatase ALP is detectable. The results suggest that laminin 22 is an ECM ligand that promotes osteogenesis in the presence of BMP-2. The ALP activity reported for Fibrinogen CG23 and RGD were lower. The mechanism is unknown.

There are no complete list of ECM ligands within specific microenviroments or niches published. The collection of ligands presented here, provides a framework for understanding the enviromental cues or niches in which muscle progenitor cells can proliferate and differentiate. This list can potentially grow and be used to characterize their interplay in other cell systems.

Perturbation with ECM ligands can be further explored with new design of peptide motifs, that specifically interact with key receptors . Sensitivity and ligand specificity using different amino acid lengths and structures can refine adhesive-signaling research.

Multi-parametric cell based screens require the combination of technical skills from informatics to cell culture. Difficulty arises in handling a large number of samples manually. Automation of sample preparation and better algorithms to process complex images is desirable to improve the output of the samples, and accuracy in interpretation of the results. Further optimization includes barcode sample tracking, online data sharing and higher resolution microscopy.

A strategy for quantitative analysis of cell-matrix interactions is presented here. The methodology can be used for (i) system biology: elucidating the biological functions of ECM adhesive sites, and their role in the regulation of cytoskeleton assembly,

and in mechano adhesive-signalling, (ii) drug discovery to treat human diseases by identifying inhibitors and activators of cell adhesion and (iii) regenerative medicine: by collecting adhesive ECM ligands that provide a framework for understating the environmental niches in which adult stem cells can adhere, proliferate and differentiate.

Bibliography

[1] Rina Aharoni, Elizabeta Aizman, Ora Fuchs, Ruth Arnon, David Yaffe, and Rachel Sarig. Transplanted myogenic progenitor cells express neuronal markers in the cns and ameliorate disease in experimental autoimmune encephalomyelitis. *J Neuroimmunol*, 215(1-2):73–83, 2009 Oct 30.

[2] S K Akiyama and K M Yamada. The interaction of plasma fibronectin with fibroblastic cells in suspension. *J Biol Chem*, 260(7):4492–4500, 1985 Apr 10.

[3] Steven K. Akiyama and Josephine C. Adams. *Methods in Cell Biology, Functional Analysis of Cell Adhesion*, volume 69. Academic Press, 2002.

[4] Antonina Y Alexandrova, Katya Arnold, Sebastien Schaub, Jury M Vasiliev, Jean-Jacques Meister, Alexander D Bershadsky, and Alexander B Verkhovsky. Comparative dynamics of retrograde actin flow and focal adhesions: formation of nascent adhesions triggers transition from fast to slow flow. *PLoS One*, 3(9):e3234, 2008.

[5] Helene Andersson and Albert van den Berg, editors. *Lab on Chips for Cellomics, Micro and Nanotechnology for Life Science*. Kluwer Academic Publishers, London, 2004.

[6] S Aota, T Nagai, and K M Yamada. Characterization of regions of fibronectin besides the arginine-glycine-aspartic acid sequence required for adhesive function of the cell-binding domain using site-directed mutagenesis. *J Biol Chem*, 266(24):15938–15943, 1991 Aug 25.

[7] Marco Arnold, Elisabetta Ada Cavalcanti-Adam, Roman Glass, Jacques Blummel, Wolfgang Eck, Martin Kantlehner, Horst Kessler, and Joachim P Spatz. Activation of integrin function by nanopatterned adhesive interfaces. *Chemphyschem*, 5(3):383–388, 2004 Mar 19.

[8] Monique Aumailley, Leena Bruckner-Tuderman, William G Carter, Rainer Deutzmann, David Edgar, Peter Ekblom, Jurgen Engel, Eva Engvall, Erhard Hohenester, Jonathan C R Jones, Hynda K Kleinman, M Peter Marinkovich, George R Martin, Ulrike Mayer, Guerrino Meneguzzi, Jeffrey H Miner, Kaoru Miyazaki, Manuel Patarroyo, Mats Paulsson, Vito Quaranta, Joshua R Sanes, Takako Sasaki, Kiyotoshi Sekiguchi, Lydia M Sorokin, Jan F Talts, Karl Tryggvason, Jouni Uitto, Ismo Virtanen, Klaus von der Mark, Ulla M Wewer, Yoshihiko Yamada, and Peter D Yurchenco. A simplified laminin nomenclature. *Matrix Biol*, 24(5):326–332, 2005 Aug.

[9] Asoka Banno and Mark H Ginsberg. Integrin activation. *Biochem Soc Trans*, 36(Pt 2):229–234, 2008 Apr.

[10] DeannaLee M Beauvais, Brandon J Burbach, and Alan C Rapraeger. The syndecan-1 ectodomain regulates alphavbeta3 integrin activity in human mammary carcinoma cells. *J Cell Biol*, 167(1):171–181, 2004 Oct 11.

[11] K A Beningo, M Dembo, I Kaverina, J V Small, and Y L Wang. Nascent focal adhesions are responsible for the generation of strong propulsive forces in migrating fibroblasts. *J Cell Biol*, 153(4):881–888, 2001 May 14.

[12] M Bernfield, M Gotte, P W Park, O Reizes, M L Fitzgerald, J Lincecum, and M Zako. Functions of cell surface heparan sulfate proteoglycans. *Annu Rev Biochem*, 68:729–777, 1999.

[13] A Bershadsky, A Chausovsky, E Becker, A Lyubimova, and B Geiger. Involvement of microtubules in the control of adhesion-dependent signal transduction. *Curr Biol*, 6(10):1279–1289, 1996 Oct 1.

[14] A D Bershadsky, I S Tint, A A Jr Neyfakh, and J M Vasiliev. Focal contacts of normal and rsv-transformed quail cells. hypothesis of the transformation-induced deficient maturation of focal contacts. *Exp Cell Res*, 158(2):433–444, 1985 Jun.

[15] Alexander D Bershadsky, Nathalie Q Balaban, and Benjamin Geiger. Adhesion-dependent cell mechanosensitivity. *Annu Rev Cell Dev Biol*, 19:677–695, 2003.

[16] Jacques Blummel, Nadine Perschmann, Daniel Aydin, Jovana Drinjakovic, Thomas Surrey, Monica Lopez-Garcia, Horst Kessler, and Joachim P Spatz.

Protein repellent properties of covalently attached peg coatings on nanostructured sio(2)-based interfaces. *Biomaterials*, 28(32):4739–4747, 2007 Nov.

[17] D Boettiger, M Enomoto-Iwamoto, H Y Yoon, U Hofer, A S Menko, and R Chiquet-Ehrismann. Regulation of integrin alpha 5 beta 1 affinity during myogenic differentiation. *Dev Biol*, 169(1):261–272, 1995 May.

[18] D W Branch, B C Wheeler, G J Brewer, and D E Leckband. Long-term stability of grafted polyethylene glycol surfaces for use with microstamped substrates in neuronal cell culture. *Biomaterials*, 22(10):1035–1047, 2001 May.

[19] M Bronner-Fraser, M Artinger, J Muschler, and A F Horwitz. Developmentally regulated expression of alpha 6 integrin in avian embryos. *Development*, 115(1):197–211, 1992 May.

[20] A Brunetti and I D Goldfine. Role of myogenin in myoblast differentiation and its regulation by fibroblast growth factor. *J Biol Chem*, 265(11):5960–5963, 1990 Apr 15.

[21] C A Buck and A F Horwitz. Cell surface receptors for extracellular matrix molecules. *Annu Rev Cell Biol*, 3:179–205, 1987.

[22] R E Burgeson, M Chiquet, R Deutzmann, P Ekblom, J Engel, H Kleinman, G R Martin, G Meneguzzi, M Paulsson, and J Sanes. A new nomenclature for the laminins. *Matrix Biol*, 14(3):209–211, 1994 Apr.

[23] K Burridge and M Chrzanowska-Wodnicka. Focal adhesions, contractility, and signaling. *Annu Rev Cell Dev Biol*, 12:463–518, 1996.

[24] Elisabetta A Cavalcanti-Adam, Alexandre Micoulet, Jacques Blummel, Jorg Auernheimer, Horst Kessler, and Joachim P Spatz. Lateral spacing of integrin ligands influences cell spreading and focal adhesion assembly. *Eur J Cell Biol*, 85(3-4):219–224, 2006 Apr.

[25] Elisabetta Ada Cavalcanti-Adam, Daniel Aydin, Vera Catherine Hirschfeld-Warneken, and Joachim Pius Spatz. Cell adhesion and response to synthetic nanopatterned environments by steering receptor clustering and spatial location. *HFSP J*, 2(5):276–285, 2008 Oct.

[26] Elisabetta Ada Cavalcanti-Adam, Tova Volberg, Alexandre Micoulet, Horst Kessler, Benjamin Geiger, and Joachim Pius Spatz. Cell spreading and focal

adhesion dynamics are regulated by spacing of integrin ligands. *Biophys J*, 92(8):2964–2974, 2007 Apr 15.

[27] A S Charonis, A P Skubitz, G G Koliakos, L A Reger, J Dege, A M Vogel, R Wohlhueter, and L T Furcht. A novel synthetic peptide from the b1 chain of laminin with heparin-binding and cell adhesion-promoting activities. *J Cell Biol*, 107(3):1253–1260, 1988 Sep.

[28] Christopher S Chen, John Tan, and Joe Tien. Mechanotransduction at cell-matrix and cell-cell contacts. *Annu Rev Biomed Eng*, 6:275–302, 2004.

[29] R Chiquet-Ehrismann. Tenascins, a growing family of extracellular matrix proteins. *Experientia*, 51(9-10):853–862, 1995 Sep 29.

[30] Colin K Choi, Miguel Vicente-Manzanares, Jessica Zareno, Leanna A Whitmore, Alex Mogilner, and Alan Rick Horwitz. Actin and alpha-actinin orchestrate the assembly and maturation of nascent adhesions in a myosin ii motor-independent manner. *Nat Cell Biol*, 10(9):1039–1050, 2008 Sep.

[31] David A Cisneros, Carlos Hung, Clemens M Franz, and Daniel J Muller. Observing growth steps of collagen self-assembly by time-lapse high-resolution atomic force microscopy. *J Struct Biol*, 154(3):232–245, 2006 Jun.

[32] E A Clark, W G King, J S Brugge, M Symons, and R O Hynes. Integrin-mediated signals regulated by members of the rho family of gtpases. *J Cell Biol*, 142(2):573–586, 1998 Jul 27.

[33] B Clement, B Segui-Real, P Savagner, H K Kleinman, and Y Yamada. Hepatocyte attachment to laminin is mediated through multiple receptors. *J Cell Biol*, 110(1):185–192, 1990 Jan.

[34] Carolina F M Z Clemente, Marcus A F Corat, Sara T O Saad, and Kleber G Franchini. Differentiation of c2c12 myoblasts is critically regulated by fak signaling. *Am J Physiol Regul Integr Comp Physiol*, 289(3):R862–70, 2005 Sep.

[35] Charlotte A Collins, Irwin Olsen, Peter S Zammit, Louise Heslop, Aviva Petrie, Terence A Partridge, and Jennifer E Morgan. Stem cell function, self-renewal, and behavioral heterogeneity of cells from the adult muscle satellite cell niche. *Cell*, 122(2):289–301, 2005 Jul 29.

[36] Charlotte A Collins and Terence A Partridge. Self-renewal of the adult skeletal muscle satellite cell. *Cell Cycle*, 4(10):1338–1341, 2005 Oct.

[37] Christian Conrad and Daniel W Gerlich. Automated microscopy for high-content rnai screening. *J Cell Biol*, 188(4):453–461, 2010 Feb 22.

[38] John R Couchman. Syndecans: proteoglycan regulators of cell-surface microdomains? *Nat Rev Mol Cell Biol*, 4(12):926–937, 2003 Dec.

[39] Geoff Cumming, Fiona Fidler, and David L Vaux. Error bars in experimental biology. *J Cell Biol*, 177(1):7–11, 2007 Apr 9.

[40] S Dufour, J L Duband, M J Humphries, M Obara, K M Yamada, and J P Thiery. Attachment, spreading and locomotion of avian neural crest cells are mediated by multiple adhesion sites on fibronectin molecules. *EMBO J*, 7(9):2661–2671, 1988 Sep.

[41] Asier Echarri, Olivia Muriel, and Miguel A Del Pozo. Intracellular trafficking of raft/caveolae domains: insights from integrin signaling. *Semin Cell Dev Biol*, 18(5):627–637, 2007 Oct.

[42] Christophe J Echeverri and Norbert Perrimon. High-throughput rnai screening in cultured cells: a user's guide. *Nat Rev Genet*, 7(5):373–384, 2006 May.

[43] C P Emerson. Myogenesis and developmental control genes. *Curr Opin Cell Biol*, 2(6):1065–1075, 1990 Dec.

[44] Heidi S Erickson, Gallya Gannot, Michael A Tangrea, Rodrigo F Chuaqui, John W Gillespie, and Michael R Emmert-Buck. High throughput screening of normal and neoplastic tissue samples. *Comb Chem High Throughput Screen*, 13(3):253–267, 2010 Mar.

[45] Yoram Etzion and Anthony J Muslin. The application of phenotypic high-throughput screening techniques to cardiovascular research. *Trends Cardiovasc Med*, 19(6):207–212, 2009 Aug.

[46] F Fang and I Szleifer. Kinetics and thermodynamics of protein adsorption: a generalized molecular theoretical approach. *Biophys J*, 80(6):2568–2589, 2001 Jun.

[47] H Fujiwara, Y Kikkawa, N Sanzen, and K Sekiguchi. Purification and characterization of human laminin-8. laminin-8 stimulates cell adhesion and migration through alpha3beta1 and alpha6beta1 integrins. *J Biol Chem*, 276(20):17550–17558, 2001 May 18.

[48] J L Funderburgh. Keratan sulfate: structure, biosynthesis, and function. *Glycobiology*, 10(10):951–958, 2000 Oct.

[49] J T Gallagher. Heparan sulfate: growth control with a restricted sequence menu. *J Clin Invest*, 108(3):357–361, 2001 Aug.

[50] J T Gallagher, M Lyon, and W P Steward. Structure and function of heparan sulphate proteoglycans. *Biochem J*, 236(2):313–325, 1986 Jun 1.

[51] Benjamin Geiger, Joachim P Spatz, and Alexander D Bershadsky. Environmental sensing through focal adhesions. *Nat Rev Mol Cell Biol*, 10(1):21–33, 2009 Jan.

[52] F G Giancotti. Complexity and specificity of integrin signalling. *Nat Cell Biol*, 2(1):E13–4, 2000 Jan.

[53] R. Glass, M. Moller, and J.P Spatz. Block copolymer micelle nanolithography. *Nanotechnology*, 14(10):1153–1160, 2003.

[54] W R Gombotz, G H Wang, T A Horbett, and A S Hoffman. Protein adsorption to poly(ethylene oxide) surfaces. *J Biomed Mater Res*, 25(12):1547–1562, 1991 Dec.

[55] B L Goode, D G Drubin, and G Barnes. Functional cooperation between the microtubule and actin cytoskeletons. *Curr Opin Cell Biol*, 12(1):63–71, 2000 Feb.

[56] J Graf, R C Ogle, F A Robey, M Sasaki, G R Martin, Y Yamada, and H K Kleinman. A pentapeptide from the laminin b1 chain mediates cell adhesion and binds the 67,000 laminin receptor. *Biochemistry*, 26(22):6896–6900, 1987 Nov 3.

[57] D S Grant, K Tashiro, B Segui-Real, Y Yamada, G R Martin, and H K Kleinman. Two different laminin domains mediate the differentiation of human endothelial cells into capillary-like structures in vitro. *Cell*, 58(5):933–943, 1989 Sep 8.

[58] S Greenberg, P Chang, and S C Silverstein. Tyrosine phosphorylation of the gamma subunit of fc gamma receptors, p72syk, and paxillin during fc receptor-mediated phagocytosis in macrophages. *J Biol Chem*, 269(5):3897–3902, 1994 Feb 4.

[59] J L Guan and R O Hynes. Lymphoid cells recognize an alternatively spliced segment of fibronectin via the integrin receptor alpha 4 beta 1. *Cell*, 60(1):53–61, 1990 Jan 12.

[60] D Gullberg, C F Tiger, and T Velling. Laminins during muscle development and in muscular dystrophies. *Cell Mol Life Sci*, 56(5-6):442–460, 1999 Oct 30.

[61] Jaime Gutierrez, Nelson Osses, and Enrique Brandan. Changes in secreted and cell associated proteoglycan synthesis during conversion of myoblasts to osteoblasts in response to bone morphogenetic protein-2: role of decorin in cell response to bmp-2. *J Cell Physiol*, 206(1):58–67, 2006 Jan.

[62] Abdelali Haoudi and Halima Bensmail. Bioinformatics and data mining in proteomics. *Expert Rev Proteomics*, 3(3):333–343, 2006 Jun.

[63] Christian Harwanegg and Reinhard Hiller. Protein microarrays for the diagnosis of allergic diseases: state-of-the-art and future development. *Clin Chem Lab Med*, 43(12):1321–1326, 2005.

[64] Michael J Heller. Dna microarray technology: devices, systems, and applications. *Annu Rev Biomed Eng*, 4:129–153, 2002.

[65] Martin E Hemler. Tetraspanin functions and associated microdomains. *Nat Rev Mol Cell Biol*, 6(10):801–811, 2005 Oct.

[66] Vera C Hirschfeld-Warneken, Marco Arnold, Ada Cavalcanti-Adam, Monica Lopez-Garcia, Horst Kessler, and Joachim P Spatz. Cell adhesion and polarisation on molecularly defined spacing gradient surfaces of cyclic rgdfk peptide patches. *Eur J Cell Biol*, 87(8-9):743–750, 2008 Sep.

[67] Pirta Hotulainen and Pekka Lappalainen. Stress fibers are generated by two distinct actin assembly mechanisms in motile cells. *J Cell Biol*, 173(3):383–394, 2006 May 8.

[68] J.A Hubbel. Biomaterials in tissue engineering. *Biotechnology 13*, pages 565–576, 1995.

[69] J.A Hubbel. Bioactive biomaterials. *Curr Opin Biotechnol 10*, pages 123–129, 1999.

[70] M J Humphries, S K Akiyama, A Komoriya, K Olden, and K M Yamada. Identification of an alternatively spliced site in human plasma fibronectin that mediates cell type-specific adhesion. *J Cell Biol*, 103(6 Pt 2):2637–2647, 1986 Dec.

[71] M J Humphries, A Komoriya, S K Akiyama, K Olden, and K M Yamada. Identification of two distinct regions of the type iii connecting segment of human plasma fibronectin that promote cell type-specific adhesion. *J Biol Chem*, 262(14):6886–6892, 1987 May 15.

[72] Richard O Hynes. Integrins: bidirectional, allosteric signaling machines. *Cell*, 110(6):673–687, 2002 Sep 20.

[73] R.O Hynes. Fibronectins. *Spinger-Verlag, New York*, 1990.

[74] R V Iozzo. Matrix proteoglycans: from molecular design to cellular function. *Annu Rev Biochem*, 67:609–652, 1998.

[75] Steffen Jaehrling, Karsten Thelen, Tobias Wolfram, and G Elisabeth Pollerberg. Nanopatterns biofunctionalized with cell adhesion molecule dm-grasp offered as cell substrate: spacing determines attachment and differentiation of neurons. *Nano Lett*, 9(12):4115–4121, 2009 Dec.

[76] D Leanne Jones and Amy J Wagers. No place like home: anatomy and function of the stem cell niche. *Nat Rev Mol Cell Biol*, 9(1):11–21, 2008 Jan.

[77] R L Juliano. Signal transduction by cell adhesion receptors and the cytoskeleton: functions of integrins, cadherins, selectins, and immunoglobulin-superfamily members. *Annu Rev Pharmacol Toxicol*, 42:283–323, 2002.

[78] R.S Kane, S. Takayama, E. Ostuni, D.R Ingber, and G.M Whitesides. Patterning proteins and cells using soft lithography. *Biomaterials*, 20:2363-76, 1999.

[79] M Kantlehner, P Schaffner, D Finsinger, J Meyer, A Jonczyk, B Diefenbach, B Nies, G Holzemann, S L Goodman, and H Kessler. Surface coating with cyclic rgd peptides stimulates osteoblast adhesion and proliferation as well as bone formation. *Chembiochem*, 1(2):107–114, 2000 Aug 18.

[80] T Katagiri, A Yamaguchi, M Komaki, E Abe, N Takahashi, T Ikeda, V Rosen, J M Wozney, A Fujisawa-Sehara, and T Suda. Bone morphogenetic protein-2 converts the differentiation pathway of c2c12 myoblasts into the osteoblast lineage. *J Cell Biol*, 127(6 Pt 1):1755–1766, 1994 Dec.

[81] Akira Katsumi, A Wayne Orr, Eleni Tzima, and Martin Alexander Schwartz. Integrins in mechanotransduction. *J Biol Chem*, 279(13):12001–12004, 2004 Mar 26.

[82] Y Kikkawa, N Sanzen, H Fujiwara, A Sonnenberg, and K Sekiguchi. Integrin binding specificity of laminin-10/11: laminin-10/11 are recognized by alpha 3 beta 1, alpha 6 beta 1 and alpha 6 beta 4 integrins. *J Cell Sci*, 113 (Pt 5):869–876, 2000 Mar.

[83] Jin-Man Kim, Won Ho Park, and Byung-Moo Min. The ppflmllkgstr motif in globular domain 3 of the human laminin-5 alpha3 chain is crucial for integrin alpha3beta1 binding and cell adhesion. *Exp Cell Res*, 304(1):317–327, 2005 Mar 10.

[84] Lily Y Koo, Darrell J Irvine, Anne M Mayes, Douglas A Lauffenburger, and Linda G Griffith. Co-regulation of cell adhesion by nanoscale rgd organization and mechanical stimulus. *J Cell Sci*, 115(Pt 7):1423–1433, 2002 Apr 1.

[85] Noriko Kotobuki, Motohiro Hirose, Hiroyuki Funaoka, and Hajime Ohgushi. Enhancement of in vitro osteoblastic potential after selective sorting of osteoblasts with high alkaline phosphatase activity from human osteoblast-like cells. *Cell Transplant*, 13(4):377–383, 2004.

[86] Vathany Kulasingam, Maria P Pavlou, and Eleftherios P Diamandis. Integrating high-throughput technologies in the quest for effective biomarkers for ovarian cancer. *Nat Rev Cancer*, 10(5):371–378, 2010 May.

[87] A B Lassar, S X Skapek, and B Novitch. Regulatory mechanisms that coordinate skeletal muscle differentiation and cell cycle withdrawal. *Curr Opin Cell Biol*, 6(6):788–794, 1994 Dec.

[88] Irena Lavelin, Avital Beer, Zvi Kam, Varda Rotter, Moshe Oren, Ami Navon, and Benjamin Geiger. Discovery of novel proteasome inhibitors using a high-content cell-based screening system. *PLoS One*, 4(12):e8503, 2009.

[89] Ki-Bum Lee, So-Jung Park, Chad A Mirkin, Jennifer C Smith, and Milan Mrksich. Protein nanoarrays generated by dip-pen nanolithography. *Science*, 295(5560):1702–1705, 2002 Mar 1.

[90] Dirk Lehnert, Bernhard Wehrle-Haller, Christian David, Ulrich Weiland, Christoph Ballestrem, Beat A Imhof, and Martin Bastmeyer. Cell behaviour on micropatterned substrata: limits of extracellular matrix geometry for spreading and adhesion. *J Cell Sci*, 117(Pt 1):41–52, 2004 Jan 1.

[91] Renhao Li, Neal Mitra, Holly Gratkowski, Gaston Vilaire, Rustem Litvinov, Chandrasekaran Nagasami, John W Weisel, James D Lear, William F DeGrado, and Joel S Bennett. Activation of integrin alphaiibbeta3 by modulation of transmembrane helix associations. *Science*, 300(5620):795–798, 2003 May 2.

[92] Yung-Feng Liao, Philip J Gotwals, Victor E Koteliansky, Dean Sheppard, and Livingston Van De Water. The eiiia segment of fibronectin is a ligand for integrins alpha 9beta 1 and alpha 4beta 1 providing a novel mechanism for regulating cell adhesion by alternative splicing. *J Biol Chem*, 277(17):14467–14474, 2002 Apr 26.

[93] Y Liron, Y Paran, N G Zatorsky, B Geiger, and Z Kam. Laser autofocusing system for high-resolution cell biological imaging. *J Microsc*, 221(Pt 2):145–151, 2006 Feb.

[94] Valeryi K Lishko, Nataly P Podolnikova, Valentin P Yakubenko, Sergiy Yakovlev, Leonid Medved, Satya P Yadav, and Tatiana P Ugarova. Multiple binding sites in fibrinogen for integrin alphambeta2 (mac-1). *J Biol Chem*, 279(43):44897–44906, 2004 Oct 22.

[95] Shuang Liu. Radiolabeled cyclic rgd peptides as integrin alpha(v)beta(3)-targeted radiotracers: maximizing binding affinity via bivalency. *Bioconjug Chem*, 20(12):2199–2213, 2009 Dec.

[96] Mingjian Lu and Kodi S Ravichandran. Dock180-elmo cooperation in rac activation. *Methods Enzymol*, 406:388–402, 2006.

[97] Yan-Qing Ma, Jun Qin, Chuanyue Wu, and Edward F Plow. Kindlin-2 (mig-2): a co-activator of beta3 integrins. *J Cell Biol*, 181(3):439–446, 2008 May 5.

[98] G Maheshwari, G Brown, D A Lauffenburger, A Wells, and L G Griffith. Cell adhesion and motility depend on nanoscale rgd clustering. *J Cell Sci*, 113 (Pt 10):1677–1686, 2000 May.

[99] M C Maiden. High-throughput sequencing in the population analysis of bacterial pathogens of humans. *Int J Med Microbiol*, 290(2):183–190, 2000 May.

[100] Neelina H. Malsch, editor. *Biomedical Nanotechnology*. Taylor and Francis, New York, 2005.

[101] S P Massia and J A Hubbell. Covalent surface immobilization of arg-gly-asp- and tyr-ile-gly-ser-arg-containing peptides to obtain well-defined cell-adhesive substrates. *Anal Biochem*, 187(2):292–301, 1990 Jun.

[102] S P Massia and J A Hubbell. An rgd spacing of 440 nm is sufficient for integrin alpha v beta 3-mediated fibroblast spreading and 140 nm for focal contact and stress fiber formation. *J Cell Biol*, 114(5):1089–1100, 1991 Sep.

[103] S P Massia, S S Rao, and J A Hubbell. Covalently immobilized laminin peptide tyr-ile-gly-ser-arg (yigsr) supports cell spreading and co-localization of the 67-kilodalton laminin receptor with alpha-actinin and vinculin. *J Biol Chem*, 268(11):8053–8059, 1993 Apr 15.

[104] A MAURO. Satellite cell of skeletal muscle fibers. *J Biophys Biochem Cytol*, 9:493–495, 1961 Feb.

[105] Ulrike Mayer. Integrins: redundant or important players in skeletal muscle? *J Biol Chem*, 278(17):14587–14590, 2003 Apr 25.

[106] Rowena McBeath, Dana M Pirone, Celeste M Nelson, Kiran Bhadriraju, and Christopher S Chen. Cell shape, cytoskeletal tension, and rhoa regulate stem cell lineage commitment. *Dev Cell*, 6(4):483–495, 2004 Apr.

[107] Kyle J McQuade, DeannaLee M Beauvais, Brandon J Burbach, and Alan C Rapraeger. Syndecan-1 regulates alphavbeta5 integrin activity in b82l fibroblasts. *J Cell Sci*, 119(Pt 12):2445–2456, 2006 Jun 15.

[108] R P Mecham. Laminin receptors. *Annu Rev Cell Biol*, 7:71–91, 1991.

[109] R P Mecham. Receptors for laminin on mammalian cells. *FASEB J*, 5(11):2538–2546, 1991 Aug.

[110] F Melo, D J Carey, and E Brandan. Extracellular matrix is required for skeletal muscle differentiation but not myogenin expression. *J Cell Biochem*, 62(2):227–239, 1996 Aug.

[111] A S Menko and D Boettiger. Occupation of the extracellular matrix receptor, integrin, is a control point for myogenic differentiation. *Cell*, 51(1):51–57, 1987 Oct 9.

[112] Harald Mikkers and Jonas Frisen. Deconstructing stemness. *EMBO J*, 24(15):2715–2719, 2005 Aug 3.

[113] Jeffrey H Miner and Peter D Yurchenco. Laminin functions in tissue morphogenesis. *Annu Rev Cell Dev Biol*, 20:255–284, 2004.

[114] H Mohri. Interaction of fibronectin with integrin receptors: evidence by use of synthetic peptides. *Peptides*, 18(6):899–907, 1997.

[115] Eloi Montanez, Siegfried Ussar, Martina Schifferer, Michael Bosl, Roy Zent, Markus Moser, and Reinhard Fassler. Kindlin-2 controls bidirectional signaling of integrins. *Genes Dev*, 22(10):1325–1330, 2008 May 15.

[116] Mark R Morgan, Martin J Humphries, and Mark D Bass. Synergistic control of cell adhesion by integrins and syndecans. *Nat Rev Mol Cell Biol*, 8(12):957–969, 2007 Dec.

[117] Markus Moser, Bernhard Nieswandt, Siegfried Ussar, Miroslava Pozgajova, and Reinhard Fassler. Kindlin-3 is essential for integrin activation and platelet aggregation. *Nat Med*, 14(3):325–330, 2008 Mar.

[118] M W Mosesson. Fibrinogen and fibrin structure and functions. *J Thromb Haemost*, 3(8):1894–1904, 2005 Aug.

[119] D F Mosher. Fibronectin. *Academic Press, New York*, 1989.

[120] F P Moss and C P Leblond. Satellite cells as the source of nuclei in muscles of growing rats. *Anat Rec*, 170(4):421–435, 1971 Aug.

[121] A P Mould and M J Humphries. Identification of a novel recognition sequence for the integrin alpha 4 beta 1 in the cooh-terminal heparin-binding domain of fibronectin. *EMBO J*, 10(13):4089–4095, 1991 Dec.

[122] H B Nader, C P Dietrich, V Buonassisi, and P Colburn. Heparin sequences in the heparan sulfate chains of an endothelial cell proteoglycan. *Proc Natl Acad Sci U S A*, 84(11):3565–3569, 1987 Jun.

[123] Suha Naffar-Abu-Amara, Tal Shay, Meirav Galun, Naomi Cohen, Steven J Isakoff, Zvi Kam, and Benjamin Geiger. Identification of novel pro-migratory, cancer-associated genes using quantitative, microscopy-based screening. *PLoS One*, 3(1):e1457, 2008.

[124] T Nagai, N Yamakawa, S Aota, S S Yamada, S K Akiyama, K Olden, and K M Yamada. Monoclonal antibody characterization of two distant sites required for function of the central cell-binding domain of fibronectin in cell adhesion, cell migration, and matrix assembly. *J Cell Biol*, 114(6):1295–1305, 1991 Sep.

[125] D Nandan, E P Clarke, E H Ball, and B D Sanwal. Ethyl-3,4-dihydroxybenzoate inhibits myoblast differentiation: evidence for an essential role of collagen. *J Cell Biol*, 110(5):1673–1679, 1990 May.

[126] John Nielsen. Combinatorial synthesis of natural products. *Curr Opin Chem Biol*, 6(3):297–305, 2002 Jun.

[127] Hyeran Noh and Erwin A Vogler. Volumetric interpretation of protein adsorption: competition from mixtures and the vroman effect. *Biomaterials*, 28(3):405–422, 2007 Jan.

[128] M Obara, M S Kang, and K M Yamada. Site-directed mutagenesis of the cell-binding domain of human fibronectin: separable, synergistic sites mediate adhesive function. *Cell*, 53(4):649–657, 1988 May 20.

[129] E N Olson. Myod family: a paradigm for development? *Genes Dev*, 4(9):1454–1461, 1990 Sep.

[130] Nelson Osses and Enrique Brandan. Ecm is required for skeletal muscle differentiation independently of muscle regulatory factor expression. *Am J Physiol Cell Physiol*, 282(2):C383–94, 2002 Feb.

[131] Nelson Osses, Juan Carlos Casar, and Enrique Brandan. Inhibition of extracellular matrix assembly induces the expression of osteogenic markers in skeletal muscle cells by a bmp-2 independent mechanism. *BMC Cell Biol*, 10:73, 2009.

[132] Nelson Osses, Jaime Gutierrez, Teresa Lopez-Rovira, Francesc Ventura, and Enrique Brandan. Sulfation is required for bone morphogenetic protein 2-dependent id1 induction. *Biochem Biophys Res Commun*, 344(4):1207–1215, 2006 Jun 16.

[133] Roumen Pankov and Kenneth M Yamada. Fibronectin at a glance. *J Cell Sci*, 115(Pt 20):3861–3863, 2002 Oct 15.

[134] Yael Paran, Micha Ilan, Yoel Kashman, Sofee Goldstein, Yuvalal Liron, Benjamin Geiger, and Zvi Kam. High-throughput screening of cellular features using high-resolution light-microscopy; application for profiling drug effects on cell adhesion. *Journal of Structural Biology*, 158(2):233–243, 2007.

[135] Yael Paran, Irena Lavelin, Suha Naffar-Abu-Amara, Sabina Winograd-Katz, Yuvalal Liron, Benjamin Geiger, and Zvi Kam. Development and application of automatic high-resolution light microscopy for cell-based screens. *Methods Enzymol*, 414:228–247, 2006.

[136] Terence A Partridge. Stem cell route to neuromuscular therapies. *Muscle Nerve*, 27(2):133–141, 2003 Feb.

[137] Manuel Patarroyo, Karl Tryggvason, and Ismo Virtanen. Laminin isoforms in tumor invasion, angiogenesis and metastasis. *Semin Cancer Biol*, 12(3):197–207, 2002 Jun.

[138] B L Patton, J H Miner, A Y Chiu, and J R Sanes. Distribution and function of laminins in the neuromuscular system of developing, adult, and mutant mice. *J Cell Biol*, 139(6):1507–1521, 1997 Dec 15.

[139] Jeffrey R Peterson and Timothy J Mitchison. Small molecules, big impact: a history of chemical inhibitors and the cytoskeleton. *Chem Biol*, 9(12):1275–1285, 2002 Dec.

[140] M Pfaff, K Tangemann, B Muller, M Gurrath, G Muller, H Kessler, R Timpl, and J Engel. Selective recognition of cyclic rgd peptides of nmr defined conformation by alpha iib beta 3, alpha v beta 3, and alpha 5 beta 1 integrins. *J Biol Chem*, 269(32):20233–20238, 1994 Aug 12.

[141] M D Pierschbacher and E Ruoslahti. Cell attachment activity of fibronectin can be duplicated by small synthetic fragments of the molecule. *Nature*, 309(5963):30–33, 1984 May 3-9.

[142] E F Plow, T A Haas, L Zhang, J Loftus, and J W Smith. Ligand binding to integrins. *J Biol Chem*, 275(29):21785–21788, 2000 Jul 21.

[143] Kate Poole, Khaled Khairy, Jens Friedrichs, Clemens Franz, David A Cisneros, Jonathon Howard, and Daniel Mueller. Molecular-scale topographic cues induce the orientation and directional movement of fibroblasts on two-dimensional collagen surfaces. *J Mol Biol*, 349(2):380–386, 2005 Jun 3.

[144] K Prime and G Whitesides. Self-assembled organic monolayers: model systems for studying adsorption of proteins at surfaces. *Science*, 252(5009):1164–1167, 1991 May 24.

[145] D J Prockop and K I Kivirikko. Collagens: molecular biology, diseases, and potentials for therapy. *Annu Rev Biochem*, 64:403–434, 1995.

[146] Karine Raymond, Marie-Ange Deugnier, Marisa M Faraldo, and Marina A Glukhova. Adhesion within the stem cell niches. *Curr Opin Cell Biol*, 21(5):623–629, 2009 Oct.

[147] K Reimhult, K Petersson, and Krozer A. Qcm-d analysis of the performance of blocking agents on gold and polystyrene surfaces qcm-d analysis of the performance of blocking agents on gold and polystyrene surfaces. *Langmuir*, 8695-8700:8695–8700, 2008.

[148] B Ringelmann, C Roder, R Hallmann, M Maley, M Davies, M Grounds, and L Sorokin. Expression of laminin alpha1, alpha2, alpha4, and alpha5 chains, fibronectin, and tenascin-c in skeletal muscle of dystrophic 129rej dy/dy mice. *Exp Cell Res*, 246(1):165–182, 1999 Jan 10.

[149] E Rozengurt. Convergent signalling in the action of integrins, neuropeptides, growth factors and oncogenes. *Cancer Surv*, 24:81–96, 1995.

[150] E Ruoslahti and Y Yamaguchi. Proteoglycans as modulators of growth factor activities. *Cell*, 64(5):867–869, 1991 Mar 8.

[151] L A Sabourin and M A Rudnicki. The molecular regulation of myogenesis. *Clin Genet*, 57(1):16–25, 2000 Jan.

[152] O Saitoh, M Periasamy, M Kan, and R Matsuda. cis-4-hydroxy-l-proline and ethyl-3,4-dihydroxybenzoate prevent myogenesis of c2c12 muscle cells and block myod1 and myogenin expression. *Exp Cell Res*, 200(1):70–76, 1992 May.

[153] Rachel Sarig, Zadok Baruchi, Ora Fuchs, Uri Nudel, and David Yaffe. Regeneration and transdifferentiation potential of muscle-derived stem cells propagated as myospheres. *Stem Cells*, 24(7):1769–1778, 2006 Jul.

[154] Rachel Sarig, Ora Fuchs, Lilach Tencer, Avi Panski, Uri Nudel, and David Yaffe. Cloned myogenic cells can transdifferentiate in vivo into neuron-like cells. *PLoS One*, 5(1):e8814, 2010.

[155] M Sasaki, H K Kleinman, H Huber, R Deutzmann, and Y Yamada. Laminin, a multidomain protein. the a chain has a unique globular domain and homology with the basement membrane proteoglycan and the laminin b chains. *J Biol Chem*, 263(32):16536–16544, 1988 Nov 15.

[156] David T Scadden. The stem-cell niche as an entity of action. *Nature*, 441(7097):1075–1079, 2006 Jun 29.

[157] N Schutze. sirna technology. *Mol Cell Endocrinol*, 213(2):115–119, 2004 Jan 15.

[158] Anthony Scime, Annabelle Z Caron, and Guillaume Grenier. Advances in myogenic cell transplantation and skeletal muscle tissue engineering. *Front Biosci*, 14:3012–3023, 2009.

[159] A G Secchi, V Grigoriou, I M Shapiro, E A Cavalcanti-Adam, R J Composto, P Ducheyne, and C S Adams. Rgds peptides immobilized on titanium alloy stimulate bone cell attachment, differentiation and confer resistance to apoptosis. *J Biomed Mater Res A*, 83(3):577–584, 2007 Dec 1.

[160] Christine Selhuber-Unkel, Monica Lopez-Garcia, Horst Kessler, and Joachim P Spatz. Cooperativity in adhesion cluster formation during initial cell adhesion. *Biophys J*, 95(11):5424–5431, 2008 Dec.

[161] A P Skubitz, J B McCarthy, Q Zhao, X Y Yi, and L T Furcht. Definition of a sequence, ryvvlpr, within laminin peptide f-9 that mediates metastatic fibrosarcoma cell adhesion and spreading. *Cancer Res*, 50(23):7612–7622, 1990 Dec 1.

[162] M H Snow. An autoradiographic study of satellite cell differentiation into regenerating myotubes following transplantation of muscles in young rats. *Cell Tissue Res*, 186(3):535–540, 1978 Jan 31.

[163] W K Song, W Wang, H Sato, D A Bielser, and S J Kaufman. Expression of alpha 7 integrin cytoplasmic domains during skeletal muscle development: alternate forms, conformational change, and homologies with serine/threonine kinases and tyrosine phosphatases. *J Cell Sci*, 106 (Pt 4):1139–1152, 1993 Dec.

[164] L M Sorokin, F Pausch, M Frieser, S Kroger, E Ohage, and R Deutzmann. Developmental regulation of the laminin alpha5 chain suggests a role in epithelial and endothelial cell maturation. *Dev Biol*, 189(2):285–300, 1997 Sep 15.

[165] J. P. Spatz, V. Z. H. Chan, S. Mossmer, F. M. Kamm, A. Plettl, P. Ziemann, and M. Moller. A combined top-down/bottom-up approach to the microscopic localization of metallic nanodots. *Adv. Mater*, 14(24):1827–1832, 2002.

[166] Joachim P Spatz and Benjamin Geiger. Molecular engineering of cellular environments: cell adhesion to nano-digital surfaces. *Methods Cell Biol*, 83:89–111, 2007.

[167] J.P. Spatz, S. Mossmer, C. Hartmann, M. Moller, T. Herzog, M. Krieger, H.G Boyen, P. Ziemann, and B. Kabius. Ordered deposition of inorganic clusters from micellar block copolymer films. *Langmuir*, 16(2):407–415, 2000.

[168] A Spradling, D Drummond-Barbosa, and T Kai. Stem cells find their niche. *Nature*, 414(6859):98–104, 2001 Nov 1.

[169] Charles H Streuli and Nasreen Akhtar. Signal co-operation between integrins and other receptor systems. *Biochem J*, 418(3):491–506, 2009 Mar 15.

[170] Seiji Tadokoro, Sanford J Shattil, Koji Eto, Vera Tai, Robert C Liddington, Jose M de Pereda, Mark H Ginsberg, and David A Calderwood. Talin binding to integrin beta tails: a final common step in integrin activation. *Science*, 302(5642):103–106, 2003 Oct 3.

[171] J.L Tan, J Tien, and CS Chen. Microcontact printing of proteins on mixed self assemble monolayers. *Langmuir 18*, pages 519–523, 2002.

[172] K Tashiro, G C Sephel, B Weeks, M Sasaki, G R Martin, H K Kleinman, and Y Yamada. A synthetic peptide containing the ikvav sequence from the a chain of laminin mediates cell attachment, migration, and neurite outgrowth. *J Biol Chem*, 264(27):16174–16182, 1989 Sep 25.

[173] L Teboul, D Gaillard, L Staccini, H Inadera, E Z Amri, and P A Grimaldi. Thiazolidinediones and fatty acids convert myogenic cells into adipose-like cells. *J Biol Chem*, 270(47):28183–28187, 1995 Nov 24.

[174] Peter ten Dijke, Olexander Korchynskyi, Gudrun Valdimarsdottir, and Marie-Jose Goumans. Controlling cell fate by bone morphogenetic protein receptors. *Mol Cell Endocrinol*, 211(1-2):105–113, 2003 Dec 15.

[175] A ten Wolde. Nanotechnology: Toward a molecular construction kit. *Netherlands Study Centre for Technology Trends, The Hague*, 1998.

[176] Robert W Tilghman and J Thomas Parsons. Focal adhesion kinase as a regulator of cell tension in the progression of cancer. *Semin Cancer Biol*, 18(1):45–52, 2008 Feb.

[177] R Timpl and J C Brown. Supramolecular assembly of basement membranes. *Bioessays*, 18(2):123–132, 1996 Feb.

[178] Richard P Tucker and Ruth Chiquet-Ehrismann. The regulation of tenascin expression by tissue microenvironments. *Biochim Biophys Acta*, 1793(5):888–892, 2009 May.

[179] C E Turner. Paxillin and focal adhesion signalling. *Nat Cell Biol*, 2(12):E231–6, 2000 Dec.

[180] Tatiana P Ugarova, Valeryi K Lishko, Nataly P Podolnikova, Nobuo Okumura, Sergei M Merkulov, Valentin P Yakubenko, Vivien C Yee, Susan T Lord, and Thomas A Haas. Sequence gamma 377-395(p2), but not gamma 190-202(p1), is the binding site for the alpha mi-domain of integrin alpha m beta 2 in the gamma c-domain of fibrinogen. *Biochemistry*, 42(31):9365–9373, 2003 Aug 12.

[181] M R Urist. Bone: formation by autoinduction. *Science*, 150(698):893–899, 1965 Nov 12.

[182] M R Urist and B S Strates. Bone morphogenetic protein. *J Dent Res*, 50(6):1392–1406, 1971 Nov-Dec.

[183] Helga von der Mark, Inka Williams, Olaf Wendler, Lydia Sorokin, Klaus von der Mark, and Ernst Poschl. Alternative splice variants of alpha 7 beta 1 integrin selectively recognize different laminin isoforms. *J Biol Chem*, 277(8):6012–6016, 2002 Feb 22.

[184] S Vukicevic, F P Luyten, H K Kleinman, and A H Reddi. Differentiation of canalicular cell processes in bone cells by basement membrane matrix components: regulation by discrete domains of laminin. *Cell*, 63(2):437–445, 1990 Oct 19.

[185] Michiko R Wada, Masayo Inagawa-Ogashiwa, Shirabe Shimizu, Shigeru Yasumoto, and Naohiro Hashimoto. Generation of different fates from multipotent muscle stem cells. *Development*, 129(12):2987–2995, 2002 Jun.

[186] Kate L Wegener, Anthony W Partridge, Jaewon Han, Andrew R Pickford, Robert C Liddington, Mark H Ginsberg, and Iain D Campbell. Structural basis of integrin activation by talin. *Cell*, 128(1):171–182, 2007 Jan 12.

[187] H Weintraub. The myod family and myogenesis: redundancy, networks, and thresholds. *Cell*, 75(7):1241–1244, 1993 Dec 31.

[188] James R Whiteford and John R Couchman. A conserved nxip motif is required for cell adhesion properties of the syndecan-4 ectodomain. *J Biol Chem*, 281(43):32156–32163, 2006 Oct 27.

[189] Sabina E Winograd-Katz, Shalev Itzkovitz, Zvi Kam, and Benjamin Geiger. Multiparametric analysis of focal adhesion formation by rnai-mediated gene knockdown. *J Cell Biol*, 186(3):423–436, 2009 Aug 10.

[190] Haguy Wolfenson, Yoav I Henis, Benjamin Geiger, and Alexander D Bershadsky. The heel and toe of the cell's foot: a multifaceted approach for understanding the structure and dynamics of focal adhesions. *Cell Motil Cytoskeleton*, 66(11):1017–1029, 2009 Nov.

[191] Myra H Wyckoff, Chirine El-Turk, Abbot Laptook, Charles Timmons, Francis H Gannon, Xiafang Zhang, Steven Mumm, and Michael P Whyte. Neonatal lethal osteochondrodysplasia with low serum levels of alkaline phosphatase and osteocalcin. *J Clin Endocrinol Metab*, 90(2):1233–1240, 2005 Feb.

[192] J P Xiong, T Stehle, B Diefenbach, R Zhang, R Dunker, D L Scott, A Joachimiak, S L Goodman, and M A Arnaout. Crystal structure of the extracellular segment of integrin alpha vbeta3. *Science*, 294(5541):339–345, 2001 Oct 12.

[193] D Yaffe and O Saxel. Serial passaging and differentiation of myogenic cells isolated from dystrophic mouse muscle. *Nature*, 270(5639):725–727, 1977 Dec 22-29.

[194] V P Yakubenko, D A Solovjov, L Zhang, V C Yee, E F Plow, and T P Ugarova. Identification of the binding site for fibrinogen recognition peptide gamma 383-395 within the alpha(m)i-domain of integrin alpha(m)beta2. *J Biol Chem*, 276(17):13995–14003, 2001 Apr 27.

[195] Valentin P Yakubenko, Valeryi K Lishko, Stephen C-T Lam, and Tatiana P Ugarova. A molecular basis for integrin alphambeta 2 ligand binding promiscuity. *J Biol Chem*, 277(50):48635–48642, 2002 Dec 13.

[196] K M Yamada and D W Kennedy. Dualistic nature of adhesive protein function: fibronectin and its biologically active peptide fragments can autoinhibit fibronectin function. *J Cell Biol*, 99(1 Pt 1):29–36, 1984 Jul.

[197] N Yamamoto, S Akiyama, T Katagiri, M Namiki, T Kurokawa, and T Suda. Smad1 and smad5 act downstream of intracellular signalings of bmp-2 that inhibits myogenic differentiation and induces osteoblast differentiation in c2c12 myoblasts. *Biochem Biophys Res Commun*, 238(2):574–580, 1997 Sep 18.

[198] C C Yao, B L Ziober, A E Sutherland, D L Mendrick, and R H Kramer. Laminins promote the locomotion of skeletal myoblasts via the alpha 7 integrin receptor. *J Cell Sci*, 109 (Pt 13):3139–3150, 1996 Dec.

[199] Fumiharu Yokoyama, Nobuharu Suzuki, Yuichi Kadoya, Atsushi Utani, Hiroko Nakatsuka, Norio Nishi, Masahiro Haruki, Hynda K Kleinman, and Motoyoshi Nomizu. Bifunctional peptides derived from homologous loop regions in the laminin alpha chain lg4 modules interact with both alpha 2 beta 1 integrin and syndecan-2. *Biochemistry*, 44(28):9581–9589, 2005 Jul 19.

[200] Peter D Yurchenco, Peter S Amenta, and Bruce L Patton. Basement membrane assembly, stability and activities observed through a developmental lens. *Matrix Biol*, 22(7):521–538, 2004 Jan.

[201] Ronen Zaidel-Bar and Benjamin Geiger. The switchable integrin adhesome. *J Cell Sci*, 123(Pt 9):1385–1388, 2010 May 1.

[202] Ronen Zaidel-Bar, Shalev Itzkovitz, Avi Ma'ayan, Ravi Iyengar, and Benjamin Geiger. Functional atlas of the integrin adhesome. *Nat Cell Biol*, 9(8):858–867, 2007 Aug.

[203] Ronen Zaidel-Bar, Zvi Kam, and Benjamin Geiger. Polarized downregulation of the paxillin-p130cas-rac1 pathway induced by shear flow. *J Cell Sci*, 118(Pt 17):3997–4007, 2005 Sep 1.

[204] E Zamir and B Geiger. Molecular complexity and dynamics of cell-matrix adhesions. *J Cell Sci*, 114(Pt 20):3583–3590, 2001 Oct.

[205] Fabian Zanella, James B Lorens, and Wolfgang Link. High content screening: seeing is believing. *Trends Biotechnol*, 28(5):237–245, 2010 May.

[206] Xian Zhang, Guoying Jiang, Yunfei Cai, Susan J Monkley, David R Critchley, and Michael P Sheetz. Talin depletion reveals independence of initial cell spreading from integrin activation and traction. *Nat Cell Biol*, 10(9):1062–1068, 2008 Sep.

[207] Wolfgang H Ziegler, Alex R Gingras, David R Critchley, and Jonas Emsley. Integrin connections to the cytoskeleton through talin and vinculin. *Biochem Soc Trans*, 36(Pt 2):235–239, 2008 Apr.

[208] Dov Zipori. The nature of stem cells: state rather than entity. *Nat Rev Genet*, 5(11):873–878, 2004 Nov.

[209] Dov Zipori. Mesenchymal stem cells: harnessing cell plasticity to tissue and organ repair. *Blood Cells Mol Dis*, 33(3):211–215, 2004 Nov-Dec.

[210] Dov Zipori. The stem state: plasticity is essential, whereas self-renewal and hierarchy are optional. *Stem Cells*, 23(6):719–726, 2005 Jun-Jul.

[211] Dov Zipori. The stem state: mesenchymal plasticity as a paradigm. *Curr Stem Cell Res Ther*, 1(1):95–102, 2006 Jan.

Acknowledgments

I wish firstly to express my appreciation to Prof. Thomas Holstein, for lending his support at Heidelberg University. I would like to thank Prof. Joachim Spatz for his invaluable encourage, entrusting me and supporting this multidisciplinary project to get off the ground. I wish to thank the Max Planck Institute for Metal Research, for the financial support of my studies and also for enabling me to travel to Israel and Germany on the conference and research cooperation circuit.

Extended appreciation is expressed to the Group of Prof. Spatz at the Max Planck Institute for Metal Research. It is only through participation and sometimes pointless conversations that insight and motivation strikes. For the project itself, many thanks are due: To Dr. Ada Cavalcanti-Adam and Dr. Letizia Carramusa for informal discussions. To Dr. Roberto Fiamengo for showing me how to handle peptides. To Dr. Alex de Beer, who assisted me with the focal adhesion algorithm to analyze my data, Laura Valiente for useful MatLab hints, and Dr. Iain Dunlop for his assistance in microscopy. To Dr. Cornelia Lee-Thedieck and Dr. Jens Ulmer for reviewing parts of my work. To Dr. Ferdinand Belz for providing the PEG polymer neccesary for my experiments. Special thanks to technicians Christine Mollenhauer, Margit Kaap, Maria Sycha, Henriette Ries and Janis Grigoridis and the administrative staff Dorothee Klink and Elizabeth Pfeilmeier, all of whom I gratefully acknowledge here with my sincere thanks.

I am grateful to our main collaborator Prof. Benny Geiger, for countless informal discussions, scientific induction, patience and understanding throughout this project. I have enjoyed working with you so much and learnt a lot. Without the retroviral infection expertise of Dr. Irena Lavelin, it would have been impossible to proceed with the paxillin focal adhesion studies upon which the report depends. I also want to thanks to Prof. Dr. David Yaffe and Dr. Heli Sarig of the Department of Molecular Biology at the Weizmann Institute of science for providing me the C2 cells and for valuable discussions. I also wish to thank Dr. Tova Volberg for help in tissue culture, and to Dr. Sabina Winogratz and Dr. Suha Naffar-Abu-Amara for their lab support in the screening project in the Weizmann Institute of Science

during 2006-2008. Appreciation to Prof. Bershadsky, Prof Zvi Kam, and their group members. Thanks to Prof. "Spilke" for the interesting philosophical conversations of the human nature. Thanks to Prof. Dov Zipori for his lectures. Thanks to Etty Hirsch, secretary of Prof. Geiger for her assistance during my visits in Israel.

I also wish to thank to Dr. Nadine Walter, Dr. Silvie Roke, Dr. Kristen Mills, Dr. Stefan Kudera, Dr. Alexandra Goldyn, Burak Ozdol, Burcu Ogut and Hilton Barbosa de Aguiar and George for showing me the sun in days of disappointing experiments. Special thanks to Adriana, Moritz, Angela, Dirk, Carol, Wieland, Gil, Ana, Karsten, Yael, Julia, Ruppa, Thomas, Miles, Juan, Maya and Rafael who keep me grounded and sane.

And although metaphorically speaking, I feel like a satellite of the many places I once called home, finally I wish to thank my mother... who takes my phonecalls wherever I am, and reminds me that taking care of myself is just as important as writing my thesis. Thanks mother for your unfailing love and strength.